

Exosome Trafficking in the Acute Myeloid Leukemia Microenvironment

By

Noah I. Hornick

A DISSERTATION

Presented to the Department of Molecular Microbiology & Immunology
and the Oregon Health & Science University

School of Medicine

in partial fulfillment of

the requirements for the degree of

Doctor of Philosophy

April 2015

School of Medicine
Oregon Health & Science University

CERTIFICATE OF APPROVAL

This is to certify that the PhD dissertation of
Noah I. Hornick
has been approved

Peter Kurre, MD; Mentor/Advisor

Eric D. Cambronne, PhD; Chair

David M. Lewinsohn, MD, PhD; Member

Philip J. Stork, MD; Member

Jeffrey W. Tyner, PhD; Member

David B. Jacoby, MD; Member

TABLE OF CONTENTS

List of Figures	iii
List of Abbreviations	v
ACKNOWLEDGEMENTS	vii
ABSTRACT	ix
CHAPTER 1: Introduction	1
<i>Acute Myeloid Leukemia</i>	2
<i>Bone Marrow Microenvironment</i>	6
<i>Extracellular Vesicles and Exosomes</i>	11
<i>MicroRNA</i>	14
<i>General Hypothesis and Specific Aims</i>	17
CHAPTER 2: AML Vesicle Biogenesis and Trafficking	20
<i>Abstract</i>	21
<i>Introduction</i>	21
<i>Results</i>	22
<i>Discussion</i>	32
<i>Materials & Methods</i>	34
CHAPTER 3: Exosome Impact on the Marrow Niche	41
<i>Abstract</i>	42
<i>Introduction</i>	42
<i>Results</i>	43
<i>Discussion</i>	54
<i>Materials & Methods</i>	55
CHAPTER 4: AML Exosomes as Serum Biomarkers	61
<i>Abstract</i>	62
<i>Introduction</i>	63
<i>Results</i>	64
<i>Discussion</i>	78
<i>Materials & Methods</i>	81
CHAPTER 5: AML Exosome MicroRNA Target Analysis	88
<i>Abstract</i>	89
<i>Introduction</i>	89
<i>Results</i>	90
<i>Discussion</i>	95
<i>Materials & Methods</i>	98
CHAPTER 6: Conclusions and Future Directions	101
<i>Future directions</i>	102
<i>Conclusions</i>	107

REFERENCES

112

List of Figures

- 1.1 Organization of the Marrow Microenvironment
- 1.2 MicroRNA Processing

- 2.1 Exosome Release by AML Blasts
- 2.2 Total RNA Content of Exosomes
- 2.3 AML Blasts Concentrate Mature MicroRNA in Exosomes
- 2.4 Exosomes Contain Distinct Selected MicroRNA
- 2.5 AML Exosomes are Internalized By Neighboring Cells of Multiple Types

- 3.1 Molecular Impact of AML Exosomes on Stroma
- 3.2 AML Exosomes Compromise HSPC Function *In Vitro*
- 3.3 Intrafemoral Injection of AML Exosomes Recapitulates In Vitro Exosome Exposure
- 3.4 Molm-14 and HL-60 Produce Distinct Disease Kinetics, Distribution
- 3.5 AML Xenograft Causes Hematopoietic Suppression in NSG Mice

- 4.1 Molm-14 Engraft in NSG Mice and Contribute to Compartment Exosome Secretion
- 4.2 Molm-14 and Stromal Exosomes Concentrate Selected MicroRNA
- 4.3 Conventional Markers Are Limited; Chemotherapy is a Confounder
- 4.4 Serum Exosome RNA Yield and Quality are Independent of Serum Volume

- 4.5 Serum Exosome miRNA Distinguishes Leukemia From Hematopoiesis
- 4.6 Expansion of the Scope of the Serum Exosome miRNA Biomarker

- 5.1 Packaging and Import of miRs -155 and -1246
- 5.2 RISCTrap mRNA Targeting of miR-155
- 5.3 Validation of miRNA Targeting

List of Abbreviations

3'UTR, 3' untranslated region
AGO, Argonaute
AML, acute myeloid leukemia
ANGPT1, angiopoietin 1
CAR, CXCL12-abundant reticular cell
CFU-C, colony-forming unit in culture
CLL, chronic lymphocytic leukemia
CML, chronic myelogenous leukemia
cMYB, v-myb avian myeloblastosis viral oncogene homolog
CXCL12, C-X-C motif chemokine 12
CXCR4, C-X-C motif chemokine receptor 4
DIC, differential interference contrast
DLS, dynamic light scattering
FBS, fetal bovine serum
FDR, false discovery rate
FLT3, FMS-like tyrosine kinase 3
FLT3L, FMS-like tyrosine kinase 3 ligand
GFP, green fluorescent protein
GM-CSF, granulocyte and macrophage colony-stimulating factor
GVHD, graft versus host disease
HSC, hematopoietic stem cell
HSPC, hematopoietic stem and progenitor cell
IGF-IR, insulin-like growth factor I receptor
IL-2 γ , interleukin 2 receptor gamma
ILV, intraluminal vesicle
KITLG, Kit ligand
Lin-, lineage depleted
LSC, leukemic stem cell
MEF, murine embryonic fibroblast
miRNA, microRNA
MRD, minimal residual disease
MSC, mesenchymal stem/stromal cell
MVB, multivesicular body
NMSC, nonmyelinating Schwann cell
NOD, non-obese diabetic
NRhPE, N-(lissamine rhodamine B sulfonyl) phosphatidylethanolamine
NSG, NOD/SCID/IL-2 γ ^{null}
NTA, nanoparticle tracking analysis
PABPC, cytoplasmic poly-A binding protein
PBMC, peripheral blood mononuclear cells
PBS, phosphate buffered saline
PCR, polymerase chain reaction
PPP, picropodophyllin
qPCR, quantitative polymerase chain reaction

qRT-PCR, quantitative reverse transcriptase - polymerase chain reaction
R-, insulin-like growth factor I receptor knockout
R+, insulin-like growth factor I receptor overexpressing
RISC, RNA-induced silencing complex
RNA, ribonucleic acid
RT-PCR, reverse transcriptase - polymerase chain reaction
SCF, stem cell factor
SCID, severe combined immunodeficiency
T-Reg, T-regulatory cell
TEM, transmission electron microscopy
TGF- β , transforming growth factor β
Tie-2, TEK tyrosine kinase
VEGF, vascular endothelial growth factor
VF-FBS, vesicle-free fetal bovine serum

ACKNOWLEDGEMENTS

The research outlined herein would not have been possible without the contributions of a great many people, and my writing this thesis has only been made possible through their guidance and support. I would first like to thank Peter Kurre, for welcoming me into his lab and training me despite a work history that included essentially no relevant experience and a CV that caused him to question my suitability for admission to this university. I am therefore in his debt for teaching me to write and edit a CV, in addition to scientific reasoning; the composition of abstracts, manuscripts, and grants; and the presentation of results. He has given me a role model in balancing the practices of basic science and clinical medicine, supported my opinion of my own work, and helped me to judge which projects are worth pursuing from another angle and which are simply not going to work. I am deeply grateful for his mentorship, and for the opportunity to spend these years in his lab. I would like to thank all of the current and former members of the Kurre lab for giving me the benefit of their experience, assistance, and camaraderie. Thanks to Matt Shurtleff, Amy Skinner (who performed the initial live cell NRhPE imaging described here), and Andrea McBeth, for my initial training in many lab techniques. Many thanks to Ashley Kamimae-Lanning for her friendship, lab assistance, and providing many examples of successful graduate student work. I am very grateful to have worked with Jianya Huan, Natalya Goloviznina, and Ben Doron, whose collaboration and assistance has been instrumental not only in many of the experiments described in this thesis (and especially in mouse work), but in the writing of many manuscripts and abstracts, in the planning of experiments, and the interpretation of results. Thanks to Santhosh Chakkaramakkil Verghese, for his impressive molecular biology expertise and for his inexplicably unflagging cheerfulness in the face of (what to me seemed to be) endless cloning setbacks. Thanks to Shelton Viola for his help with and advice on both medical training and stromal cell culture. Thanks to Thomas Russell for scientific discussion and Neil Diamond Friday. Thanks to Lauriel Earley, Tae Ha, Rajani Kaimal, Katy Lawson, Michael Layoun, Kyle Lenz, Shannon Liudahl, John Powers, Kelsie Storm, Lauren Uhde, and Jennifer Wherley for discussions, feedback, and assistance.

I am grateful to my co-mentor David Lewinsohn, and to the members of my thesis advisory committee, Eric Cambronne, Jeff Tyner, and Phil Stork, for a great deal of helpful feedback and suggestions, as well as for helping to keep me pointed in a productive direction.

I owe a great deal to David Jacoby, for his assistance and support as the director of the MD/PhD program, as well as for serving on my dissertation defense. His ability to make himself available and helpful to his students despite an alarmingly full schedule is truly impressive and greatly appreciated, as is his enthusiasm both for education and for science. I am also grateful to Johanna Colgrove for many types of assistance, from scheduling to grant writing to flat tires, and to the

MD/PhD program generally, its committee and students, for an excellent training environment, support, and encouragement.

I thank the Department of Pediatrics, the Papé Family Pediatric Research Institute, and the Oregon Stem Cell Center. I am grateful to the Grompe, Impey, and Fleming labs for sharing advice, reagents, and equipment, and particularly to Devorah Goldman and Ronn Leon for their help in unraveling several particularly challenging problems. Thanks to Qianyu Yang for her help and support with the hypoxia chamber, centrifuges, and other equipment. Thanks to Leslie Lublink and Kirsten Groener for their administrative support and advice, and thanks to Dale Braden, without whom I would have no grants submitted, let alone funded.

I would like to thank Muneesh Tewari and John Chevillet for their collaboration on and assistance with nanoparticle tracking analysis. I would like to thank Aurelie Snyder of the Advanced Light Microscopy Core, Claudia Lopez of the Electron Microscopy Core, and Pamela Canaday and Mandy Gilchrist of the Flow Cytometry Core. I am grateful to Chris Harrington, Kristina Vartanian, Trevor McFarland, Amiee Potter, Tomi Mori, and Solange Mongoue-Tchokote of the Gene Profiling Shared Resource for bioanalyzer and microarray assistance. I am indebted to Amy Laird and Jodi Lapidus of the Department of Public Health for statistical advice and assistance.

I am fortunate to have had Lulu Cambronne and Rongkun Shen of the Richard Goodman lab as collaborators on the RISCTrap experiments. Their support has not only been instrumental in performing those initial experiments, but in data analysis and result interpretation. Since our original collaboration, they have done far more than could be expected in helping me to get this technology working in our own lab, and I am thankful for their assistance.

I am grateful to the Program for Cell and Molecular Biosciences, the Department of Molecular Microbiology and Immunology, and my funding sources: the National Cancer Institute, N.L. Tartar Trust, and the T32 Inflammation and Immunology training grant. I would like to thank the American Society for Hematology and the International Society for Extracellular Vesicles, for their annual meetings and workshops, for their support of my niche research, and for giving me an opportunity to present our work.

Lastly, I would like to thank my amazing girlfriend and yolo partner Ruby Larisch, my family (whose examples in the scientific and writing worlds have been instrumental in essentially everything I do), and my friends, for their unwavering love and support, for tolerating my variable availability and communication, for being interested in my work (and, sometimes, for not asking about it). There is no way to adequately express my appreciation for you all.

ABSTRACT

Homeostatic hematopoiesis is defined by the division and differentiation of rare self-renewing stem cells, maintained and regulated by the diverse constituent cells of their microenvironment. Numerous studies have investigated the supportive roles of many types of marrow stroma, and it has been proposed that leukemogenesis is accompanied by a conversion of this space. The leukemic marrow microenvironment exhibits decreased capacity for hematopoietic stem and progenitor cell (HSPC) maintenance capability, while promoting and protecting leukemic blasts. In patients and model animals, these processes eventually result in hematopoietic failure. The mechanisms for such a conversion, however, remain unclear.

HSPC support is a role that has been variously ascribed to osteoblasts, nonmyelinating Schwann cells, endothelium, and mesenchymal stromal cells, among others. As residual nonmalignant HSPC have themselves been shown to be altered in patients with acute myeloid leukemia (AML), this process requires either multiple independent specific mediators, or a highly pleiotropic mechanism. The trafficking of exosomes (small, membrane-enclosed extracellular vesicles that carry protein and nucleic acid cargo between cells) within the marrow space provides such a pleiotropic mechanism, as they have the potential to deliver regulatory messages directly to the cytoplasm of recipient cells without any known entry restriction.

In these experiments, I begin to delineate the role of AML-derived exosomes in the regulation of the marrow microenvironment. Through electron and fluorescence microscopy, nanoparticle tracking analysis, and microRNA microarray, I demonstrate that AML blasts secrete exosomes containing concentrated microRNA, the makeup of which clearly distinguishes cells from exosomes and nonmalignant hematopoietic cells from AML blasts. These exosomes are taken up by both HSPC and marrow stroma, transferring sufficient microRNA to effect as much as a 10-fold increase in cellular concentration.

In order to determine the physiologic impact of this exosome transfer, I evaluate exosome-exposed HSPC and stroma, both *in vitro* as well as through several *in vivo* models of exposure, using xenograft, intrafemoral injection of purified exosomes, and an extramedullary disease model to isolate the effects of exosomes from those of other secreted and contact-mediated factors. AML-derived exosomes suppress the expression of several HSPC retention and maintenance factors in stromal cells, and directly cause a decrease in the ability of HSPC to home along a CXCL12 gradient, as well as their clonogenicity (their ability to generate colonies of hematopoietic-lineage cells in culture).

The marked differences between the microRNA content of malignant and nonmalignant exosomes raises the possibility of tracking these molecules as a potential biomarker of disease. Exosome-based biomarkers have particular advantages in AML, as monitoring patients in remission is of central importance to treatment (> 50% of patients relapse), and as direct observation of leukemic blasts is only reliably possible in those with advanced disease. Through a series

of xenograft experiments using the Molm-14 and HL-60 cell lines, I demonstrate that exosomes present a serum-detectable microRNA signature of disease, to which both AML blasts and modified stroma contribute. This signature is durable through treatment with either cytarabine or targeted kinase inhibition. Additional experiments in an alternative AML cell line and primary patient samples provide promising support for broad applicability of serum exosome microRNA as a biomarker in AML.

Finally, I pursue a mechanistic explanation of the observed effects of AML exosomes on recipient HSPC and stroma, through in-depth investigation of selected transferred microRNA. Employing RISCTrap technology and validating 3' untranslated region (3'UTR) luciferase assays and exosome transfer studies, I capture a broad sampling of targets of miR-155, working with this microRNA because of its appreciated relevance in hematopoiesis and leukemia as well as its prominence in AML-derived exosomes. This data set both confirms previously identified targets and identifies several novel potential targets. Further, it provides a starting point for an investigation of interacting partners, in order to better identify pathways regulated by this microRNA. Included targets are of known hematopoietic relevance in numerous cell types, supporting the hypothesis that exosomal microRNA is capable of co-regulating a diverse set of processes in a diverse set of cells.

In total, these experiments represent a body of evidence that supports exosomes as a mechanism by which microRNA are transferred between AML blasts and multiple marrow-resident cell types. These microRNA contribute to

the regulation of several molecular processes, impacting the conversion of the marrow microenvironment from a hematopoietic niche to a leukemic niche, a process with the potential to mediate a major cause of morbidity and mortality in AML patients. Further, AML exosomal microRNA are detectable in the peripheral blood, where they carry a detectable signature of disease, providing a promising avenue for development of a minimally invasive, clinically-relevant biomarker.

CHAPTER 1: Introduction

Acute Myeloid Leukemia

Leukemia was first recognized as a disease process in 1845, described separately in autopsy reports by John Hughes Bennett and Rudolf Virchow, in which were noted "hypertrophy of the Spleen and Liver" and "everywhere in the vessels a mass thoroughly resembling blood." Both reports called attention to the aberrantly high proportion of white cells in the blood, prompting Virchow to label the disease 'leukemia' (a combination of the Greek 'λευκός' / 'leukos' and 'αἷμα' / 'haima'), literally "white blood" in 1847¹. Typically thought to be a chronic disease, an acute (meaning rapidly progressive) leukemia was first recognized as a distinct clinical entity in 1857 by Nikolaus Friedreich, in a patient whose initial presentation preceded her death by only six weeks. It was not until 1872 that the role the bone marrow played in the production of both physiologic blood cells and leukemic blasts was recognized, by Ernst Neumann, who was the first to identify a myelogenous (or myeloid) form of the disease¹. However, this conclusion remained controversial until the development of the triacid stain by Paul Ehrlich in 1877 enabled more precise morphological studies of blood cells, confirming a marrow-derived, granulocytic predominance in myeloid leukemias^{1,2}. This, combined with Otto Naegeli's 1900 identification of the myeloblast as both the cell from which granulocytes descend and the cell representing the pathological population in myeloid leukemias, cemented the definition of acute myeloid leukemia (AML) as a rapidly progressive disease characterized by the overproduction and circulation of myeloblasts^{1,2}. Over the subsequent century, continuing research has revealed a stunning depth of heterogeneity within this

subset of hematopoietic malignancy. The 1976 publication of the French-American-British classification system allowed the separation of AML into six distinct groups, based on cell lineage and morphology³. This classification system, revised in 1985, allowed for productive stratification of risk and treatment strategy⁴, and its major features underlie the current World Health Organization classification system⁵. However, it failed to capture a number of features of disease which offer some clinical utility, including immunophenotype⁶, a history of myelodysplasia⁷, cytogenetics⁸, and gene expression⁹. While these distinct features have in some cases provided clinicians with guidance and patients with improved outcomes, the heterogeneity of AML is such that much of the field's research and statistical analysis addresses it as a whole, rather than restricting analyses to individual subtypes¹⁰.

AML (considering all subtypes together) is the most common acute leukemia in adults, with an annual incidence of 4 per 100,000, and it is responsible for 10,000 deaths per year in the United States¹⁰. Primarily a disease of older adults, it has a median age at diagnosis of 72 years, a number that is increasing both with an aging population and with an increase in diagnosis and treatment among the elderly¹¹. Although there have been advances in treatment – the adoption of a standard chemotherapeutic regimen combining cytosine arabinoside in 1982² and the use of hematopoietic stem cell transplant in 1979^{12,13} were significant milestones – the prognosis for patients with AML remains poor. Among pediatric patients, where AML represents less than twenty percent of leukemia, it is still responsible for the majority of all leukemia deaths¹⁴.

Patient outcomes in older adults are bleaker still, with an overall five-year survival rate across all age groups of less than 25%¹⁰. This dismal outlook exists despite a standard chemotherapy regimen that for more than fifteen years has been successful at achieving initial remission in 50% of patients over 60 years old, and as many as 80% of younger patients¹⁵. These numbers provide a clear illustration of both the significance of relapse in AML and of the importance of residual disease monitoring in patients after induction chemotherapy.

Relapse occurs in more than half of AML patients achieving initial remission, and successful treatment of relapsed AML is uncommon¹⁶. This being the case, substantial research has been devoted to the detection of minimal residual disease (MRD) in patients in remission, in the interest of guiding therapy either to eradicate residual disease, or to prevent its expansion into relapsed AML. These strategies have employed a number of technologies, including quantitative polymerase chain reaction (qPCR) for AML-specific transcripts or fusion genes¹⁷, multiparameter flow cytometry for leukemia-representative cell surface proteins¹⁸, and next-generation sequencing¹⁹. Each of these methods focuses on the direct detection of leukemic blasts, and as such requires their presence in the peripheral blood – emblematic of advanced disease – or requires marrow sampling, a procedure whose invasiveness limits the frequency with which it can be performed¹⁷. The utilization of MRD-directed therapies when possible, however, has yielded promising results¹⁷, underscoring the need for more efficient, less invasive monitoring.

Morbidity and mortality that is attributable to AML and not secondary to treatment is primarily due to one of two causes. Increased blood viscosity caused by large numbers of circulating leukemic blasts can cause localized infarction and organ damage²⁰. Alternatively (or additionally), development of leukemia is concomitant with suppression of normal hematopoiesis, leading to anemia, neutropenia, and thrombocytopenia. These cytopenias frequently require the usage of transfusions and prophylactic antimicrobials to mitigate their effects, a set of interventions with its own costs and risks^{14,21}. Despite the clinical significance of hematopoietic insufficiency in AML, its causes are poorly understood, having traditionally been ascribed to marrow infiltration by leukemic blasts and resultant overcrowding¹⁵. This explanation, however, fails to address the common clinical finding of cytopenias in AML patients with normal marrow cellularity²², or, more rarely, in those with exclusively extramedullary AML (termed granulocytic sarcoma)²³. Recently, it has been reported that AML results in an impairment of bone marrow stromal cells, which is a significant contributor to the failure of physiologic hematopoiesis²⁴. While it has long been believed that AML receives support from the marrow microenvironment, the hypothesis that this interaction extends in both directions, making the marrow less hospitable for the maintenance and proliferation of normal hematopoietic stem cells, is a potentially more comprehensive explanation for the failure of hematopoiesis in patients with AML.

Bone Marrow Microenvironment

In adult mammals, the bone marrow is the primary site of hematopoiesis. The marrow is a complex tissue, containing numerous cell types in an intricately organized spatial arrangement, polarized between the marrow vasculature (specifically fenestrated sinusoids) and the endosteum (Fig. 1.1). Since Ray Schofield first proposed the existence of a specific niche in which hematopoietic stem cells reside, interaction between these stem cells and their neighbors has been viewed as an essential determinant of their quiescence, proliferation, and differentiation²⁵. Subsequent research has revealed that this stem-cell-extrinsic regulation is a highly complex network of communications between a host of interacting partners. Cell types within this space that have been implicated in the maintenance and regulation of hematopoietic stem and progenitor cells (HSPC) include osteoblasts and osteoclasts,

endothelium, mesenchymal stem cells (MSC), sympathetic

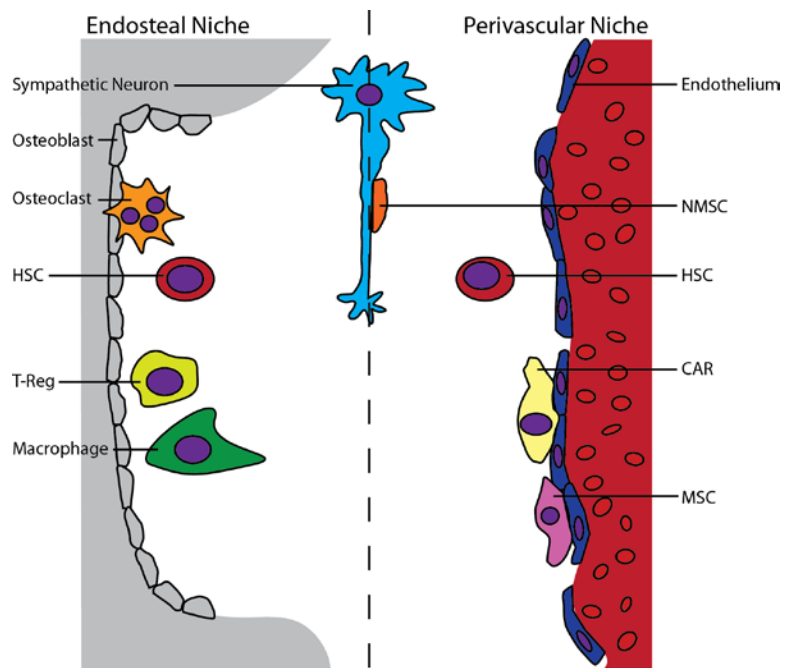


Figure 1.1: Organization of the Marrow Microenvironment

The bone marrow microenvironment contains two separate niches, each home to multiple cell types supporting a population of hematopoietic stem cells. HSC, hematopoietic stem cell; T-Reg, T-regulatory cell; NMSC, nonmyelinating Schwann cell; CAR, CXCL12-abundant reticular cell; MSC, mesenchymal stem cell.

neurons and associated glia, T-regulatory cells and macrophages, and perivascular stroma^{26,27}. These cells are organized into two communicating niches²⁷ (endosteal and perivascular) across a gradient of oxygen concentrations, providing regulation and support to HSPC of multiple types, roles, and lineages.

Structurally, the bone marrow consists of a richly vascularized network of spaces that extend from the metaphyseal plates through the diaphysis. A recent study of hematopoietic localization within the marrow identified structures (termed 'hemospheres') that are concentrated within the metaphysis and contain the majority of hematopoietic activity *in vivo*²⁸. These hemospheres span a region between microvasculature and endosteum, and are more concentrated in the arteriole-rich peripheral region of the marrow cavity, distant from the central vein²⁹. Despite this localization near the arterial side of the marrow vasculature, the marrow's overall hypoxic nature (7% O₂ average in healthy volunteers³⁰), along with rapidly decreasing oxygen tension with distance from the vessel³¹, result in a marrow microenvironment with oxygen tension ranging from hypoxia in the perivascular niche to near anoxia at the endosteal surface.

At the endosteal pole of this continuum reside osteoblasts and osteoclasts, whose importance to the hematopoietic microenvironment was among the first recognized. Although recent studies have suggested that the role of osteoblasts in support of hematopoietic stem cells (HSC) is indirect³², the fact remains that they express the HSPC chemoattractant C-X-C motif chemokine 12 (CXCL12), as well as membrane-bound ligands Jagged-1 and Angiopoietin-1,

which interact with HSC receptors Notch-1 and TEK Tyrosine Kinase (Tie-2), regulating quiescence and expansion of the stem cell pool²⁷. These interactions support a role for osteoblasts in defining the HSC niche, by contributing to the attractant CXCL12 gradient if not by direct contact. Osteoclasts, meanwhile, have been shown to contribute to the hematopoietic niche in that suppressing their activity suppresses HSC expansion, while their influence on local calcium ion concentration in the marrow supports retention of HSC in the niche²⁷. These contributions have been shown to be dispensable for HSC maintenance, however, and it has been suggested that osteoclasts themselves are a nonessential niche constituent²⁹.

The perivascular niche, similarly, is composed of its own unique constituent cell types. The walls of the sinusoids are defined by endothelial cells, that in numerous studies have been shown to express HSC-supporting molecules, including granulocyte and macrophage colony-stimulating factor (GM-CSF), Kit ligand (KITLG), FMS-like tyrosine kinase 3 ligand (FLT3L), Notch ligands, and CXCL12³³, collectively promoting HSC response to injury in addition to homeostatic maintenance²⁹. Adjacent to the endothelium lining the sinusoids within the marrow lie perivascular CXCL12-abundant reticulocytes (CAR), so called because they secrete high levels of the HSC chemoattractant³⁴. Deletion of these cells not only led to depletion of HSC, but also impaired the generation of adipocyte and osteoblast populations³², suggesting a role for these cells in generating the marrow stroma as well as supporting hematopoiesis. This proposed role of CAR as bi-potent progenitors has led to some overlap in

definition with mesenchymal stem/stromal cells (MSC). Although nomenclature varies between reports, a population of mesenchymal cells that is marked by CD146 in humans and nestin in mice contributes to the formation of the perivascular niche. These cells are positioned between HSC, endothelium, and adrenergic neurons, and promote ectopic niche formation when transplanted, demonstrating a defining role in the microenvironment^{27,33}.

In addition to the endosteal and perivascular niche-defining cell populations, the marrow is home to several cell types that are essential for hematopoietic support, without themselves defining a spatial niche. Multiple immune cell types have been implicated in forming and maintaining stem cell niches within the bone marrow. Fujisaki *et al.* demonstrated that T-regulatory immune suppressive cells colocalized with murine HSPC *in vivo*, and further demonstrated that these cells were necessary for the engraftment and survival of transplanted allogeneic HSPC³⁵, supporting the hypothesis that these cells create an immune-protected environment for hematopoiesis. Macrophages also have a defined role in maintaining the endosteal marrow niche, having been shown to be required both for osteoblast maintenance and for retention of HSC within the marrow³⁶. Both autonomic neurons and associated glial cells have also been reported to be vital in supporting hematopoiesis²⁹. Through multiple methods of dysregulation and functional complementation, norepinephrine signaling provided by adrenergic neurons has been shown to be essential for controlling HSC retention within the marrow³⁷. In close contact with these

neurons are nonmyelinating Schwann cells, a glial cell population that secretes transforming growth factor β (TGF- β) essential for HSC quiescence³⁸.

The culmination of these influences is an environment that provides protection and support to hematopoietic stem cells, both in their baseline quiescent state – HSC spend the majority of their existence outside the cell cycle – and in their proliferative stages. These effects maintain a healthy stem cell pool, allowing for lifelong maintenance of the cellular components of blood. This protection and support, however, creates an ideal environment to a nascent leukemia, as well. Leukemic stem cells (LSC) behave similarly to hematopoietic stem cells, in that they exist as rare cells at the root of a cellular hierarchy, dividing and differentiating to produce the great majority of the blast population³⁹. Utilizing many of the same molecular mechanisms as HSC⁴⁰, LSC home to and engraft within the marrow, where they produce durable modifications in the microenvironment⁴¹. These changes progressively alter the hematopoietic niche into a leukemic one, shifting away from support of HSC and toward MSC⁴². An alternative hypothesis, in which alterations in the hematopoietic microenvironment themselves lead to oncogenesis, has also been advanced⁴³, generating a chicken-and-egg causality debate. Whichever cell is initially responsible, the interaction between leukemia and the marrow confers advantages, including chemoresistance⁴⁴, and the presence of cell-extrinsic signaling provided by the marrow has been shown to be essential for LSC survival⁴⁵.

In aggregate, the bone marrow coordinately maintains hematopoiesis by regulating the proliferation and differentiation of stem and progenitor cells. These influences are, additionally, central to the process of leukemogenesis, providing migration and adhesion support, pro-growth and anti-apoptotic signaling, and resistance to chemotherapeutics. An understanding of the interaction between HSC and LSC and their niche constituents is therefore central to an understanding of normal and malignant hematopoiesis, and could provide insight into treatment of numerous human diseases, including AML.

Extracellular Vesicles and Exosomes

In 1981, Trams *et al.* described the shedding of two populations of extracellular vesicles from normal and neoplastic cell lines in culture. These vesicles were either 500-1000nm or approximately 40nm in diameter, and were shown to be both plasma membrane-derived and enzymatically active. The authors suggested that these new vesicles be termed 'exosomes'⁴⁶. In the years following this discovery, the label 'exosome' has come to refer specifically to exocytosed vesicles 30-100nm in diameter, derived from exocytosis of the internal vesicles of multivesicular endosomes⁴⁷. These exocytosed vesicles were first differentiated from the larger vesicles generated by plasma membrane budding through painstaking electron microscopy of the removal of transferrin receptor from the plasma membrane of rat reticulocytes⁴⁸, though they have since been shown to be secreted by many disparate cell types⁴⁹. Their cup-shaped morphology is similar both before and after secretion by the originating cell, with a density between 1.13 and 1.19g/mL⁴⁷. Their surface phenotype and

biogenesis, however, have resisted uniform characterization, suggesting that the collective term 'exosome' may refer to multiple populations of vesicle⁵⁰. This has led to a lack of clarity in the field with regard to what specific populations of vesicle are being studied⁵¹. In order to obviate this difficulty here, I will be using the term 'exosome' to refer generally to all nanoscale extracellular vesicles secreted by the cells being studied, although the specific experiments described herein will include more stringent characterizations of the vesicle populations concerned.

It was the integral membrane proteins of the reticulocyte-derived exosomal surface that first brought exosomes to the attention of researchers⁴⁶, and numerous subsequent studies focused on the details of this secretion led to the finding that exosomes could be retrieved from peripheral circulation in animals, and that these exosomes had multiple functions independent of their producing cells⁵². A major contributor to the appeal for early exosome researchers was that an exosome could 'simulate' cell-contact-dependent signaling at locations remote from the exosome-producing cell. An early example of this sort of function was the 1996 description of B cell-derived exosomes acting as antigen-presenting cells to activate T cells⁵³, a function previously believed to rely upon physical contact between B and T cells. In subsequent years, exosomes were implicated in viral transmission⁵⁴, in tumor progression⁵⁵, and in physiologic regulation of cytokine signaling through secretion of exosome-bound (and so, 'soluble') receptors⁵⁶. In its first twenty-five years, the field's understanding of exosomes slowly expanded from secreted enzyme activity in

reticulocytes to an evolutionarily conserved mechanism that mediates numerous diverse processes in both health and disease.

The pace of exosome research greatly accelerated following the 2007 discovery that exosomes could mediate the productive transfer of nucleic acids (messenger RNA (mRNA) and microRNA (miRNA)), which led to a surge of interest and publication⁵⁷. Within two years, exosome transfer of RNA had been investigated in the contexts of immune suppression⁵⁸, tumor progression⁵⁹, neural communication with somatic tissue⁶⁰, gene therapy delivery vehicles⁶¹, acute kidney injury⁶², and insulin resistance⁶³, among many others. One particularly promising area of research has been in the identification of novel biomarkers of disease. As exosomes have been found to equilibrate with many body fluids, including bronchoalveolar lavage fluid⁶⁴, blood⁶⁵, malignant pleural effusions⁶⁶, urine⁶⁷, saliva⁶⁸, and cerebrospinal fluid⁶⁹, they present an attractive platform for biomarker development in the context of disease of a wide variety of tissues and organs. This has led to investigations into exosome-based biomarkers of many cancers^{59,70-72}, as well as of many other diverse diseases and conditions, including multiple sclerosis⁷³, tuberculosis⁷⁴, sepsis⁷⁵, and kidney transplant failure⁷⁶.

Within the marrow, the role of exosome trafficking is still being defined. The bulk of the research into exosome secretion in the marrow has focused on mesenchymal stem/stromal cells or on malignancy. Many effects have been ascribed to the exosomes derived from MSC: tumor suppression⁷⁷ or acceleration⁷⁸, promoting regeneration after injury in many tissues⁷⁹⁻⁸¹, and

amelioration of graft-versus-host disease⁸². As diverse as these effects are, there has been substantially more investigation into the role of exosomes in cancer. It has been shown that many cancers are able to modulate the activity of cells within the marrow through their exosomes. Melanoma exosomes were demonstrated to secrete exosomes that alter marrow progenitors, leading them to increase vessel permeability and tumor-associated angiogenesis, which led to an increase in metastatic potential⁸³. Tumor-derived exosomes have also been reported to suppress immune recognition of and response to malignancy through inhibiting the activity of natural killer cells, T cells, and professional antigen-presenting cells⁸⁴. Exosomes secreted by cholangiocarcinoma altered MSC, both increasing migration and modulating cytokine expression that enhanced the growth and proliferation of tumor cells *in vitro*⁸⁵. This exosomally-mediated tumor-stroma crosstalk has been shown to be relevant to treatment as well, with MSC-exosome signaling contributing to drug resistance in multiple myeloma cells⁸⁶.

MicroRNA

MicroRNA are small (22 to 24 nucleotides in length) RNA transcripts that suppress translation of mRNA, contributing to posttranscriptional gene regulation. Since 2001, when they were first recognized as a distinct class of small regulatory RNA in *Caenorhabditis elegans*⁸⁷⁻⁸⁹, microRNA have rapidly gained recognition as a powerful, phylogenetically conserved means by which organisms orchestrate diverse biological processes⁹⁰. As miRNA require only a small degree of complementarity with their target mRNA, a single miRNA

transcript can regulate many different targets, with more than 60% of all human protein-coding transcripts being regulated by miRNA⁹¹.

MicroRNA are generally transcribed by RNA polymerase II as a long 'pri-miRNA', or primary microRNA transcript, containing a small (~70nt) hairpin structure, which contains the miRNA⁹² (Fig. 1.2).

This pri-miRNA, often an intron of another coding or non-coding gene, is then bound by the Microprocessor complex, consisting of RNA-binding protein DGCR8 and the endonuclease Drosha. This

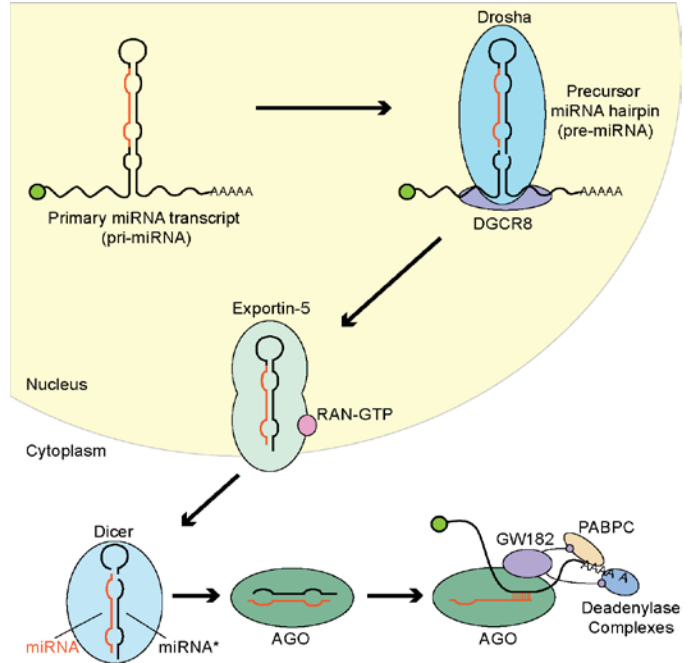


Figure 1.2: MicroRNA Processing

MicroRNA are initially transcribed as pri-miRNA, which are processed by Drosha in the nucleus into pre-miRNA hairpin structures. These pre-miRNA are brought out of the nucleus by Exportin-5, where Dicer processes them into mature miRNA. These miRNA are loaded into Argonaute (AGO) proteins, which nucleate the assembly of the RISC, which recruits mRNA and deadenylates them through enzymes associated with GW182.

complex excises the hairpin structure containing the microRNA, which is then known as a 'pre-miRNA', or precursor microRNA hairpin⁹³. These pre-miRNA are then bound by a complex of Exportin-5 and RAN-GTP, which exports them from the nucleus into the cytoplasm, where they are bound by the endonuclease Dicer. Processing by Dicer removes the hairpin, separating the pre-miRNA into two mature miRNA of approximately 22 nucleotides in length⁹². The nomenclature of the mature miRNA is somewhat murky, with human pre-miRNA

hsa-mir-155, for example, being processed into two mature miRNA variously called hsa-miR-155 and hsa-miR-155* or hsa-miR-155-5p and hsa-miR-155-3p⁹⁴. After processing, the miRNA duplex is loaded as a pair into one of several Argonaute (AGO) proteins. The duplex is then unwound, and one of the two strands is ejected, while the other remains to become a component of the mature RNA-induced silencing complex (RISC). This complex, containing the mature miRNA, AGO protein, and GW182, binds a target mRNA, selected by complementarity to the miRNA's seed sequence (nucleotides 2-8)⁹³. In the canonical human miRNA silencing pathway, GW182 then binds cytoplasmic poly-A binding protein (PABPC), which binds the polyadenylated tail of the mRNA, and several deadenylase complexes, which degrade it. The deadenylated mRNA is then released, where it is rapidly decapped by the decapping enzyme DCP2, and then broken down by the exonuclease XRN1⁹⁵. It has also been demonstrated that miRNA can function by inhibition of translation, and indeed, this was originally thought to be the exclusive means by which miRNA suppressed gene expression in animals. However, more recent studies have supported the widely held view that degradation of mRNA transcripts is the major mechanism of action of miRNA silencing in both plants and animals⁹⁶.

Among the first aspects of physiology discovered to be under miRNA control was hematopoiesis; a series of experiments published in 2004 identified miR-142, -181, and -221 as contributors to lymphoid lineage selection for B versus T cells⁹⁷. In the subsequent ten years, miRNA has been revealed to be a precise tool for shaping hematopoietic differentiation, with multiple miRNA

species known to effect nearly all decision points in the hematopoietic lineage tree⁹⁸. This has also proved true in the other cell types of the marrow microenvironment; the proliferation and fate determination of MSC has been shown to be under miRNA control⁹⁹, and miRNA have been implicated in the interaction of marrow endothelium and hematopoietic cells¹⁰⁰. Additionally, dysregulation of miRNA has been implicated in hematologic malignancy in many facets - oncogenesis, disease progression, and prognosis¹⁰¹.

General Hypothesis and Specific Aims

Current treatments for acute myeloid leukemia are highly successful at achieving initial remission, but the high rate of relapse, coupled with the difficulty of treating relapsed AML, keeps the overall five-year survival rate of this disease unacceptably low. Additionally, a significant mediator of AML morbidity – suppression of hematopoiesis – lacks a satisfactory explanation, when the ability to prevent or ameliorate its effects has the potential to yield substantial benefit to AML patients. The research described in this dissertation addresses these issues by evaluating the role of AML-secreted exosomes in the pathophysiology of this disease. The overall hypothesis tested is twofold: that secreted exosomes simultaneously influence cells of the marrow microenvironment, including stromal cells and HSPC, resulting in hematopoietic failure; and that secreted exosomes escape the marrow, equilibrating with the bloodstream and providing an earlier biomarker of residual disease than is available through more traditional, cell-based methods.

Specific Aims:

1. Characterize exosome production by Acute Myeloid Leukemia cells

Exosomes have been shown to be produced by many different malignancies, both *in vitro* and *in vivo*, but this has not yet been demonstrated in the case of AML. An evaluation of exosome production and content, and particularly of RNA content, by AML primary blasts and cell lines will shed substantial light on the potential roles of these vesicles to be examined in aims 2 and 3.

2. Evaluate AML exosome RNA as an early biomarker of disease

Existing studies have demonstrated the potential for exosomes as biomarkers of disease. Because of their equilibration between body compartments, I hypothesize that exosomes will be detectable in the peripheral circulation of AML-engrafted mice and of AML patients at earlier time points than are AML blasts themselves. If this hypothesis is correct, exosomes could provide a biomarker that would enable earlier detection of disease than is currently possible. RNA is a particularly attractive target in this regard, as the ability to amplify specific transcripts with PCR will improve detection sensitivity beyond what is possible with protein- or lipid-based metrics.

3. Determine the impact of AML exosomes on HSPC and marrow stroma

It has been established in many model systems that exosomes can be taken up by nearby cells of diverse types, wherein exosomal mRNA and miRNA

is biologically active. The regulatory role of miRNA is of particular interest, as its small size and target diversity potentially allow for signals of greater regulatory potency in smaller physical space. I will determine whether AML-secreted exosomes are taken up by neighboring cells within the marrow, specifically HSPC and mesenchymal stromal cells. Upon identifying recipient cells of AML exosomes, I will determine whether these vesicles play a role in the suppression of hematopoiesis, either directly through action on HSPC, or indirectly through conditioning of marrow stroma.

CHAPTER 2: AML Vesicle Biogenesis and Trafficking

Compiled from Huan, *et al.*, Cancer Research, 2013, and Huan, *et al.*, in preparation.

Abstract

Extracellular vesicles are known to be produced by many human malignancies, including acute myeloid leukemia, although information about the content and pathophysiological role of these vesicles is lacking. In the experiments described in this chapter, I evaluate the extracellular vesicles produced by AML blasts, their RNA content, and their uptake by other cells of the leukemic microenvironment. Examining these vesicles in multiple ways, I demonstrate that they consist predominantly of exosomes, containing concentrated and selected microRNA cargo. These primarily mature microRNA include both species implicated in hematopoiesis and AML and others about which little has yet been discovered. Through direct observation and subsequent molecular assays, I demonstrate that these exosomes are taken up into multiple cell types within the hematopoietic niche, delivering miRNA cargo to HSPC and stromal cells. In a set of experiments dovetailing with exosome characterization, I determine the contributions of the low oxygen tension within the marrow to the biology of exosome trafficking within the microenvironment. In total, this work demonstrates the exosomal trafficking by AML of select miRNA within the hematopoietic niche.

Introduction

In many patients with acute myeloid leukemia, disease-driven morbidity is largely the result of the erosion of physiologic hematopoiesis, rather than a direct consequence of the presence of malignant blasts. This effect was long believed to be the result of overcrowding of the bone marrow; too great a physical mass of

leukemia was thought to create an environment lacking sufficient physical space for the production of homeostatic blood cells¹⁵. This hypothesis, however, fails to account for AML patients with normocellular marrow, or a low percentage of blasts in the marrow, who still suffer from cytopenias characteristic of impaired hematopoiesis^{22,23}.

The recently discovered secretion of extracellular vesicles by AML blasts provides fertile ground for the exploration of alternative hypotheses. Carriers of messenger and microRNA as well as proteins⁵⁷, these nanoscale, membrane-enclosed particles equilibrate across body compartments, and are capable of transporting biologically active molecules to recipient cells within the local microenvironment as well as to distant parts of the body⁶⁴⁻⁶⁹. The trafficking of these vesicles could therefore exert many distinct or coordinated effects across a variety of recipient cell types, and their role in AML leukemogenesis, pathophysiology, and progression, if any, remains undefined. The experiments described in this chapter are the results of an investigation into the biogenesis of these vesicles, their content, and their trafficking to the cell of the bone marrow microenvironment.

Results

Previous investigations into extracellular vesicle secretion had used an ultracentrifugation-based approach to isolate vesicles from culture media or patient serum, whereas subsequent work had characterized 'exosomes' specifically as vesicles with particular density (1.13 and 1.19g/mL) and size (30-

100nm) ranges. We therefore undertook an investigation into the populations of extracellular vesicles secreted by AML cells, using the cell lines Molm-14 and HL-60, in addition to primary patient samples. We compared vesicles isolated by ultracentrifugation followed by sucrose gradient (density-based) purification (**Fig. 2.1A**) to those isolated by ultracentrifugation alone (**Fig. 2.1B**) using transmission electron microscopy (TEM), and found that extracellular vesicles were indeed released by these cells in culture, with the addition of the sucrose gradient step yielding a more homogeneous, less concentrated population of vesicles. In order to determine whether these vesicles could be termed 'exosomes' according to the biogenesis proposed for that nomenclature (fusion of late endosomes containing multiple sub-vesicles with the plasma membrane), we used live cell deconvolution microscopy to monitor primary AML blasts in culture after labeling with the nuclear stain Hoechst 33342 and the lipid dye N-(lissamine rhodamine B sulfonyl) phosphatidylethanolamine (NRhPE). NRhPE is endocytosed by cells and concentrated within late endosomes, where it labels exosomes that are then secreted¹⁰². Monitoring blasts stained with this dye in 2.5-minute intervals, we observed fusion of labeled subcellular compartments with the plasma membrane, and, subsequently, labeled extracellular vesicles (**Fig. 2.1C**), supporting the hypothesis that extracellular vesicles secreted by AML include exosomes. Comparing the size distribution of vesicles isolated with and without sucrose gradient purification using transmission electron microscopy (TEM) and dynamic light scattering (DLS), we identified vesicles of similar sizes using both preparation methods, although preparations without a density selection step were

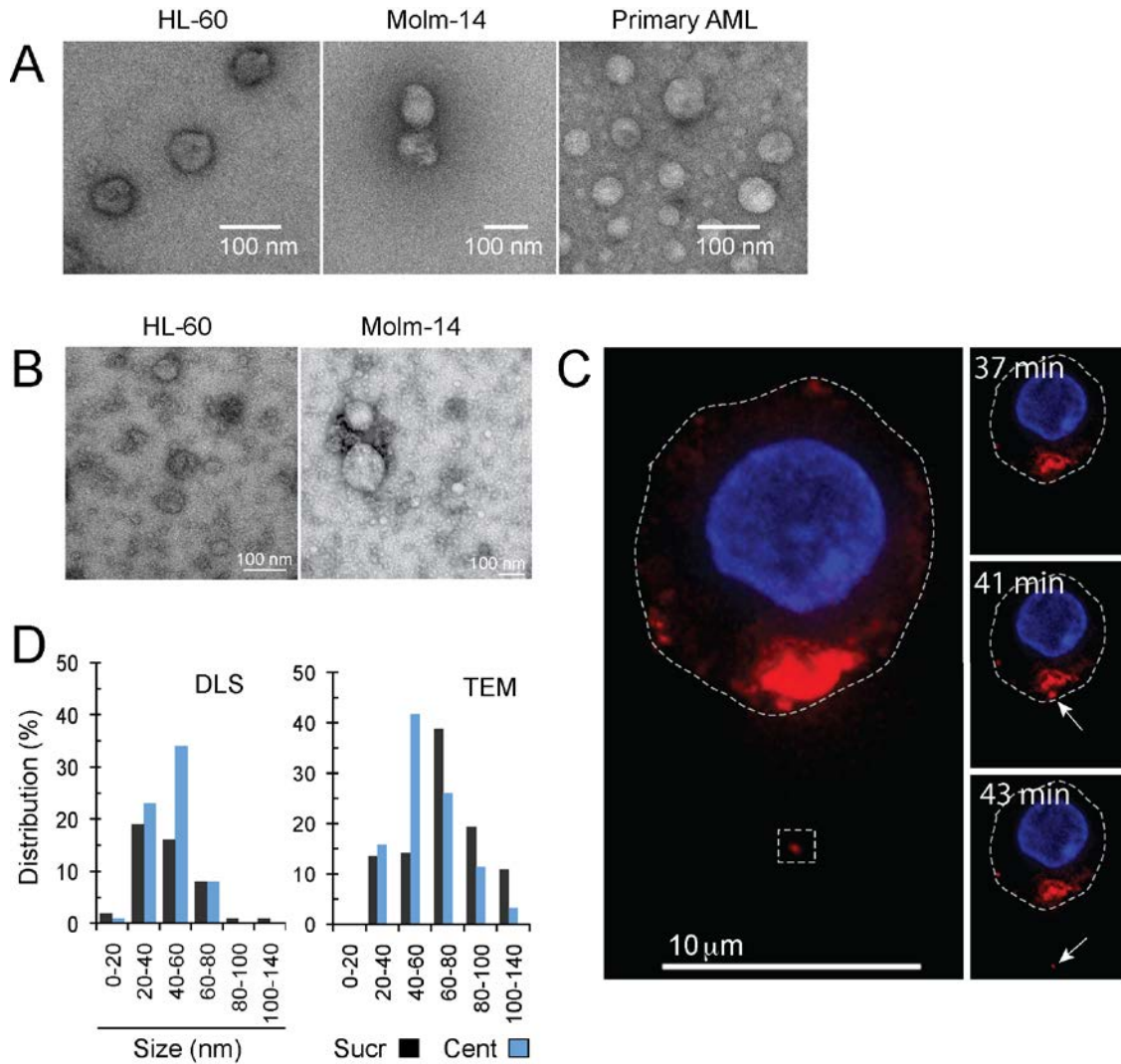


Figure 2.1: Exosome Release by AML Blasts

(A) Vesicles isolated from HL-60, Molm-14, and primary AML cells using sucrose gradient centrifugation, visualized by TEM. Scale bars: 100 nm. (B) Vesicles isolated from HL-60 and Molm-14 cells using ultracentrifugation without density isolation, visualized by TEM. Scale bars: 100nm. (C) Left: Projection image (merged z-stack) of primary cell stained with Hoechst 33342 (blue) and NRhPE (red). Right: z-plane captured every 2.5 minutes. Dotted line: cell margin; arrows: MVB and subsequent extracellular vesicle. (D) Comparison of size distribution of vesicles from sucrose gradient ('Sucr') and differential centrifugation ('Cent') analyzed by dynamic light scattering (DLS) and TEM.

somewhat broader in distribution (**Fig. 2.1D**). Based upon the loss of sample incurred during gradient preparation and our preference for a more inclusive set of extracellular vesicles, we chose to utilize the ultracentrifugation protocol (without additional density gradient purification) for our subsequent

experimentation. Similarly, because AML-derived vesicles are primarily 'exosomes' as defined narrowly (density between 1.13 and 1.19g/mL, endocytic origin), and because our chosen preparatory method includes 'exosomes' as defined broadly (extracellular vesicles with potential biological effects), I have adopted the term 'exosomes' for describing AML-derived extracellular vesicles.

In order to begin to determine the bioregulatory potential of exosome trafficking within the marrow niche, we investigated the RNA content of AML-derived exosomes. Our initial investigations focused on RNA content rather than other classes of macromolecule due to the increased potential for phenotypic alteration in the recipient cell; each transferred molecule of mRNA has the potential to produce many copies of its encoded protein, and each transferred molecule of miRNA can potentially suppress the translation of many mRNA transcripts. Quantifying total RNA in exosome preparations from primary AML blasts and cell lines as well as nonmalignant human CD34+ hematopoietic cells (**Fig. 2.2A**) revealed that all of these cell types secrete substantial (and roughly comparable) amounts of exosomal RNA in culture. As hypoxia has been reported to increase exosome secretion in breast cancer cells¹⁰³, and the bone marrow represents a hypoxic environment relative to standard tissue culture conditions³⁰, we investigated whether hypoxic conditioning would similarly affect AML blasts. After seven passages in culture at 1% O₂, we prepared exosomes from HL-60 and Molm-14 cells, comparing the RNA yields to the same cells

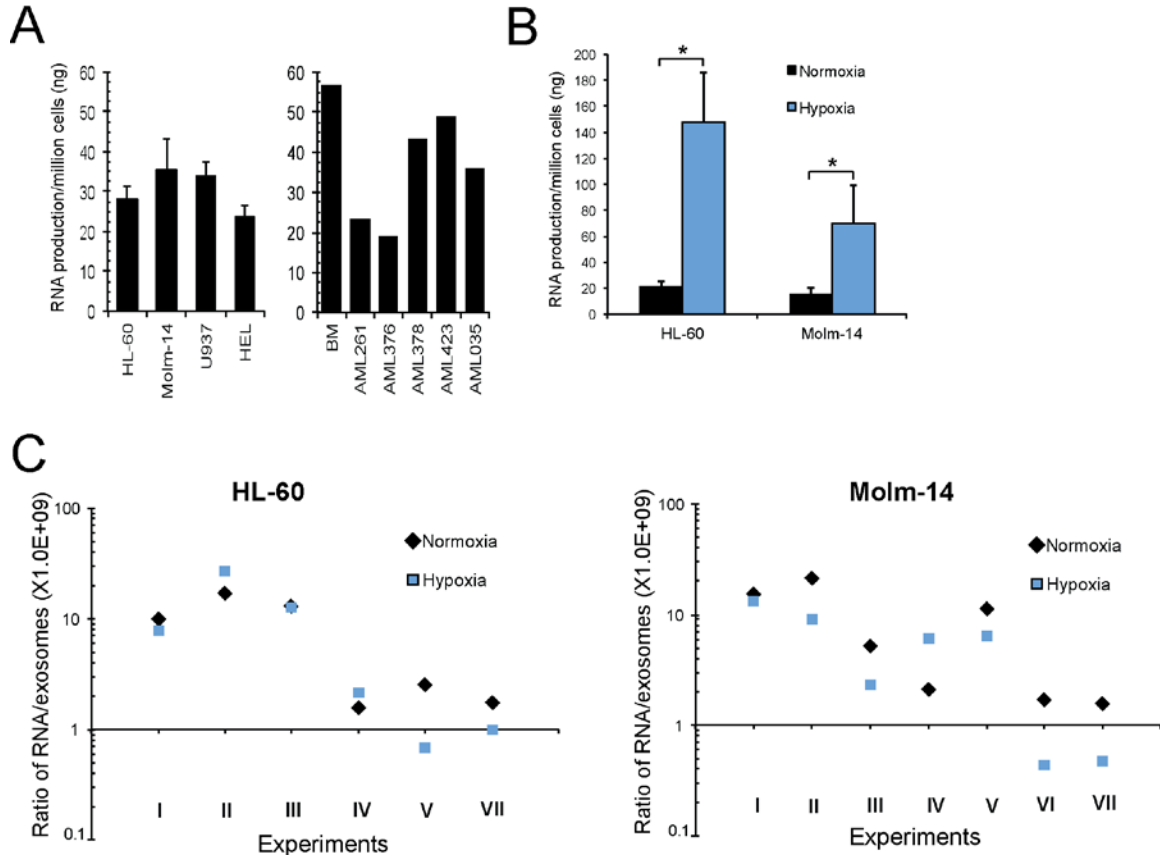


Figure 2.2: Total RNA Content of AML Exosomes

(A) RNA isolated from exosomes collected from cultures of HL-60, Molm-14, U937, nonmalignant CD34+ human hematopoietic (BM), and primary AML cells was quantified using spectrophotometry. (B) RNA yields of exosome preps generated from HL-60 and Molm-14 cells cultured at 21% (normoxia) and 1% (hypoxia) O₂, per million producing cells. *, *p*<0.05. (C) Comparison of the amount of RNA packaged (ng / billion exosomes) in exosomes produced under normoxic and hypoxic conditions.

grown under standard tissue culture conditions (21% O₂). In both cell lines, hypoxia dramatically increased the release of exosomal RNA (**Fig. 2.2B**). We then used nanoparticle tracking analysis (NTA) to determine whether this increase in RNA secretion represented an increase in the number of exosomes, or an increase in RNA packaging per exosome. Although there was substantial variability between experiments in the ratio of exosomal RNA to number of exosomes released, there was no difference between packaging under normoxic

versus hypoxic conditions (**Fig. 2.2C**), indicating that hypoxia increases AML exosome secretion without changing the amount of RNA packaged per exosome.

We next examined the size profile of AML exosomal RNA using a bioanalyzer, in order to roughly quantify the different types of RNA packaged into these vesicles. When comparing RNA profiles of primary or cell line AML cells and exosomes, there was a clear concentration of small RNA inside exosomes secreted by these cells (**Fig. 2.3A**), indicating a greater potential for transfer of miRNA than for the transfer of larger mRNA species. We therefore sought to capture a picture of the miRNA contained within AML exosomes, as a potentially rich source of regulatory content. By conducting a microarray characterization of Molm-14 cell and exosome miRNA under both normoxic and hypoxic conditions, we were able to describe in broad strokes the microRNA packaged into exosomes by AML, and to determine whether the packaging of particular miRNA was dependent upon oxygen status in the producing cell. We found that the vast majority of miRNA in exosomes, as in the producing cells, was mature (as compared to the originating pre-miRNA hairpins) under both normoxic and hypoxic conditions (**Fig. 2.3B**). This finding was true not only generally, but also of specific candidate miRNA with established relevance to leukemia or hematopoiesis (**Fig. 2.3C**). We next pursued comparisons of specific miRNA content of cells and exosomes as it relates to oxygen status. In comparisons of exosomal miRNA in hypoxia and normoxia (**Fig. 2.3D**), along with cellular miRNA under the same conditions (**Fig. 2.3E**), we found that the vast majority of miRNA

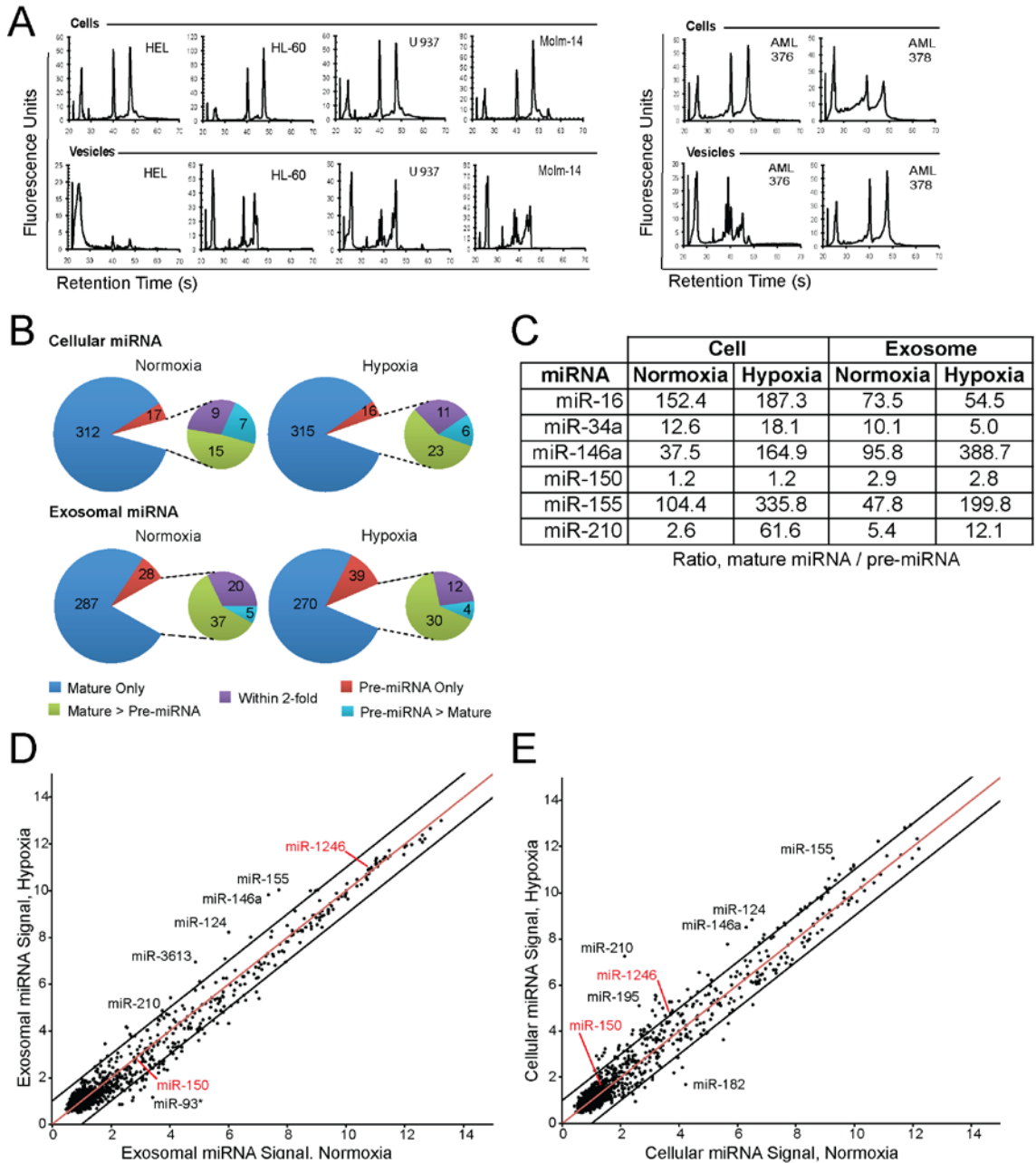


Figure 2.3: AML Blasts Concentrate Mature MicroRNA in Exosomes

(A) RNA isolated from exosomes and cells of AML cell lines (left) and primary samples (right) were analyzed using a bioanalyzer. (B) MicroRNA from Molm-14 cells and exosomes, cultured in normoxic (21%) and hypoxic (1%) conditions, were analyzed using an Affymetrix microRNA microarray. Signals for all detected human miRNA and their originating pre-miRNA hairpins were compared in each condition, and the miRNA species were categorized based on whether the preponderance of signal was detected from mature or pre-miRNA. (C) Ratio of pre versus mature miRNA for selected literature candidate miRNA, based on the microarray data. (D, E) Comparison of hypoxia versus normoxia levels of miRNA in exosomes (D) and cells (E). The heavy black lines indicate 2-fold change between oxygenation conditions.

in cells and exosomes were essentially unaltered by hypoxia, with certain interesting exceptions. Several miRNA with established relevance to AML, including miR-124¹⁰⁴, miR-146a¹⁰⁵, and miR-155¹⁰⁶ were present in increased amounts in both cells and exosomes cultured under hypoxic conditions, underscoring the relevance of microenvironmental conditions to AML exosome biology.

Expanding the scope of our characterization of exosomal miRNA, we conducted additional microarray experiments, this time comparing Molm-14 cellular and exosomal miRNA to that of the HL-60 AML cell line, nonmalignant human CD34+ cells, and their exosomes. Comparing all miRNA common to all samples using principal component analysis, we found that separation along the axes of the two first principal components was by cell *versus* exosome, and then by AML *versus* nonmalignant (**Fig. 2.4A**). A closer look at the 14 most enriched / most excluded miRNA in exosomes revealed that although many excluded miRNA had established roles in leukemia¹⁰⁷⁻¹⁰⁹, the most enriched targets were largely unstudied (**Fig. 2.4B**). As we considered this a potentially exciting finding for further study, we validated several of the enriched targets with known hematopoietic or leukemic function along with miR-1246, one of the most consistently upregulated targets in leukemic exosomes as compared to producing cells or nonmalignant exosomes, using qRT-PCR (**Fig. 2.4C**). This assay, normalized to U6 snRNA, revealed substantial enrichment of these targets in AML exosomes, up to several thousand fold in the case of miR-1246.

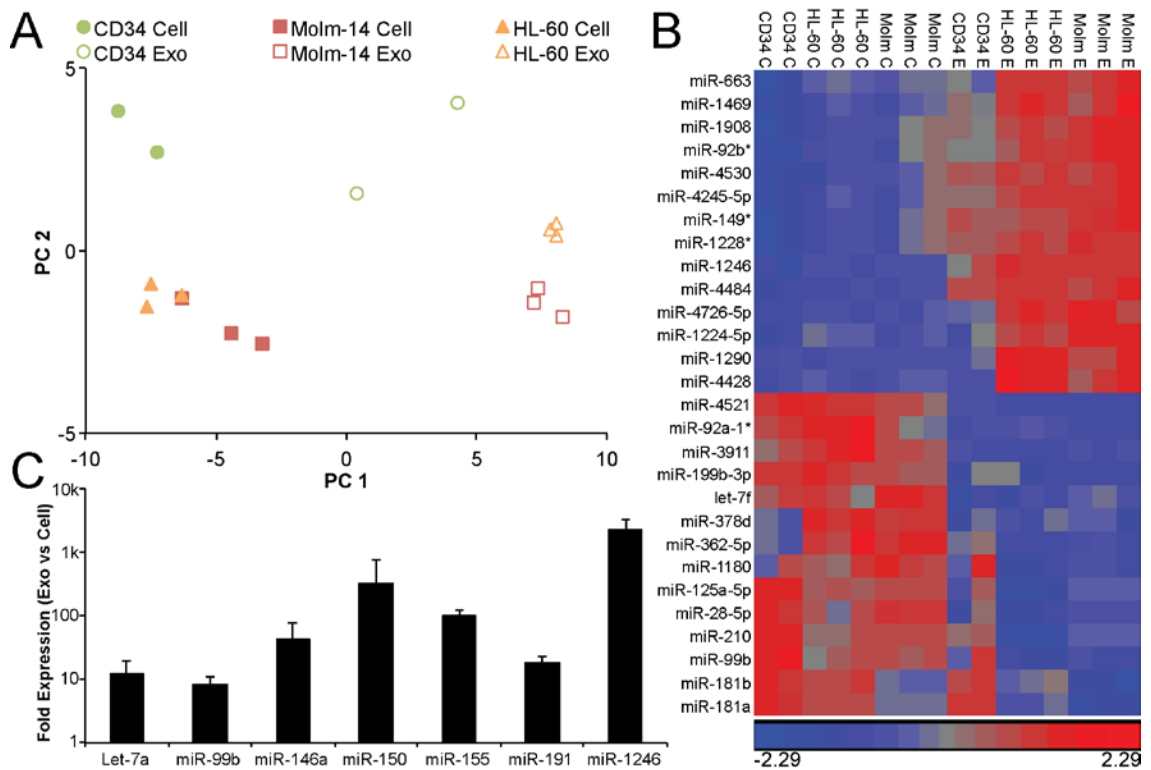


Figure 2.4: Exosomes Contain Distinct Selected MicroRNA

Microarray surveys of miRNA expression were conducted on Molm-14, HL-60, and normal human CD34+ cells and exosomes. **(A)** Principal component analysis was performed following gene selection for all (63) targets both demonstrating significant (FDR < 0.05) difference in level between leukemic cell and exosome samples and uniform detection in all samples. X-axis, first principal component; Y-axis, second principal component. **(B)** Heat map depicting expression of those miRNA with the greatest difference in expression between cells and exosomes. **(C)** qRT-PCR validation of specific miRNA targets in Molm-14 cells versus exosomes, normalized to U6 snRNA. Microarray data shown are from three biological replicates (for AML lines) from two experiments, CD34+ microarray data is two pilot samples shown for descriptive comparison; qRT-PCR data represents at least three independent experiments per target. The log₂ transformed signal intensity data shown in the heat map is standardized to have a mean of 0 and standard deviation of 1.

Having demonstrated that exosomes containing microRNA are secreted into the microenvironment by AML blasts, we next investigated whether these vesicles were trafficked to other cells within the marrow niche. Although exosome uptake has been demonstrated in a wide variety of cell types, the internalization of these vesicles in the cells of the marrow has not yet been shown. In order to focus on uptake in stromal cells, we made use of the well-

established murine stromal cell line OP9¹¹⁰, which we transduced to express green fluorescent protein (GFP). These cells were exposed to exosomes that were isolated from HL-60 cells in culture and subsequently stained with the red fluorescent lipid dye PKH-26. On imaging using deconvolution microscopy, we were able to clearly see internalized exosomes within the cytoplasm of the recipient cells (**Fig. 2.5 A,B**). As it was possible for crystallized PKH-26 to be coprecipitated with the labeled exosomes, we quantified fluorescent events in exosome-exposed cells compared to those treated with PKH-26-labeled diluent, demonstrating that the number of events per cell was well above background in the exosome-treated cells (**Fig. 2.5C**). We also evaluated exosome uptake into HSPC, using primary murine c-kit⁺ cells. These cells were exposed to NRhPE-labeled exosomes produced by Molm-14 cells, a procedure which avoids the possibility of coprecipitating dye particles. Deconvolution microscopy again showed that c-kit⁺/sca-1⁺/lin⁻ cells internalized exosomes (**Fig. 2.5D**). In order to determine whether oxygenation played a role in the uptake process, we grew Molm-14 cells with NRhPE under both hypoxic and normoxic conditions, and collected the exosomes they produced. These exosomes were then placed in culture with 293T cells, again under normoxic or hypoxic conditions, for 3 hours, after which the cells were collected, washed, and analyzed for NRhPE fluorescence by flow cytometry (**Fig. 2.5E**). Although the uptake of exosomes was clearly visible when comparing exosome-treated cells to untreated controls, oxygenation status of the donor or recipient cells made no difference in exosome internalization. As an initial indication of miRNA content transfer between AML

and recipient cells, we isolated c-kit⁺ cells from murine marrow and exposed them to exosomes secreted by HL-60 or Molm-14 cells (**Fig. 2.5F**). After exposure to exosomes, c-kit⁺ cells exhibited a substantial (3-8 fold) increase in their levels of the exosomally-enriched miR-155, as normalized to U6 snRNA. Although increased endogenous expression cannot be ruled out based on this experiment, such a dramatic change in such a short time frame supports the hypothesis that AML exosomes transfer miR-155 to these HSPC.

Discussion

Failure of hematopoiesis in the context of acute myeloid leukemia is both central to the pathophysiology of this disease and the mediator of a significant clinical problem, yet it remains unexplained. In the absence of an explanation from contact-dependent signaling or cytokines, we must look to other effectors for answers. Exosomes, recently described as carriers of protein and nucleic acids between cells of many types, may represent a promising target for investigation in this regard.

In these experiments, we establish that AML blasts secrete extracellular vesicles, the primary constituents of which are exosomes. These exosomes carry a selected set of miRNA, processed and ready to impact translation, that is distinct from the exosomal miRNA output of nonmalignant progenitors. Many of these miRNA are of established prognostic significance in AML, and some have been shown to cause myelodysplasia when overexpressed^{111,112}. Exosomes carry this

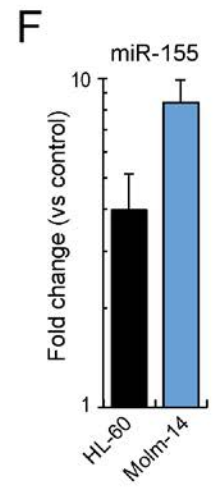
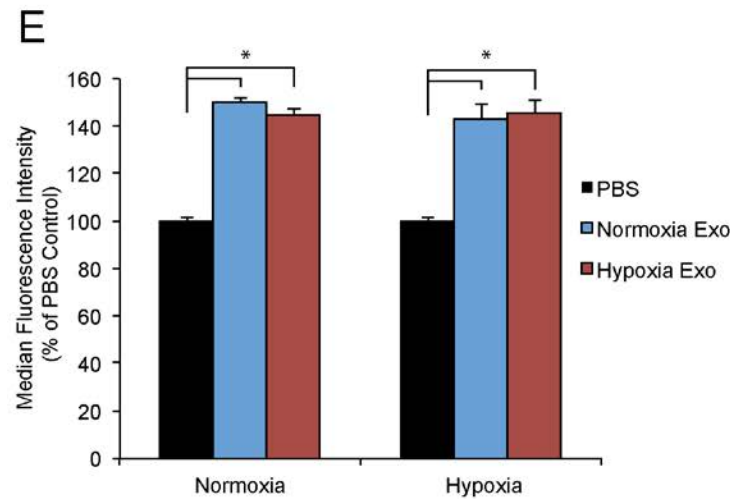
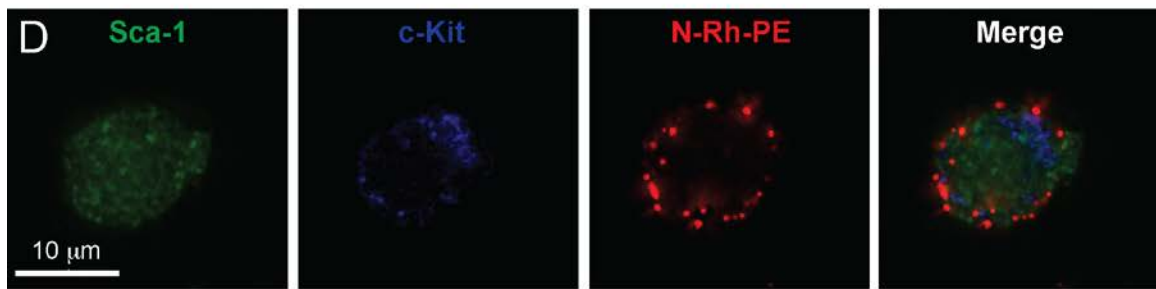
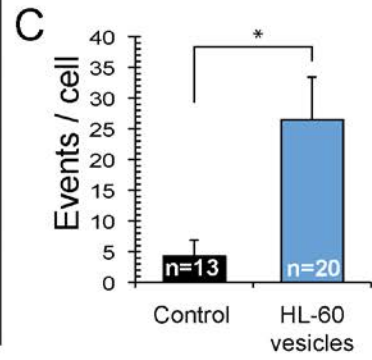
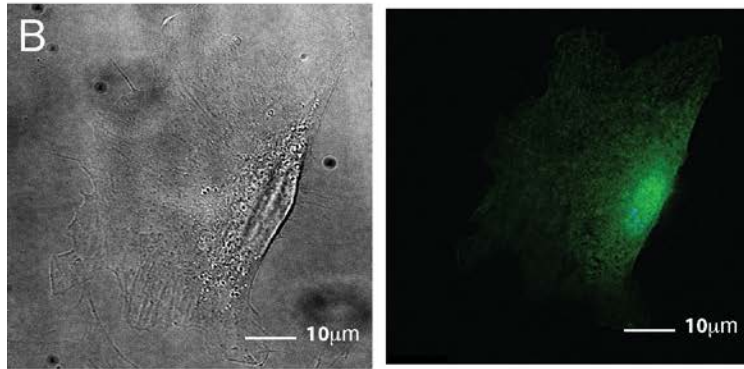
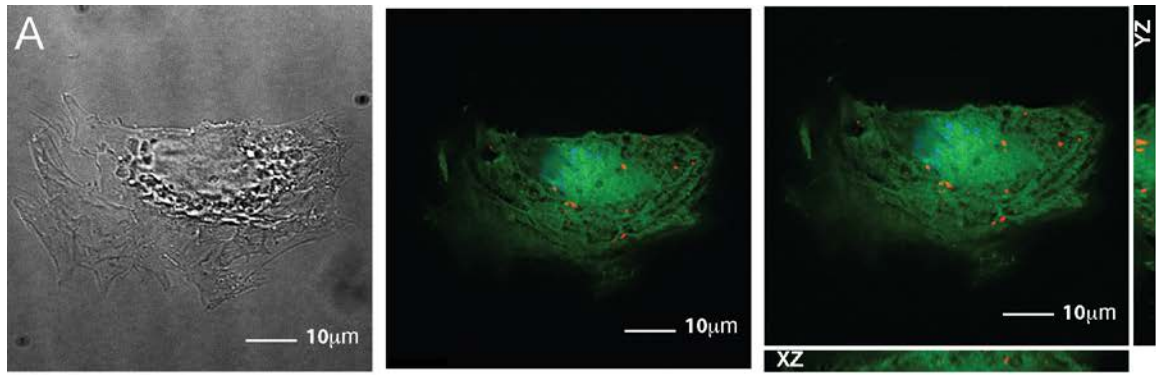


Figure 2.5: AML Exosomes are Internalized by Neighboring Cells of Multiple Types (A,B) PGK-GFP OP9 cells were exposed to PKH-26-labeled HL-60 exosomes (A) and PKH-26-labeled Diluent C (B) for 2 hrs. Images in (A): DIC, single z-slice showing labeled exosomes (red), and Z-stack in the xy-, xz-, and yz- planes. In (B): DIC, single z-slice. Scale bars: 10µm. (C) Quantification of labeled exosomes within cells. *,P<0.006 by Student's t. (D) Murine c-kit+/sca-1+/lin- cells exposed to NRhPE labeled Molm-14 exosomes for 3h, imaged using deconvolution microscopy. Scale bar: 10 µm. (E) 293T cells (under hypoxia or normoxia) were exposed to NRhPE-labeled Molm-14 exosomes (generated under hypoxia or normoxia) or PBS for 6h, then analyzed by flow cytometry. Results are presented as percent of control median fluorescence intensity. (F) qRT-PCR analysis of miR-155 expression in c-kit+ progenitor cells exposed to HL-60 or Molm-14 exosomes for 3h, normalized to U6 snRNA, presented as fold change vs untreated.

miRNA from AML blasts to recipient HSPC and stromal cells, drastically altering the level of these regulatory molecules in the recipients. Strikingly, several of these processes are accelerated in the context of an oxygen tension similar to that which exists in the physiologic or leukemic bone marrow. In total, these findings suggest the potential for a potent method of paracrine regulation.

It remains to be demonstrated what phenotypic impact AML exosomes have on the HSPC and stroma that internalize them. Although miRNA are a potent class of regulatory molecule, they have diverse targets, and additional experimentation is required to show what impact they exert after delivery in exosomes. In the subsequent chapters of this dissertation, I will address these questions.

Materials & Methods

Cell lines and cell culture

AML cell lines (HEL, HL-60, Molm-14, U937) were provided by Dr. Jeffrey Tyner and cultured in RPMI (Invitrogen) with 10% vesicle-free (VF-) FBS. VF-FBS was produced by centrifugation of FBS (Gemini Bio-Products) at 2,000g for 20 min, at 10,000g for 20 min, and at 100,000g for 2 hrs. AML patient samples were

obtained under OHSU-IRB approved protocol from treatment-naive patients at presentation (no additional selection bias) and >90% enriched for leukemic blasts. Primary cells were cultured in EGM2 (Lonza). OP9 cells, provided by Dr. William H. Fleming, were cultured in α -MEM (Invitrogen) with 20% FBS and 60 μ M 2-mercaptoethanol. Non-stimulated, cryopreserved human CD34+-enriched bone marrow cells (Stem Cell Technologies) were cultured in serum-free expansion media with the StemSpan CC110 cytokine cocktail and expanded for 5~7 days. All cells were cultured with 50 μ g/ml Pen/Strep (Invitrogen). As our cell lines were obtained directly from reliable sources who had recently published work involving these cells, we performed no formal testing or authentication beyond what is demonstrated in the content of the experiments described.

Vesicle preparation and staining

Vesicles were isolated from cell lines and primary AML cells after 48-72 hrs culture via centrifugation at 300g for 10 min. The supernatant was sequentially centrifuged at 2,000g for 20 min, at 10,000g for 20 min, and at 100,000g for 2 hrs. The resulting pellet was washed with PBS and then centrifuged at 100,000g for 2 hrs. For sucrose gradient density purification, the pellet from the first 100,000g spin was resuspended in 200 μ l PBS by shaking for 4 hrs at 4°C. The suspension was transferred to a sucrose step gradient (8%/15%/30%/45%/60%) and centrifuged at 150,000g for 90 min. The 30%/45% interface was harvested and diluted 10-fold with PBS and the ultracentrifugation was repeated. The resulting pellet was resuspended in 200 μ l of PBS.

Transmission electron microscopy

Exosome preparations (10 μ l) were deposited onto UV-activated carbon formvar 400-mesh copper grids (Ted Pella 01822-F) for 3min, rinsed and stained in filtered 1.33% uranyl acetate, and then air-dried. Samples were imaged at 100kV on a Philips CM120 transmission electron microscope, or at 120kV on a FEI Tecna Spirit TEM system. Images were acquired as 2048 \times 2048 pixel, 16-bit gray scale files using the FEI's TEM Imaging & Analysis (TIA) interface on an Eagle 2K CCD multiscan camera. The size distribution of exosomes was determined by averaging the maximum and minimum diameters of at least 100 vesicles imaged at 37,000x magnification.

Fluorescence microscopy

For PKH26 (Sigma) staining, exosomes were isolated with the following changes: following the first 100,000g centrifugation, the pellet was resuspended in 1ml PKH26 membrane dye-diluent C (Sigma) by shaking for 30 min at 4°C, along with a control aliquot containing diluent only. For NRhPE exosome labeling, donor cells (Molm-14) were exposed to 1 mg/mL NRhPE (Avanti Polar Lipids) for 1h at 37°C, then washed twice in PBS before 48-hr culture in RPMI + 10% VF-FBS and subsequent exosome preparation as above. Cells were exposed to 25 μ l of PKH26-stained, sucrose-purified exosomes or PKH26-stained diluent C for 2hrs, followed by wash and fixation in 4% paraformaldehyde (Sigma) before treatment with Fluoromount G (Southern Biotech). Lineage-depleted (lin-) cells were exposed to 30 μ L of NRhPE-stained exosomes overnight, followed by wash

and fixation in 4% paraformaldehyde before treatment with Fluoromount G. Fluorescence microscopy was performed with an Olympus IX71 microscope and DeltaVision SoftWoRx™, using a 60x 1.4NA oil lens. Z-stacks were acquired every 0.2µm for the complete depth of the cells. A reference bright-field image was captured from the center of each Z-stack. Particle quantification was performed using ImarisCell (Bitplane, Inc.). For live-cell imaging, cells were plated on poly-L-lysine (Sigma)-coated chamber wells, treated with 5µg/ml Hoechst 33342 and 2.5µM NRhPE (Avanti Polar Lipids) for 1.5hrs followed by wash and resuspension in RPMI media with 9% horse serum (Invitrogen) and 9% FBS (Gemini Bioproducts). Images were acquired every 2.5 minutes over the course of 2 hrs, at 37°C and 5% CO₂.

Dynamic light scatter (DLS)

Light-scattering experiments were conducted in a DynaPro molecular sizing instrument (Protein Solutions). A sample in PBS buffer was loaded into a quartz cuvette and analyzed with a 488nm laser. Fifty spectra were collected at 25°C to estimate diffusion coefficient and relative polydispersity. Data were analyzed with Dynamics software V.5.25.44 (Protein Solutions) and vesicle size was measured as the mean hydrodynamic radius.

Nanoparticle tracking analysis (NTA)

Exosome samples were resuspended and serial dilutions were prepared in nanofiltered (Whatman Anotop 25, 0.02-µM) molecular-grade water (Thermo Scientific) using low-adhesion 1.7-mL tubes (Genemate). Diluted samples were

loaded into the NanoSight LM10 chamber, the laser engaged, and microparticles visualized. Sixty second videos were acquired with a Hamamatsu C11440 ORCA-Flash 2.8 camera and analyzed by Nanosight NTA 2.3 software. Individual samples were diluted to 1×10^8 - 1×10^9 particles/mL.

RNA analysis, cDNA synthesis, and qRT-PCR

RNA was extracted using miRNeasy (Qiagen) or RNeasy (Qiagen) kits and quantified using a Nanodrop 2000c. RNA integrity was measured using the Agilent Bioanalyzer 'Pico Chip' or 'small RNA Chip' (Agilent). For miRNA quantitation, Taqman assay kits (Applied Biosystems) were used for both reverse transcription and qRT-PCR, normalized to U6 snRNA.

Microarrays

Microarray assays were performed in the OHSU Gene Profiling Shared Resource. For each sample, 130 ng of total RNA was labeled using the Flash-Tag Biotin HSR miRNA Labeling Kit (Affymetrix) by polyadenylation and ligation with biotinylated 3'DNA dendrimers. Labeled RNA was mixed with hybridization controls and incubated overnight with the GeneChip miRNA 3.0 array (Affymetrix) as per manufacturer recommendations. Arrays were scanned using the GeneChip Scanner 3000 7G with autoloader (Affymetrix). Image processing was performed using Affymetrix GeneChip Command Console software followed by analysis with Expression Console software (Affymetrix). Array performance and general data quality were assessed using Signal All, mean background intensity, number of detected probe sets, % P, all probe set mean, all probe set

standard deviation, all probe set RLE mean, and % species specific small RNA probe sets detected. All arrays passed standard performance quality thresholds.

Microarray statistical analysis and data visualization

Individual array data (.cel files) were uploaded to R software package and analyzed using Bioconductor's Oligo package. Normalization was conducted on all samples in a single set using RMA Background and Quantile Normalization sub-routine. Signal intensities were log₂ transformed and probe set values summarized using Median Polish Summarization Method. Final data set included paired samples from exosome and cell samples. Further analysis included 3391 mature and pre-mature human miRNA probe sets. Data visualization tools (e.g., box plot, hierarchical clustering, matrix plots and multi-dimensional scaling) were used to assess general data quality and outliers. To determine differentially expressed miRNA genes, the mixed model was used to assess differences in miRNA probe expression between exosome samples and cell samples. Unadjusted statistical significance was set at $p \leq 0.05$ with FDR correction at $p \leq 0.05$ for multiple testing where relevant. Fold change values of 2.0 were used as a cut-off to identify up- and down-regulated probes.

Normalized log₂ transformed signal data for all human mature miRNAs were imported into Partek Genomics Suite 6.6 software and filtered to include only miRNA signal data of interest prior to generating individual heat maps. The Tools Discover Hierarchical Clustering subroutine was invoked to create each

clustered heat map. Samples and miRNA were clustered using Pearson's Dissimilarity as the measure of distance with complete linkage.

For principal component analysis, normalized log₂ transformed signal data was imported into R following gene selection performed based upon significant differences between leukemic cell and exosome samples as described above. This data was used to generate principal component values, which were then exported to Microsoft Excel for visualization.

Flow cytometry analysis

For NRhPE exosome uptake, NRhPE-stained exosomes were collected as described above. 1×10^5 HEK-293T cells were exposed to 30 μ L of exosomes or PBS x 6h at 37°C, washed twice, propidium iodide (PI) was added and cells analyzed with a FACSCalibur (BD Biosciences). Data was analyzed using FlowJo software (Tree Star).

CHAPTER 3: Exosome Impact on the Marrow Niche

Compiled from Huan, *et al.*, Cancer Research, 2013, and Huan, *et al.*, in preparation.

Abstract

Having established in the experiments detailed in Chapter 2 that AML-secreted exosomes carry concentrated, select microRNA cargo to both neighboring stroma as well as to residual HSPC within the marrow, I next focused on the consequences of this transfer. In the experiments described in this chapter, I demonstrate that exposure to AML exosomes profoundly alters the hematopoietic microenvironment. Stromal cells are durably altered after exposure to exosomes, impairing HSPC retention and support. Additionally, HSPC themselves are directly impaired by AML exosome exposure, exhibiting a loss of clonogenicity, a decreased ability to home to chemoattractants, and derangement of key transcription factors. These defects are evident both after *in vitro* and *in vivo* treatment with purified exosomes as well as after coculture or xenograft with AML blasts. The data presented herein strongly supports a role for exosome trafficking in leukemic progression as well as the concomitant failure of hematopoiesis.

Introduction

The inception and expansion of a nascent leukemia has been shown to produce a variety of alterations in numerous cell types within the marrow niche⁴². Many of these changes have to date not been adequately explained. Although direct cell contact-based and cytokine-mediated signaling may contribute, these methods are restricted based on the presence of specific protein receptors on the surface of downstream cells. These signaling paradigms therefore require active participation on the part of the recipient, limiting the range of messages that can

be delivered. Exosome trafficking allows for a total subversion of these restrictions. As there are currently no known protein or cell type-specific requirements for exosome entry¹¹³, and as exosomes have been shown to be taken up by essentially every cell type studied to date, these particles allow for direct, nonspecific delivery of nucleic acid or protein messages to the cytoplasm irrespective of recipient cell phenotype. This allows for the delivery of receptors, changing what signals a cell can respond to, or bypassing traditional signaling molecules altogether, through the direct delivery of downstream proteins or regulatory transcripts. Because of this broad applicability, and based upon the demonstrated entry of AML-derived exosomes into both HSPC and stroma of the marrow niche, our next set of experiments focused on the effects exosome delivery exerts on the disparate cell types receiving these messages. As the delivered message could take the form of essentially any molecular component or activity, we focused on phenotypic changes with direct applicability to the downstream defect under investigation (*i.e.*, hematopoietic suppression) as well as on the expression of transcripts with known capacity to effect these changes.

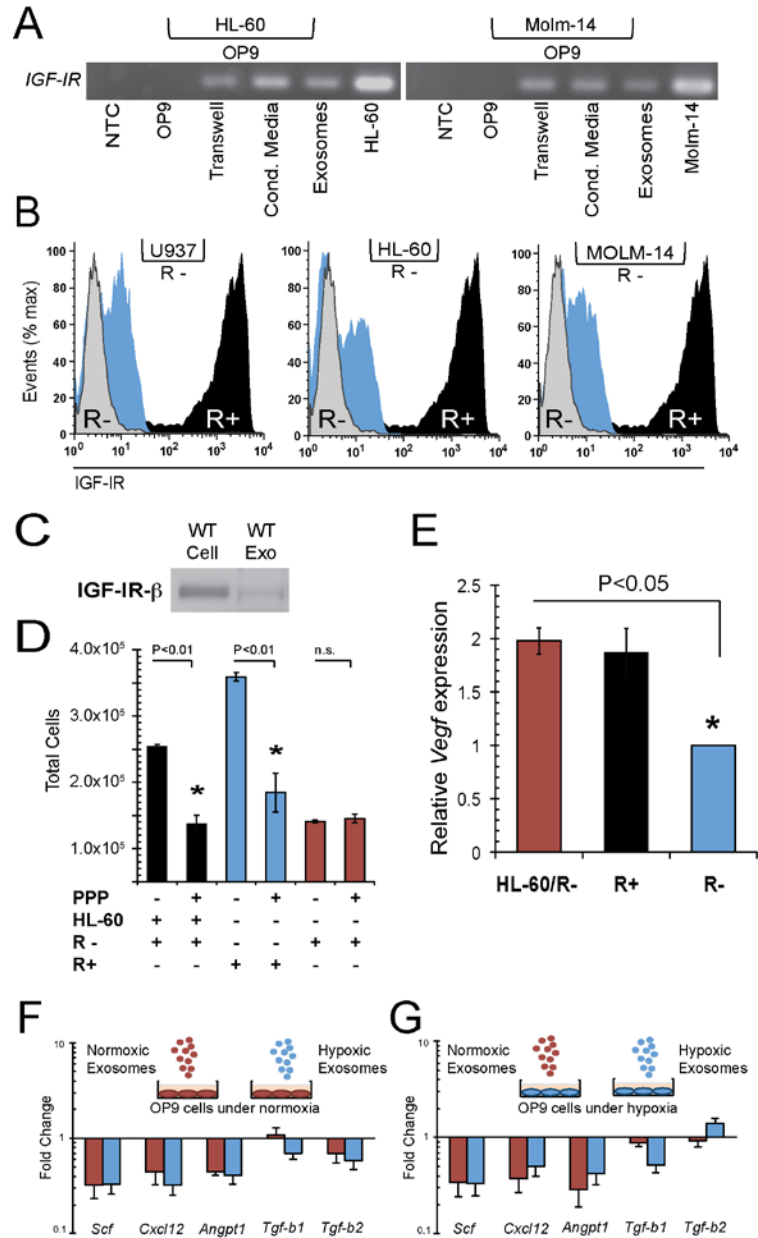
Results

Although division of HSPC is the source of mature blood cell lineages, physiologic hematopoiesis requires the support of many other cell types within the marrow. As exosomal signaling or uptake has no known cell or tissue restriction¹¹³, and as we had observed *in vitro* the entry of these vesicles into both HSPC and stroma (**Fig. 2.5**), we pursued the separate effects of AML exosomes on each cell type in order to explore the impact this communication

process has on the leukemic niche as a whole. Beginning with murine OP9 stromal cells as recipients, we evaluated the transfer of RNA between AML and stroma using three exposure modalities: coculture of AML and OP9 separated by a 0.4 μ m-pore transwell, treatment of cultured OP9 with conditioned media from AML blasts, and treatment of OP9 with purified AML exosomes. In each of these conditions, transfer of human *IGF-IR* by both Molm-14 and HL-60 was readily detected by RT-PCR (**Fig. 3.1A**). We next made use of murine embryonic fibroblasts (MEFs) from IGF-IR knockout (R-) mice in order to evaluate the viability of transferred *IGF-IR* mRNA. After coculture with any of three AML cell lines (Molm-14 and HL-60 in addition to U937), R- MEFs exhibited clear surface expression of IGF-IR, although not at the same level as the same cells stably overexpressing this protein (R+) (**Fig. 3.1B**). While exosomal transfer of protein is not excluded by this experiment, Western blot demonstrated only minimal exosome IGF-IR protein content, even when 3x greater protein was loaded as compared to the cellular fraction (**Fig. 3.1C**), suggesting that transfer of *IGF-IR* mRNA is responsible for this effect. As IGF-IR signaling promotes cell division, we evaluated proliferation of MEFs in the presence or absence of IGF-IR signaling, manipulated by HL-60 coculture, IGF-IR knockout or overexpression, and the presence or absence of the specific IGF-IR inhibitor picropodophyllin (PPP). R- MEFs proliferated more rapidly in the presence of

Figure 3.1: Molecular Impact of AML Exosomes on Stroma

(A) RT-PCR for human *IGF-IR* in murine OP9 after 48h 0.4µm transwell coculture or exposure to conditioned media or purified exosomes from HL-60 or Molm-14. (B) Flow cytometry analysis of IGF-IR knockout (R-) MEFs with or without 48h of transwell coculture with U937, HL-60, or Molm-14 AML cell lines, or IGF-IR overexpressing (R+) MEFs. (C) Western blot for IGF-IRβ on 10µg cellular and 30µg exosomal protein from HL-60. (D) Proliferation of R- or R+ MEFs after coculture with HL-60s or IGF-IR inhibitor PPP. Cells were grown alone or in transwell coculture in the presence or absence of PPP for 48 hours. (E) Relative expression of *Vegf* in R+ MEFs or R- MEFs cocultured with HL-60 for 12h, compared to R- MEFs alone. (F, G) The stromal regulatory gene profile in OP9 under normoxia (red bar) or hypoxia (blue bar) after exposure to exosomes or ECM from Molm-14 cultured under normoxia (F) or hypoxia (G) was evaluated by qRT-PCR normalized to GAPDH.



IGF-IR signaling provided endogenously (by stable overexpression) or exogenously (by HL-60 coculture), a response that was eliminated by coadministration of PPP (Fig. 3.1D). We also investigated the expression of *Vegf* (a downstream target of IGF-IR signaling), and found that coculture with HL-60 produced an increase in *Vegf* mRNA in recipient R- MEFs equivalent to that measured in R+ MEFs (Fig. 3.1E). In aggregate, these results support the

exosomal transfer of functional mRNA between AML blasts and marrow stroma, and its subsequent translation. In order to examine other targets of relevance to the stroma's ability to support hematopoiesis, we performed qRT-PCR for *Scf*, *Cxcl12*, *Angpt1*, *Tgf-β1*, and *Tgf-β2* on OP9 exposed to Molm-14 exosomes. We further sought to determine whether hypoxia played a role in any such change, either in the exosome-producing Molm-14 or in the recipient OP9. While *Scf*, *Cxcl12*, and *Angpt1* were indeed decreased as much as 70% after treatment with AML exosomes, *Tgf-β1* and *Tgf-β2* were unaffected, with hypoxia playing little apparent role (**Fig. 3.1F**). Still, the combination of an increase in IGF-IR signaling seen in MEF along with decreased expression of *Scf*, *Cxcl12*, and *Angpt1* in OP-9 produces a set of influences with the potential to proliferate stroma with decreased capacity for HSPC support.

We next sought to determine whether AML-derived exosomes exert direct effects on HSPC in the marrow compartment, in addition to the changes seen in the stroma. Intrigued by the suppression of *Cxcl12* expression seen in stromal cells, we first evaluated its receptor, CXCR4, in lineage-depleted (Lin-) murine bone marrow cells from NOD/SCID/IL-2 γ ^{null} (NSG) mice. We found that these cells had suppressed surface expression of CXCR4 by flow cytometry, along with a decreased ability to migrate across a CXCL12 gradient (**Fig. 3.2A**) after exposure to Molm-14-derived exosomes. In concert with a decrease in stromal CXCL12, such a deficit would interfere with HSPC homing to and retention in the

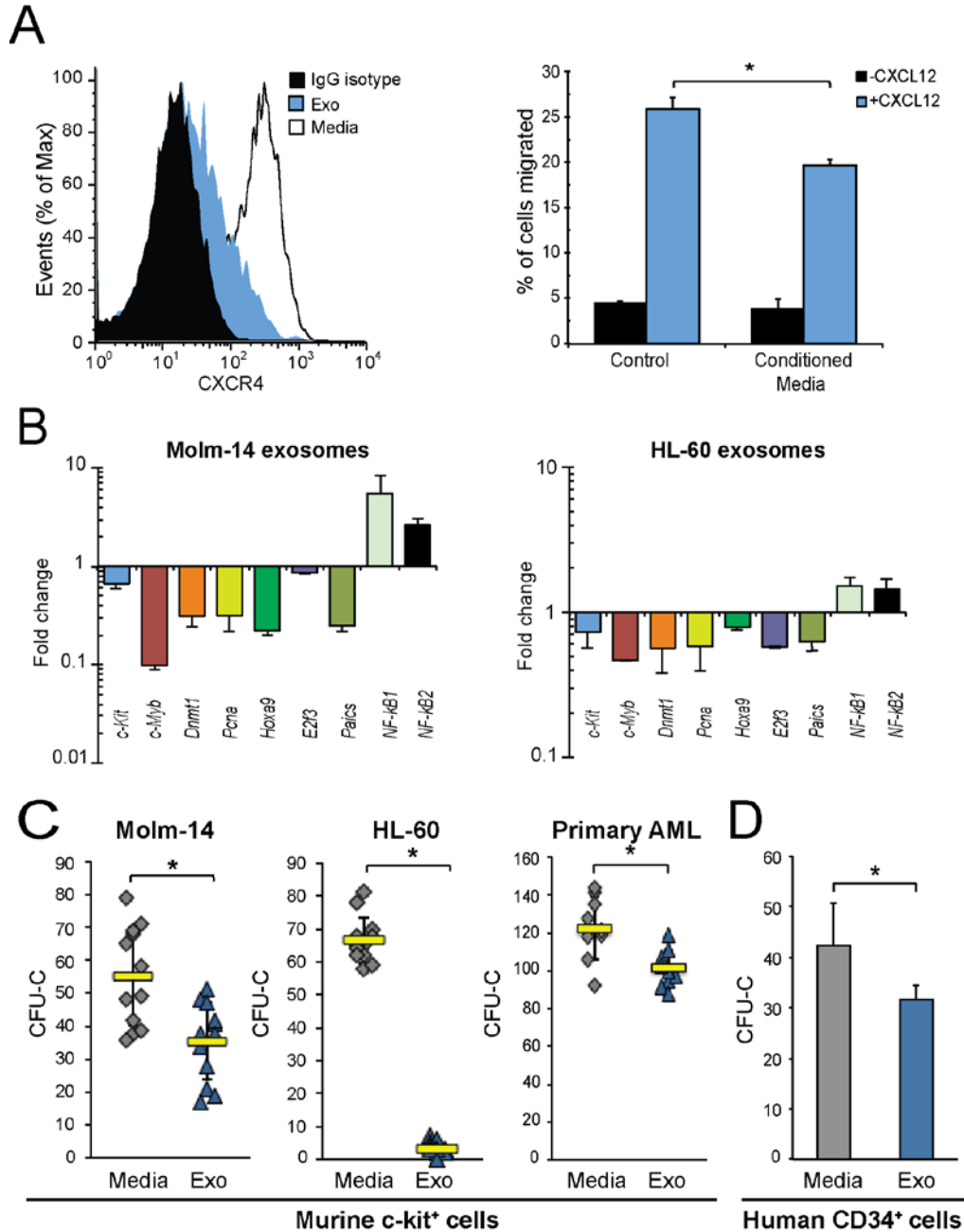


Figure 3.2: AML Exosomes Compromise HSPC Function *In Vitro*

(A) CXCR4 in lineage-depleted, AML exosome-exposed marrow cells. (Left) Lin⁻ cells from NSG marrow were exposed to Molm-14 exosomes (Exo) or media alone (Media) for 24 hours, after which they were assayed for surface CXCR4 by flow cytometry. (Right) Lin⁻ cells were cultured in Molm-14 conditioned or control media for 24 hours, after which they were exposed to a CXCL12 gradient across an 8 μ m transwell for 2 hours. (B) RNA was isolated from c-Kit⁺ NSG marrow cells and exposed to exosomes from Molm-14 (left) or HL-60 (right) cells, then subjected to qRT-PCR for the indicated transcripts, normalized to GAPDH. (C) CFU-C performed on c-Kit⁺ NSG marrow cells after exposure to exosomes from Molm-14, HL-60, or primary human AML cells, or to media control for 48h. (D) CFU-C performed on human cord blood-derived CD34⁺ cells after exposure to Molm-14 exosomes or media control for 48 hours.

marrow niche. Expanding our investigation of exosomal impact on HSPC, we evaluated the expression of a panel of hematopoietic transcription factors and regulatory genes (*c-Kit*, *c-Myb*, *Dnmt1*, *Pcna*, *Hoxa9*, *E2F3*, *Paics*, *Nf-κB1*, and *Nf-κB2*)¹¹⁴⁻¹¹⁹ in *c-Kit*⁺ murine cells exposed to exosomes from Molm-14 or HL-60 for 48 hours. While changes in expression varied from gene to gene, and Molm-14 exosomes produced larger changes than HL-60 exosomes, the HSPC exhibited consistent downregulation of *c-Myb* (50-90%), as well as *Dnmt1* and *Pcna* (40-70%). To determine whether these changes were able to cause a phenotypic alteration in recipient HSPC, we plated exosome-exposed *c-Kit*⁺ cells in methylcellulose for a colony forming unit in culture (CFU-C) assay. Treated cells had reduced capacity for colony formation, most strikingly in those treated with HL-60 exosomes, although both Molm-14 and primary AML blasts were also able to cause significant suppression (**Fig. 3.2C**). This effect was not exclusive to murine HSPC; exposing human cord blood-derived CD34⁺ cells to exosomes from Molm-14 produced a similar result (**Fig. 3.2D**). In aggregate, these results indicate that AML-derived exosomes not only suppress stromal support of HSPC, but target both sides of the HSPC-stroma interaction, exerting direct effects on the HSPC themselves.

We next sought to carry these observations into *in vivo* models of AML exosome exposure. Beginning with isolated exosomes, we performed intrafemoral (IF) injections, comparing exosome-injected femurs to media-injected controls (in separate animals). Under these conditions, exosomes were

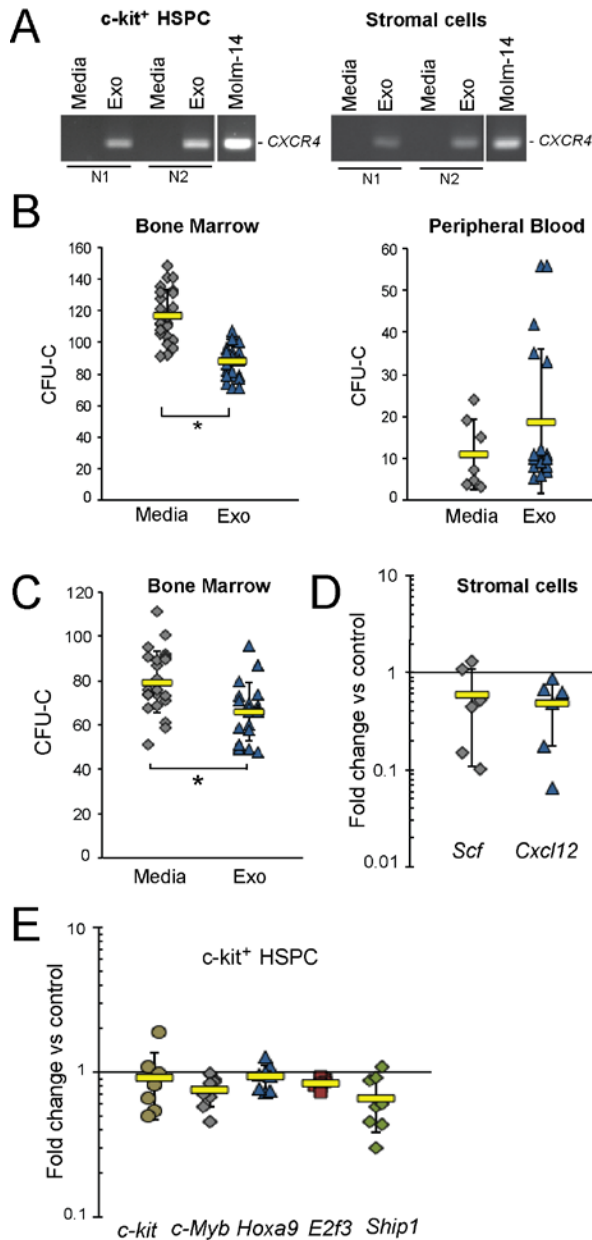


Figure 3.3: Intrafemoral Injection of AML Exosomes Recapitulates *In Vitro* Exosome Exposure

(A) NSG mice were intrafemorally injected with Molm-14 exosomes or media control. After 48h, stromal and c-Kit-selected cells were isolated, RNA was extracted, and RT-PCR was performed using human-specific *CXCR4* primers. RNA from Molm-14 cells was included as a positive control. Exo, exosome-injected animal; Media, media-injected control animal. (B) Marrow-derived c-Kit-selected cells and PBMCs from Molm-14 exosome IF-injected mice were plated in methylcellulose for CFU-C assay. *, $P < 0.01$ by Student's t. Exo, exosome-injected animal; Media, media-injected control animal. (C) Marrow-derived c-Kit-selected cells from HL-60 exosome IF-injected mice (Exo, exosome-injected femur; Media, contralateral control) were plated in methylcellulose for CFU-C assay. quantification of labeled exosomes within cells. *, $P < 0.01$ by Student's t. (D,E) qRT-PCR comparing expression of hematopoietically-relevant genes in stroma (D) or c-Kit⁺ HSPC (E) from the marrow of NSG mice intrafemorally injected with HL-60-derived exosomes. Exo, exosome-injected femur; Media, contralateral control.

able to deliver human transcripts to recipient HSPC and stromal cells, as detected by RT-PCR (**Fig. 3.3A**). Furthermore, c-Kit⁺ cells isolated from marrow in these animals exhibit the same suppression of clonogenicity observed *in vitro*. CFU-C performed on peripheral blood mononuclear cells (PBMC) of these animals suggested that mobilization of progenitors to the periphery may have occurred, but this effect did not reach statistical significance (**Fig. 3.3B**). In order to broaden the applicability of this finding, we repeated these experiments, this

time using exosomes from the HL-60 cell line with contralateral media-injected controls (in the same animal). In this model, the suppression of colony-forming capacity was more subtle, but remained significant when analyzed with a paired Student's t-test (**Fig. 3.3C**). Taking advantage of the opportunity to compare to same-animal controls, we isolated stroma and c-Kit⁺ HSPC from these mice, and investigated the expression of genes relevant to hematopoiesis (**Fig. 3.3D,E**). While HSPC demonstrated minimal alterations in gene expression, perhaps due to the change in exosome dose or timing, stromal cells recapitulated the suppression of *Scf* and *Cxcl12* that we had observed *in vitro*.

The development of leukemia within the marrow is accompanied by a host of changes, and AML's impact on the microenvironment is expected to include cell-cell contact-mediated signaling, cytokine secretion, and indirect effects from nearby cells and tissues that are triggered by the presence of a malignancy. As these influences cannot be captured by injection of isolated exosomes, we sought to reproduce our findings in two xenograft models of AML. Using NSG mice as hosts, we introduced either Molm-14 or HL-60 cells via tail vein injection, providing two distinct models of leukemia progression. In Molm-14-engrafted animals, leukemia aggressively invaded the bone marrow, producing fatal disease between 3 and 4 weeks post-injection, with minimal peripheral blood involvement (**Fig. 3.4A,B**). In contrast, HL-60-engrafted animals exhibited a somewhat slower-growing disease, fatal between 5 and 6 weeks

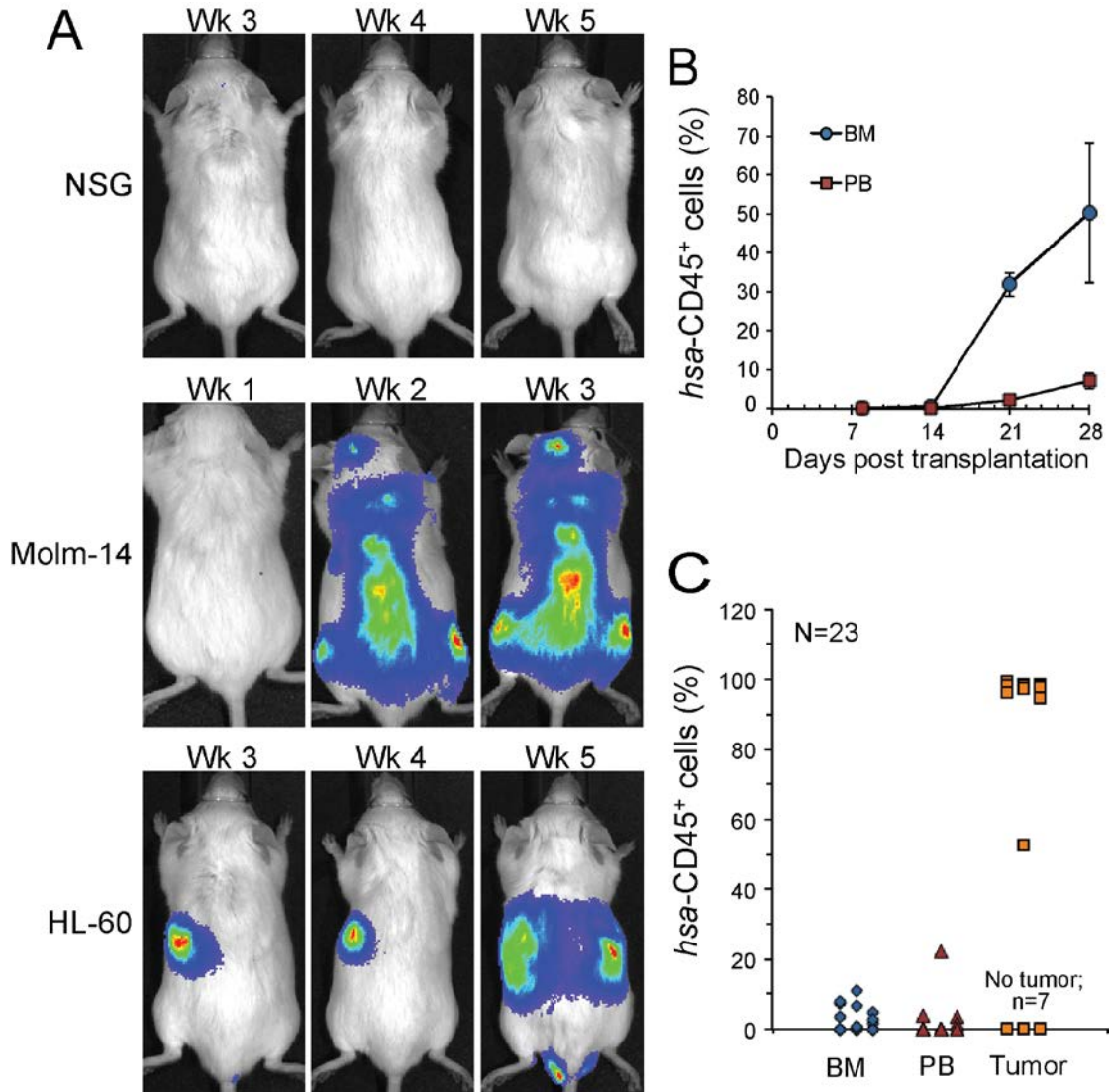


Figure 3.4: Molm-14 and HL-60 Produce Distinct Disease Kinetics, Distribution
(A) NSG mice were engrafted with luciferase-expressing Molm-14 or HL-60 cells by tail vein injection. Luciferin injection and intravital imaging was performed at the indicated time points post-leukemia injection. **(B)** Progression of peripheral blood (PB) and bone marrow (BM) chimerism in Molm-14-engrafted animals, by flow cytometry for human CD45. **(C)** Bone marrow (BM), peripheral blood (PB), and tumor chimerism in HL-60-engrafted animals at 4 weeks post-transplantation, by flow cytometry for human CD45.

post-injection, with most animals showing minimal-to-no evidence of disease in the bone marrow. Instead, these animals developed disease that was confined to the spleen, or developed large myeloid sarcomas containing the bulk of disease (**Fig. 3.4A,C**). The differing engraftment patterns of these two cell lines

allows a unique opportunity to compare the effects of marrow-resident AML with those of a primarily extramedullary leukemia.

We began this comparison by studying the colony forming capacity of c-Kit⁺ cells from the marrow alongside PBMC of engrafted animals. In Molm-14-engrafted mice, there was a clear redistribution of colony-forming capacity from the marrow to the peripheral blood (**Fig. 3.5A,B**). This finding corresponded well with analysis of gene expression in marrow stroma from these animals, which had substantially reduced levels of *Scf* and *Cxcl12* mRNA, suggesting a decrease in capacity for hematopoietic support (**Fig. 3.5C**). Surprisingly, there was similar suppression of colony-forming capacity in the marrow of mice engrafted with HL-60, despite the absence of leukemic cells in this compartment (**Fig 3.5D**). CFU-C on PBMC from these animals did not reveal an increase in circulating progenitors, however (**Fig. 3.5E**), perhaps indicating a different mechanism of hematopoietic suppression. An examination of stromal expression of *Scf* and *Cxcl12* similarly demonstrated a slight but variable decrease (**Fig. 3.5F**), and qRT-PCR performed on RNA from c-Kit⁺ cells from the marrow echoed our *in vitro* observations, with a smaller magnitude (**Fig. 3.5G**). In total, our HL-60 engraftment findings support an *in vivo* effect of engraftment that mimics the effects of purified exosomes, but to a lesser extent, potentially due to a lower dose of exosomes received in the marrow from an extramedullary leukemia.

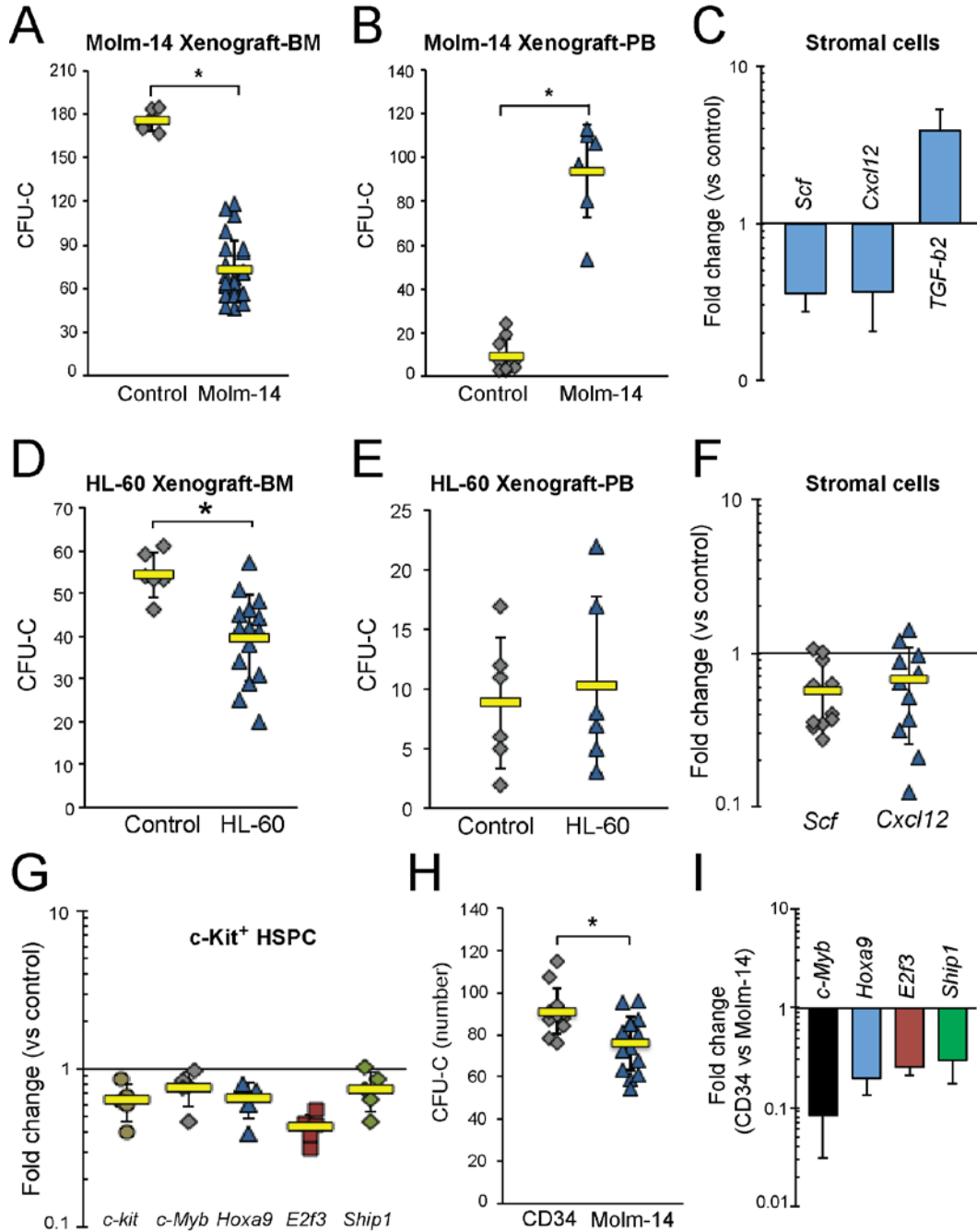


Figure 3.5: AML Xenograft Causes Hematopoietic Suppression in NSG Mice

(A-C) NSG mice were engrafted with 1×10^5 Molm-14 cells by tail vein injection. After 3 weeks, marrow c-Kit⁺ and stromal cells and PBMCs were collected. (A) CFU-C on marrow c-Kit⁺ cells. (B) CFU-C on PBMC. (C) qRT-PCR for expression of indicated genes in stroma. (D-G) NSG mice were engrafted with 5×10^6 HL-60 cells by tail vein injection. After 5 weeks, marrow c-Kit⁺ and stromal cells and PBMCs were collected. (D) CFU-C on marrow c-Kit⁺ cells. (E) CFU-C on PBMC. (F) qRT-PCR on stromal RNA. (G) qRT-PCR on marrow c-Kit⁺ cell RNA. (H,I) Comparison of c-Kit⁺ marrow cells from NSG mice engrafted with 1×10^5 Molm-14 or CD34⁺ human cord blood cells. (H) CFU-C; (I) qRT-PCR for indicated genes. All qRT-PCR was normalized to GAPDH; *, $P < 0.01$ by Student's t.

As these experiments were performed entirely in a xenograft environment (using human AML in mice), we performed additional control experiments to ensure that the changes we observed were not simply due to the presence of human hematopoietic cells. We therefore engrafted a cohort of NSG mice with CD34⁺ human cord blood cells, and compared colony forming capacity in the marrow, as well as gene expression in HSPC, with Molm-14-engrafted animals. These experiments revealed that engraftment of AML suppressed marrow clonogenicity when compared to that of animals engrafted with normal human hematopoietic cells (**Fig. 3.5H**). Although this suppression was more modest than that observed in the experiments in which we used unengrafted NSG mice as controls, gene expression in c-Kit⁺ cells from the marrow of these animals was dysregulated to a substantially greater extent (**Fig. 3.5I**), suggesting that multiple mechanisms of hematopoietic regulation are involved in these effects.

Discussion

The secretion of exosomes by AML blasts suggests that cytoplasmic material from these cells is transferred to diverse bystander cells, as no known targeting mechanism for these particles exists. The observation that AML-derived exosomes contain not a random sampling of cytoplasmic content, but instead carry selected transcripts, and often those of recognized relevance to hematopoietic regulation, suggests that determination of exosome content contributes to adaptive selection, which in turn suggests accrued benefit to the leukemic blasts from their secretion. Determining what this benefit may be, and what downstream processes are involved, requires careful evaluation of putative

target cells with attention to reciprocal effects on a developing AML. Focusing on suppression of HSPC function and the conversion of the hematopoietic niche to the leukemic niche is therefore a promising avenue of investigation, as it combines a plausible benefit to the leukemia – antiapoptotic and progrowth signaling from the niche – with a definite and direct negative result for patients. Additionally, niche conversion requires diverse changes in multiple cell types, a role for which exosomes are uniquely well-suited.

These experiments clearly demonstrate that AML-derived exosomes are sufficient to cause suppression of hematopoiesis in both *in vitro* and *in vivo* niche models. To show that exosome trafficking is necessary, however, would require either a way to specifically halt exosome secretion in the leukemic blasts, or additional insight into the mechanism by which suppression occurs. In the absence of a known way to accomplish the former, I attempt to elucidate the specific mediators of these effects in the experiments described in the subsequent chapter.

Materials & Methods

Cells, cell lines and low-oxygen cell culture

Molm-14, U937, and HL-60 cell lines were provided by Dr. Jeffrey Tyner and cultured in RPMI (Life Technologies) with 10% vesicle-free (VF-) FBS. OP9 were provided by Dr. William H. Fleming and cultured in α -minimum essential media with 20% VF-FBS and 60 μ mol/L 2-mercaptoethanol. Igf-1R knockout (R-) or overexpressing (R+) MEFs were provided by Drs. Briony Forbes and Douglas

Yee, respectively, and cultured in Dulbecco's Modified Eagle's Media (Invitrogen) with 9% VF-FBS. All cultures contained 100 U/mL penicillin/streptomycin (Invitrogen). For low O₂ culture, cells were cultured in RPMI with 10% VF-FBS using a G-Rex gas-permeable flask (Wilson-Wolf Corp.) in a BioSpherix chamber at 1-3% O₂ or a standard incubator at 20% O₂ and at 5% CO₂. VF-FBS was produced by centrifugation of FBS (Gemini Bio-Products) at 100,000xg for 6 hrs, discarding the pellet. Primary AML cells were maintained in EGM-2 media (Lonza) according to OHSU IRB-approved protocols. Primary human CD34+ cord blood progenitors (New York Blood Center) were enriched using MACS cell separation (Miltenyi Biotec) and cultured in serum-free media (SFEM) (StemCell Technologies) supplemented with 100 U/mL penicillin/streptomycin, 40 ng/mL FLT3L, 25 ng/mL SCF, and 50 ng/mL TPO (Miltenyi Biotec). For IGF-IR inhibitor studies, picropodophyllin (PPP; CalBiochem) was added at 100nmol/L.

Exosome preparation and RNA extraction

AML cells were cultured for 48 hrs, media spun at 300xg for 10 min, supernatant at 2,000xg for 20 min and 10,000xg for 20 min followed by supernatant centrifugation at 100,000xg for 2 hrs. Exosome pellets were resuspended in 10% VF-FBS/RPMI or used for RNA extraction. Media collected from exosome preparations after the 10,000xg spin is defined as conditioned media. Two mL of conditioned media was cultured with 3x10⁴ OP9 stromal cells per well in a 6-well plate (4.8x10⁹ Molm-14 exosomes/well by NTA analysis). Concentrated exosomes were resuspended in 2mL of 10% VF-FBS RPMI before use.

Murine xenograft studies

Six to eight-week-old NOD/SCID/IL-2 γ ^{null} (NSG) xenograft recipients were used with IACUC approval. 1×10^5 conditioned Molm-14 cells, cord blood CD34⁺ cells, or 5×10^6 HL-60 cells were injected via tail vein. Human CD45 chimerism (BioLegend, HI30) was monitored by flow cytometry. Animals were sacrificed at 3-5 weeks post-engraftment, and peripheral blood (PB) and BM were collected. Adherent BM stromal cells were propagated in Iscove's MDM (Life Technologies) with 10% VF-FBS. For intravital imaging, animals were engrafted as above, using AML cell lines transduced to express luciferase. At weekly time points, animals were injected with 150 μ L luciferin, then anesthetized and imaged 10min later using an IVIS Spectrum imaging system (Perkin Elmer).

Intrafemoral (IF) injection

AML exosomes ($5.8-6.8 \times 10^{11}$ Molm-14 exosomes or $5.2-6.0 \times 10^{11}$ HL-60 exosomes by NTA quantification) or saline were injected into one femur of isoflurane-anesthetized animals; in animals with contralateral controls, saline was injected contralaterally in the same animal. Animals were sacrificed 48 hrs later for BM collection and c-Kit⁺ progenitor cell enrichment.

RNA analysis and qRT-PCR

RNA was extracted using miRNeasy or RNeasy (Qiagen) and quantified using a Nanodrop 2000c (Thermo). cDNA was synthesized using a SuperScript III First Strand Synthesis kit (Invitrogen) with oligo-dT priming, followed by PCR. SYBR

Green PCR (Applied Biosystems) was used for qRT-PCR analysis. The $\Delta\Delta CT$ method was used for quantification, normalized to GAPDH. All primers were species-specific.

Nanoparticle tracking analysis (NTA)

Exosome samples were resuspended and serial dilutions were prepared in nanofiltered (Whatman Anotop 25, 0.02- μ M) molecular-grade water (Thermo Scientific) using low-adhesion 1.7-mL tubes (Genemate). Diluted samples were loaded into the NanoSight LM10 chamber, the laser engaged, and microparticles visualized. Sixty second videos were acquired with a Hamamatsu C11440 ORCA-Flash 2.8 camera and analyzed by Nanosight NTA 2.3 software. Individual samples were diluted to 1×10^8 - 1×10^9 particles/mL.

In vitro exosome treatment and colony-forming unit (CFU) assay

BM and PB from NSG or C57BL/6 mice were harvested and resuspended in hemolytic buffer and PBMCs collected by centrifugation. For enrichment, c-Kit-PE antibody (BD, clone 2B8) and EasySep Mouse PE Selection kits (StemCell Technologies) were used (90-93% mCD45 / c-Kit purity confirmed by flow cytometry). Murine c-Kit-enriched cells were cultured in IMDM/10% VF-FBS/50ng/mL mIL-3 and mSCF (R&D Systems). 1×10^6 c-Kit⁺ cells were incubated with exosomes harvested from $6\text{-}7 \times 10^7$ Molm-14 or HL-60 cells (at $5.8\text{-}6.8 \times 10^{11}$ exosomes/well from Molm-14 cells or $5.2\text{-}6.0 \times 10^{11}$ exosomes/well from HL-60 per NTA analysis), $2.5\text{-}4 \times 10^7$ primary AML cells or $3\text{-}3.5 \times 10^7$ human CD34⁺ cells for 48-hrs with VF media controls. Transwell cell-cell transfer was performed in 6-

well plates using 0.4- μm pore size inserts (Corning). Target cells were seeded at 2×10^4 cells per well and settled overnight. $1-2 \times 10^6$ cells were added into the transwell insert and co-cultured for 48 hrs. Mouse Methylcellulose Complete media (R&D Systems) was used for CFU-C assays in triplicate with 3×10^3 c-Kit⁺ cells or 2×10^5 PBMCs /35-mm dish (37°C, 5% CO₂, $\geq 95\%$ humidity, x 7 days). Human CD34⁺ cells were cultured in SFEM media, with cytokines as above. Human Methylcellulose media (StemCell Technologies) was used for CFU-C assays with 100 CD34⁺ cells/35-mm dish cultured for 14 days.

Cell migration assay

Lineage-depleted (Lin-) BM (Progenitor enrichment kit, StemCell Technologies) was cultured in triplicate at 5×10^5 cells in 2 mL IMDM, 10% VF-free FBS, 50 ng/mL SCF and IL-3 for 24 hrs +/- 1 mL of ECM (at 2.4×10^9 Molm-14 exosomes/well by NTA analysis). Washed cells were placed on 8- μm transwell inserts (Corning) in plates containing media +/- CXCL12 (50 ng/mL). After 2 hrs, transwells were removed and migrated cells were counted using a Guava PCA (Millipore).

Flow cytometry analysis

Flow cytometry was performed on Calibur/ CANTO/ LSR II cytometers (BD Biosciences) using anti-human or anti-mouse CD45 (BioLegend), murine c-Kit⁺ (BioLegend) or CXCR4 (Clone 2811, eBioscience) antibodies, or mouse anti-human IGF-1R antibodies (BioLegend) and analyzed with FlowJo (Tree Star).

Western blotting

Protein lysates were generated using RIPA buffer with protease inhibitors (Thermo Scientific) and protein concentrations were quantified using the BCA Protein Assay (Pierce). Lysates were loaded on 4-15% SDS-PAGE gels (Bio-Rad) for transfer. IGF-IR was detected using rabbit anti-human IGF-IR β (Cell Signaling Technology) and anti-rabbit HRP (Thermo Scientific). Chemiluminescence was detected by the Supersignal West Pico Chemiluminescent substrate (Pierce).

Statistical analysis

Continuous variables are summarized as mean \pm standard deviation. A two-sample t-test was employed for comparison between samples derived from the same source, but different conditions. For comparisons between cells and exosomes, or left-versus-right femur IF-injection, a paired t-test was used. Statistical significance was set at $p \leq 0.05$.

CHAPTER 4: AML Exosomes as Serum Biomarkers

Submitted for publication; Hornick *et al.*, Scientific Reports, 2015.

Abstract

Post-remission relapse remains the major cause of mortality for patients diagnosed with Acute Myeloid Leukemia (AML). Improved postremission tracking of minimal residual disease (MRD) holds the promise of timely adjustments to treatment to preempt frank relapse. Current surveillance techniques rely on molecular or immunophenotypic detection of circulating blasts that coincide with advanced disease and poorly reflect MRD levels in the marrow during early relapse. Here, we investigate exosomes as a minimally invasive platform for a microRNA (miRNA) biomarker. We identify a set of miRNA highly enriched in AML exosomes and quantitatively track the levels of circulating exosome miRNA that distinguish animals with leukemic xenografts from both non-engrafted and human CD34+ controls. We develop biostatistical models that reveal the emergence of circulating exosomal miRNA at low marrow tumor burden and well before circulating blasts can be detected. Remarkably, both leukemic blasts and marrow stroma contribute to serum exosome miRNA. We propose development of serum exosome miRNA as a platform for a novel, sensitive compartment biomarker for prospective tracking and early detection of AML recurrence.

Implications: Exosome-contained microRNA provide a serum AML biomarker that reflects contributions from leukemic and stromal cells of the AML microenvironment and outperforms conventional cell-based MRD metrics.

Introduction

Acute Myeloid Leukemia (AML)¹⁰ causes more than 10,000 deaths annually in the United States, with a 5-year overall survival rate of approximately 25%¹⁰. Induction treatment of AML achieves disease remission in up to 80% of patients, yet a majority among adults and children experience relapse. This, along with the aggressive kinetics of relapsing AML (2.5 log/month in one recent study¹²⁰), underscores the need for improved early detection of residual disease after induction chemotherapy. Indeed, end of induction minimal residual disease (MRD) is the most powerful marker of poor outcome for childhood AML¹²¹ and alters clinical decision making^{120,122}. However, current MRD metrics do not perform well at later time points, in part because conventional detection of relapse is uniformly based on identifying leukemia at the cellular level¹²³. Peripheral blood assays require the presence of leukemic blasts in the circulation, which generally connotes advanced disease burden, while bone marrow aspirates are invasive and rely on a sample from a single physical location. Ineffective surveillance strategies are illustrated by a recent retrospective study on pediatric AML that found that forty-one routine bone marrow aspirates were performed for every case of relapse detected¹²⁴. Additionally, both flow cytometry and PCR require the presence of a known leukemia-specific marker. Unlike *BCR-ABL1* in chronic myeloid leukemia, AML lacks a molecular marker whose detection specifically identifies leukemia. Combined, these features have to date precluded the development of a clinically useful and timely prospective surveillance strategy.

Cytokines¹²⁵ and circulating cell-free nucleic acids^{126,127} have been explored for MRD tracking, and more recently, microRNA (miRNA) have attracted attention as a potential source of novel AML biomarkers^{128,129}. MicroRNA expression profiles have been associated with AML subtypes¹³⁰, mutations¹³¹, and overall survival¹³². Exosomes – small, membrane-enclosed extracellular vesicles – are directly secreted by AML blasts¹³³, carrying a select panel of cellular RNA and protein^{47,61,134}. Exosomes equilibrate between tissue compartments and can be isolated from many body fluids^{135,136}, including both plasma¹³⁷ and serum¹³⁸; and while their potential as biomarkers is beginning to be explored¹³⁸⁻¹⁴⁰, exosome miRNA have not yet been investigated as a marker of AML disease burden. Based on our recent findings that AML blasts secrete exosomes that contain selected miRNA¹³³, we hypothesized that leukemia patient serum contains exosomes bearing miRNA that uniquely identify AML, providing potential advantages in both sensitivity and specificity over conventional biomarkers based on direct measures of plasma-associated miRNAs¹⁴¹.

Results

NSG xenograft of Molm-14 produces a model of AML disease with characteristic exosome secretion

As a model for high-risk AML with rapid growth kinetics, we developed a xenograft model using the Molm-14 cell line in NOD/SCID/IL-2 γ ^{null} (NSG) mice¹⁴²⁻¹⁴⁴. Upon tail vein injection of as few as 1x10⁵ Molm-14 cells, we found predictable establishment of disease in NSG mice. We avoided irradiation

conditioning in order to maintain vascular integrity and the native microenvironment. Engrafted animals were sacrificed at serial time points and human CD45 was readily detected in sectioned femurs by immunohistochemistry (**Fig. 4.1A**). In a series of experiments comprising leukemias in more than 30 animals, we found that disease was rapidly progressive, leading to death or morbidity requiring sacrifice within a 4-week time frame. In order to establish the source of exosomes within the leukemia niche, we isolated leukemic cells from mice engrafted with Molm-14 AML (bone marrow chimerism between 69-77% by human CD45 positivity). Using PCR for FLT3-ITD verified that these animals contained leukemic cells similar to Molm-14 stock (**Fig. 4.1B**). As the bone marrow microenvironment promotes leukemic growth, proliferation, and anti-apoptotic signaling, and has been shown to confer chemoresistance in NSG models¹⁴⁵⁻¹⁴⁷, we additionally isolated stroma by adhesion of cells from whole bone marrow to culture flasks, and then evaluated them in culture after 4-6 passages. Expansion cultures of both murine stromal cells and NSG-engrafted Molm-14 produced exosomes with typical size (**Fig. 4.1C**) and morphology (**Fig. 4.1D**). These results indicate that both leukemic cells and marrow stroma can contribute to serum exosomes, providing a potential compartment-level indicator of disease.

AML cell- and AML-conditioned stroma-secreted exosomes carry a select miRNA subset

We previously showed that AML-secreted exosomes, including those from Molm-14, contain a concentrated miRNA population that is proportionally different from

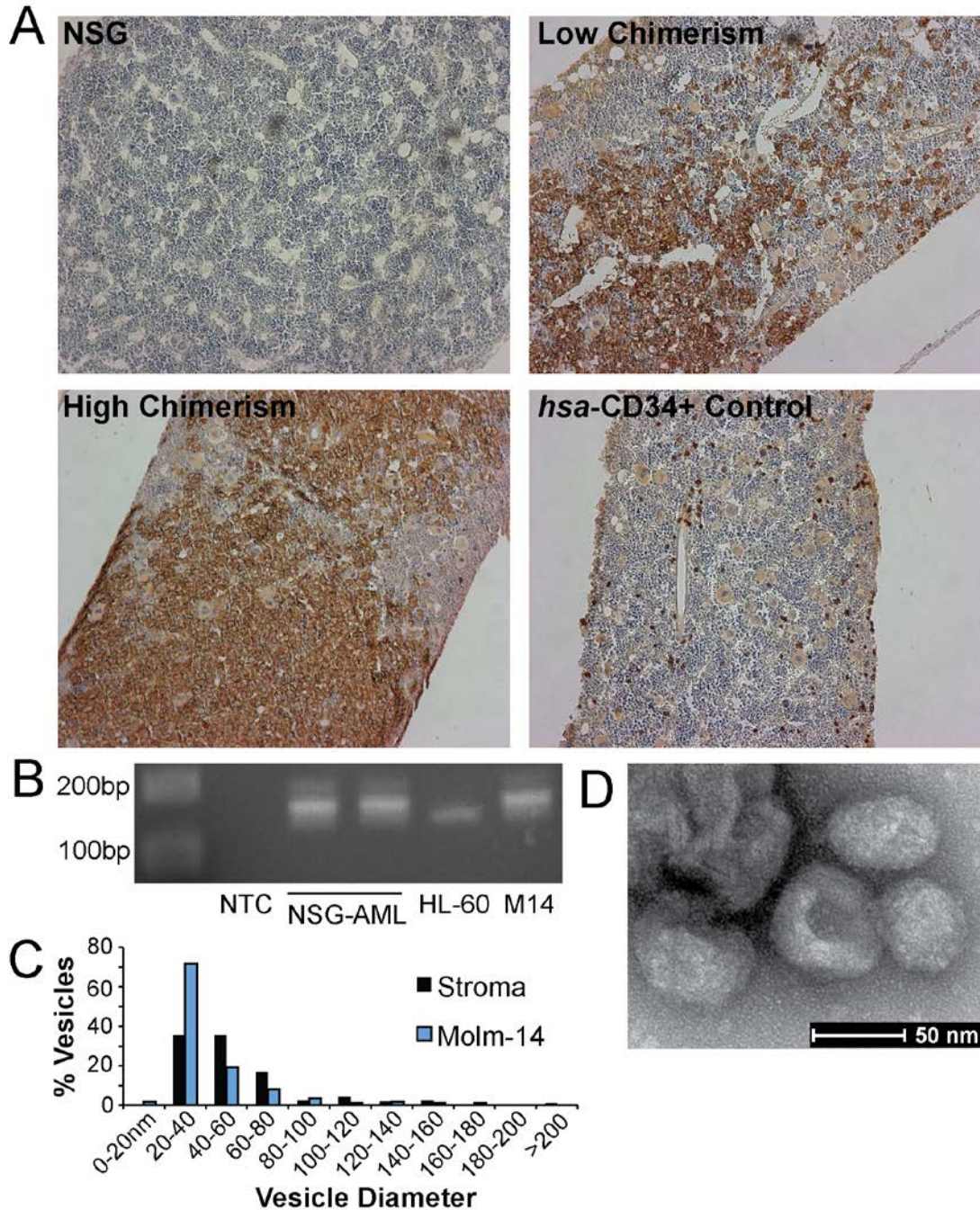


Figure 4.1: Molm-14 Engraft in NSG Mice and Contribute to Compartment Exosome Secretion

(A) Immunohistochemistry of Molm-14-engrafted NSG femurs collected from mice at 3 weeks post-engraftment, sectioned, and stained for human CD45. (B) PCR identification of NSG-engrafted AML. Molm-14 isolated from engrafted NSG mice retained their characteristic FLT3-ITD mutation, detected by 40 cycles of PCR. NTC: null-template control; NSG-AML: isolated Molm-14; HL-60: cell line exhibiting WT FLT3; M14: Molm-14 stock culture. (C,D) TEM of exosomes isolated from the culture media of Molm-14 and NSG stroma. Sizing of > 100 vesicles per sample is presented in (C); representative image is presented in (D).

the cellular miRNA¹³³. In extension of those observations, we found an enrichment of small RNA within the total RNA of exosomes derived from *ex vivo* Molm-14 after engraftment in NSG mice (**Fig. 4.2A**) as well as exosomes derived from NSG stroma, (**Fig. 4.2B**) when compared to the RNA from cell of origin. As miRNA are highly conserved¹⁴⁸, and thus unlikely to be unique to a particular disease process (or species), we pursued a wider characterization of the respective cellular / exosomal miRNA levels in order to determine whether an predictive panel could be identified¹²⁶. We evaluated Molm-14 exosomal *versus* cellular miRNA using the Affymetrix GeneChip miRNA 3.0 microarray (GEO Accession GSE55025), containing almost 20,000 unique probes based on miRBase v17. This revealed stark differences between the miRNA content of exosomes and the cells that produce them (**Fig. 4.2C**). Of the mature miRNAs detected in both cell and exosome, 161 of 1733 were at least two-fold increased in exosomes, while 108 were at least 2-fold decreased. We used quantitative reverse transcriptase-PCR to validate our microarray findings for select targets noted in the recent literature to be relevant to AML biology^{105,149}. After normalizing to U6, we found substantially enriched concentrations of let-7a, miR-99b, -146a, -155, -191, and -1246, concentrations of up to 1000-fold above cellular levels (**Fig. 4.2D**). We also evaluated several of these miRNA in exosomes isolated from *ex vivo* stromal cell cultures (**Fig. 4.2E**). Although these miRNA tended to be abundant in exosomes compared to the producing stromal cells, there was no significant difference between cell and exosome, nor between

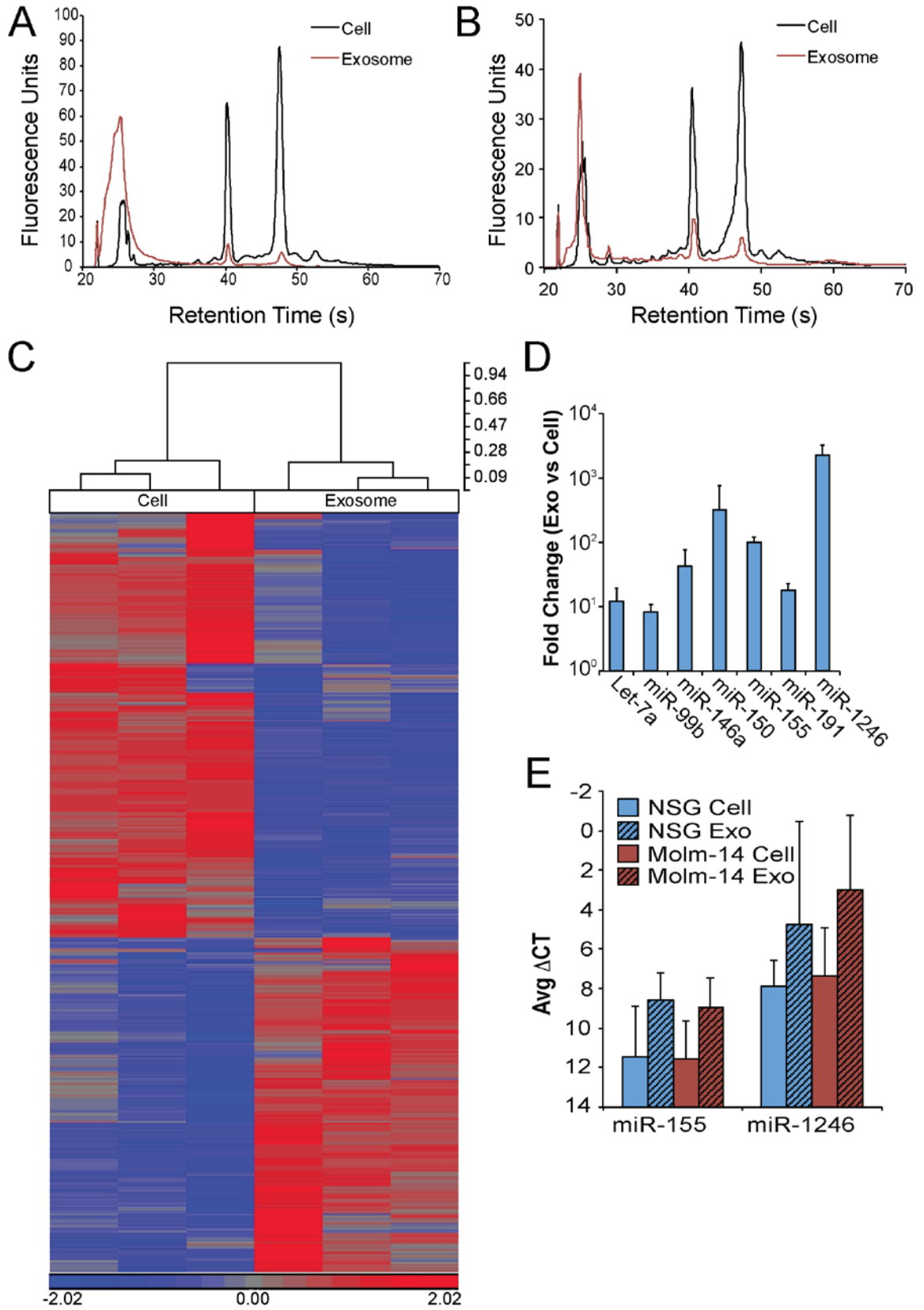


Figure 4.2: Molm-14 and Stromal Exosomes Concentrate Selected MicroRNA

(A,B) RNA size profiles of exosomes. RNA was collected from Molm-14 (A) and NSG Stromal (B) cells and their exosomes after 72 hours in culture, and miRNA was evaluated using a bioanalyzer. (C) Microarray comparison of cell, exosome miRNA. Molm-14 cell and exosome microRNA was evaluated using an Affymetrix microRNA microarray. All targets with more than 2-fold mean difference between producing cell and exosome are represented, RMA-corrected and standardized to a mean of 0 and a SD of 1. Dendrogram values are 1 - Pearson's R. (D,E) qRT-PCR for miRNA in cells *versus* exosomes. Selected targets from NSG stromal (D) and Molm-14 (E) cells and exosomes were validated using Taqman qRT-PCR, normalized to U6 snRNA. Fold change was calculated by $2^{-\Delta\Delta Ct}$.

stroma from Molm-14 engrafted animals and controls. The array studies provided us with a candidate panel of miRNA targets, derived from both AML and its surrounding stroma, to pursue in our investigations into total serum exosome miRNA profiles.

Conventional surveillance strategies provide a limited window into leukemic burden

For reference to existing leukemia monitoring strategies, we evaluated flow cytometry and complete blood count (CBC) in our model. Flow cytometry on PBMCs proved to be an unreliable means of detection; disease was first reliably detectable by this method (using the threshold of 0.3% human CD45 positivity¹⁵⁰) within two days of the earliest animal death, reflecting human disease and speaking to the vascular integrity of the BM sinusoids and the physiology of the model. Across multiple experiments, human CD45 chimerism in the marrow developed approximately seven days earlier than in the periphery (**Fig. 4.3A**). To track disease burden through treatment, we used cytarabine (ara-C), a nucleoside analog and backbone of AML chemotherapy¹⁵¹. Treatment with cytarabine effectively eliminated Molm-14 cells from the blood. Leukemic chimerism within the marrow, however, was unaffected (**Fig. 4.3A**), underscoring

the problems inherent in the reliance on peripheral leukemia cells as an indicator of disease burden. When we followed complete blood count measures of hemoglobin and platelet counts we found significant differences ($p < 0.05$) in Molm-14 engrafted versus control animals as early as two weeks after engraftment (**Fig. 4.3C**), at which time peripheral blood chimerism by flow cytometry was still zero (**Fig. 4.3A**). As anticipated, CBC metrics were globally suppressed following treatment of mice with ara-C, illustrating one of several confounders in a clinical post-treatment scenario. Illustrating the more complex situation in patients, however, treatment of unengrafted NSG mice resulted in a significant suppression of hemoglobin measures, effectively mimicking the anemia seen in engrafted animals (**Fig. 4.3C**). As Molm-14 express FLT3-ITD, we investigated whether this established MRD marker transcript was detectable in exosomes isolated from the serum of engrafted mice (**Fig. 4.3B**). Although murine GAPDH was readily found in the serum exosomes of both engrafted – with peripheral blood (PB) and bone marrow (BM) chimerism ranging from 0.4-10% and 41-67% respectively – and control animals, neither Molm-14-specific FLT3-ITD nor human-specific GAPDH was detectable after 45 cycles of PCR, broadly consistent with the comparatively lower abundance of larger RNA species by bioanalyzer. We therefore evaluated the enriched exosomal miRNA population in pursuit of biomarker candidates. As a prerequisite for a robust biomarker, AML exosome miRNA must either be unaltered by exposure of the cells to chemotherapy, or be shifted in a systematic and predictable way; this requirement complicates leukemia surveillance with CBC and flow cytometry. In

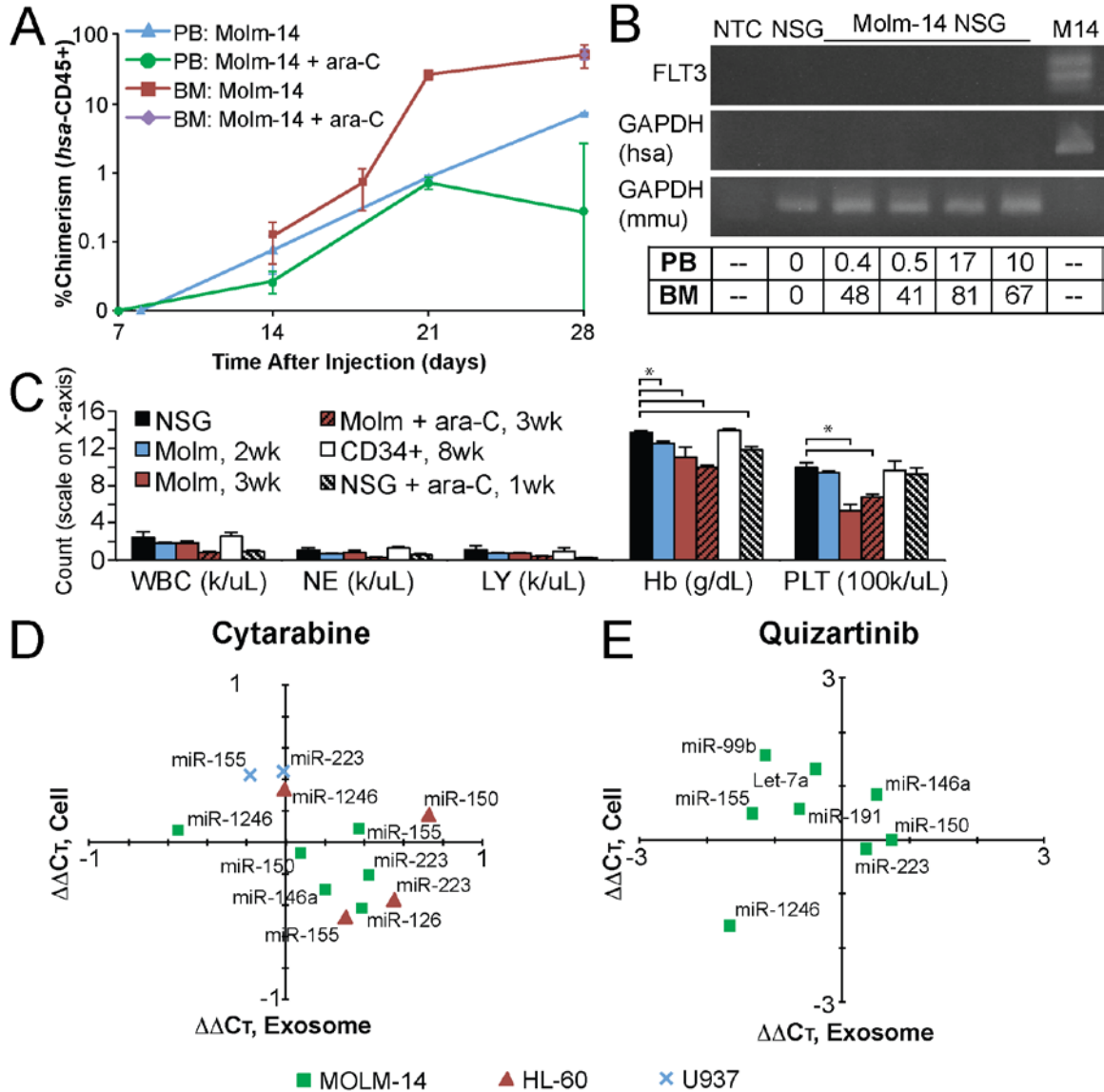


Figure 4.3: Conventional Markers Are Limited; Chemotherapy is a Confounder
 (A) Molm-14 xenograft chimerism. Flow cytometry for human CD45 was performed on the peripheral blood and bone marrow of Molm-14-engrafted NSG mice, +/- ara-C treatment. (B) mRNA RT-PCR on serum exosomes. Serum exosomes from Molm-14-engrafted mice were tested for human FLT3 and GAPDH and murine GAPDH using PCR. NTC: null-template control. M14: Molm-14. PB: Peripheral blood; BM: Bone marrow chimerism by flow for human CD45. (C) CBC of mice, comparing NSG (n=31), NSG + Molm-14 at 2 (n=16) and 3 (n=5) weeks post-engraftment, NSG + Molm-14 + ara-C (n=8) at 3 weeks, control NSG + ara-C (n=4), and NSG + nonmalignant CD34+ human cells (n=4). WBC, white blood cells; LY, lymphocytes; NE, neutrophils; Hb, hemoglobin; PLT, platelets (x1000/uL). *, $p < 0.05$ by Student's *t*. Error bars represent SEM. (D,E) *In vitro* chemotherapy and exosomal miRNA. Molm-14, HL-60, and U937 cells were exposed to cytarabine (25ng/mL, D) overnight, and Molm-14 were exposed to quizartinib (0.1nM, E) overnight. Cellular (on the x-axis) and exosomal (on the y-axis) miRNA were measured by qRT-PCR, and are presented as ddCT (a -1 ddCT represents a 2-fold increase in miRNA).

order to determine whether AML exosomal miRNA was sensitive to drug treatment, we exposed several AML cell lines to chemotherapeutics *in vitro*, and then evaluated the resulting changes in cellular and exosomal miRNA. In a series of experiments in which we exposed multiple AML cell lines to cytarabine, we found that no candidate miRNA exhibited a shift of 2-fold or more after ara-C exposure (**Fig. 4.3D**). Similarly, exposure to the targeted kinase inhibitor Quizartinib (which inhibits FLT3 kinase activity¹⁵²) was associated with only minor shifts in exosomal miRNA levels (**Fig. 4.3E**). These findings support exosomal miRNA as a biomarker that is representative of disease burden, rather than fluctuating expression or exosome release modified as a result of treatment.

Exosomal miRNA in the serum echoes AML-engraftment kinetics

To develop an *in vivo* exosome biomarker platform, we tested quality and quantity of miRNA isolated from small amounts of murine serum. We collected blood from Molm-14 xenograft and control NSG mice and extracted exosomes from the serum. Assessing the amount and quality of RNA yielded in exosome preparations from varying volumes of serum established that exosomal miRNA could be collected from as little as 20uL of serum (**Fig. 4.4**). Based on this finding, we settled on a serum volume of 20-50 miRNA for RNA measurements. In a series of experiments comprising more than sixty mice, we systematically determined serum levels of four candidate miRNA chosen for their relevance to leukemia^{105,141,149} and incorporation in exosomes (**Fig. 4.1**): miR-150, miR-155, miR-221, and miR-1246. Using Molm-14-engrafted animals at 14 days (d14) and 21 days (d21) post-engraftment as our experimental groups, we

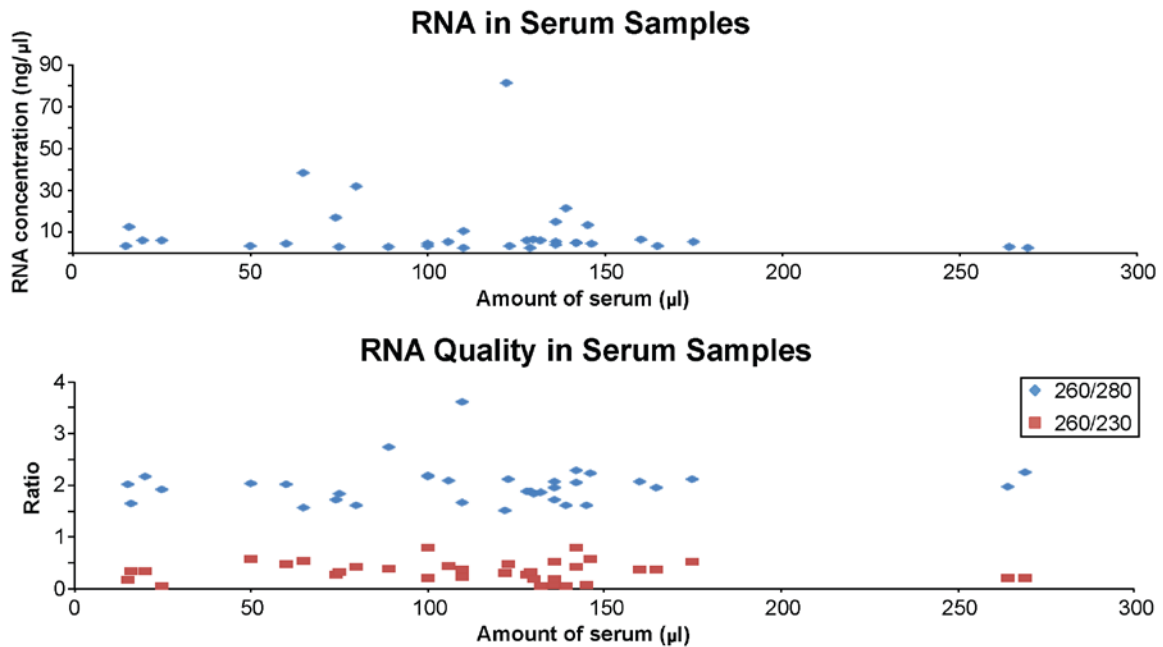


Figure 4.4: Serum Exosome RNA Yield and Quality are Independent of Serum Volume

Serum was collected from Molm-engrafted or control NSG mice, and exosomes were collected by ExoQuick precipitation. Total RNA was isolated, and concentration, 260/280, and 260/230 values were measured by spectrophotometer.

compared to unengrafted NSG mice as well as to mice engrafted with healthy human CD34+ cells derived from cord blood. In spite of the anticipated substantial inter-animal variability, this panel of miRNA reproducibly distinguished between cohorts (**Fig. 4.5A**): miR-155 was elevated in Molm-14- and CD34+-engrafted animals but not NSG controls, miR-150 separated Molm-14 from CD34+ engraftment, miR-221 was altered at late but not early leukemia time points, and miR-1246 increased over time in leukemia-, but not nonmalignant CD34+ cell-engrafted mice. In an effort to test statistical strength, models of receiver operating characteristic (ROC) were generated by logistic regression. These highlight the added discriminatory capacity conferred by combining the top performing markers (**Fig. 4.5B**). By evaluating multiple combinations, we developed a model that produces a single exosomal miRNA score (linear

combination of miR-150, -155, and -1246) which was best able to separate leukemia-engrafted mice from controls, achieving an area under the curve (AUC) of 0.80, compared to individual marker AUC's of 0.68 for miR-155 and 0.67 for miR-1246. (**Fig. 4.5B, Table 4.1**). These models were generated using data collected from mice 14 days post-engraftment, in whom peripheral blood

Model	Day 14			Day 21		
	n (control)	n (AML)	AUC	n (control)	n (AML)	AUC
1246	20	18	0.6722	20	18	0.9583
150	35	40	0.4600	35	31	0.5217
155	34	40	0.6912	34	31	0.8065
1246, 150	20	18	0.8083	20	18	0.9667
1246, 155	20	18	0.7944	20	18	0.9528
150, 155	34	40	0.7463	34	31	0.8643
1246, 150, 155	20	18	0.8028	20	18	0.9944

Table 4.1: Comparison of miRNA marker combinations

Logistic regression was used to create weighted linear combinations of serum exosome miRNA markers, which were evaluated for their capacity to discriminate between xenografted mice (*n* in column n (AML)) and unengrafted controls (*n* in column n (control)) at 14 and 21 days post-engraftment. Areas under receiver operating characteristic (ROC) curves are presented as AUC.

leukemic blasts ranged between undetectable to less than 0.1% by flow cytometry for human CD45 positivity. Using the coefficients calculated for the combined miR-150/ -155/ -1246 model (-0.2175, -0.3837, and 0.0017, respectively), we scored serum exosome miRNA from a separate validation set of animals engrafted with human cord blood-derived CD34+ cells or with Molm-14, then treated with ara-C at 14 days post-engraftment as described above. We chose three separate cutoff scores (circled in **Fig. 4.5B**) statistically emphasizing sensitivity, specificity, or a balance of the two, and sorted the scores generated by measuring serum exosomal miRNA in the validation set (**Fig. 4.5B**). Optimizing sensitivity or specificity allowed complete elimination of false

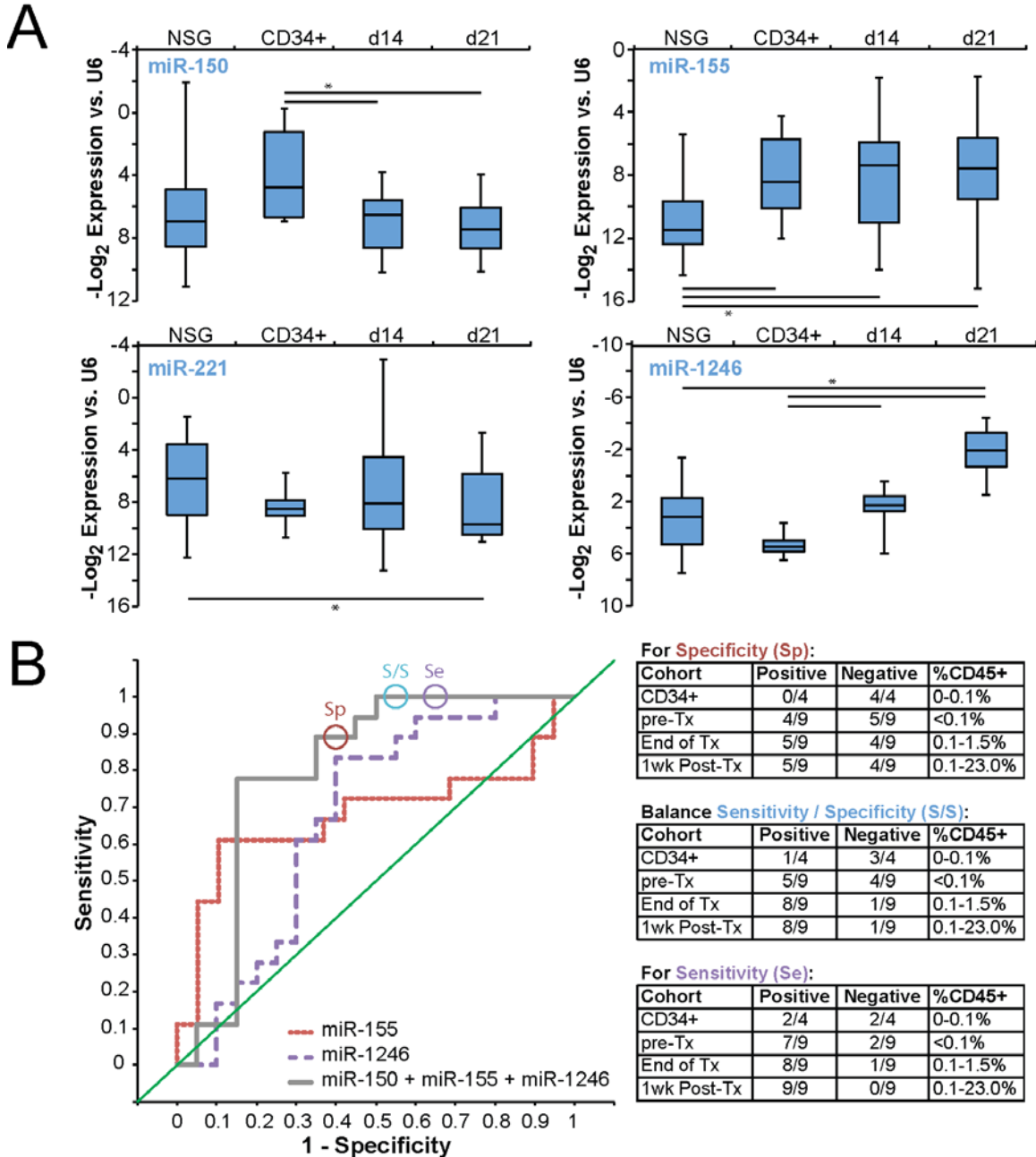


Figure 4.5: Serum Exosome miRNA Distinguishes Leukemia From Hematopoiesis
(A) Serum exosome miRNA levels. Exosomes were isolated from peripheral blood of control NSG mice as well as NSG mice engrafted with Molm-14 (after 14 or 21 days; d14 and d21, respectively) or human CD34+ cells. MicroRNA levels were measured by qRT-PCR. *, $p < 0.05$ by Student's t . **(B)** Serum exosome miRNA score performance. Receiver operating characteristic (ROC) curves are presented for single miRNA and for the combination of miRNA-150, -155, and -1246. The circles represent points on the ROC curves whose alphas were chosen as cutoff values emphasizing specificity, sensitivity, or a balance of the two, respectively. These cutoff values and the coefficients generated by the regression were used to evaluate mice engrafted with Molm-14 and treated with cytarabine, alongside control mice engrafted with human CD34+ cells. Exosome miRNA panel performance for each cohort and cutoff is presented alongside peripheral blood chimerism (by flow cytometry for human CD45).

negatives or false positives, respectively, while balancing the two in choosing a cutoff value resulted in detection of 8/9 leukemias with only 1/4 controls being scored positive. These results demonstrate both the reproducibility of alterations in serum exosomal miRNA as a marker of leukemia and the independence of this score from both treatment and the level of circulating blasts.

Exosomal miRNA as a general AML biomarker

In order to determine the broader preclinical potential for exosome miRNA as biomarkers we interrogated an additional model of promyelocytic AML by xenografting HL-60 cells into NSG mice. This corroborated the significant differences between serum exosome levels of miR-150, -155, and-1246 in leukemia engrafted mice and levels in baseline NSG or in human CD34+ cell-engrafted controls (**Fig. 4.6A**). As in our Molm-14 xenograft experiments, individual miRNA levels provided variable contributions to the ability to discriminate between cohorts. We therefore applied the scoring algorithm we derived from our Molm-14 xenografts to the miRNA levels obtained from HL-60 xenografted mice (**Fig. 4.6B**). When we applied the three cutoffs described in Figure 4B, we found that the sensitivity / specificity balanced cutoff correctly predicted 100% of HL-60 engrafted animals at 3 weeks post-engraftment; a time point at which human CD45 could not be identified by flow cytometry in 5/7 animals (**Table 4.2**). Interestingly, we found that a majority of animals engrafted with HL-60 developed peripheral chloromas (**Fig. 4.6C**), in addition to, but primarily in lieu of bone marrow disease, further highlighting the potential for detecting extramedullary disease.

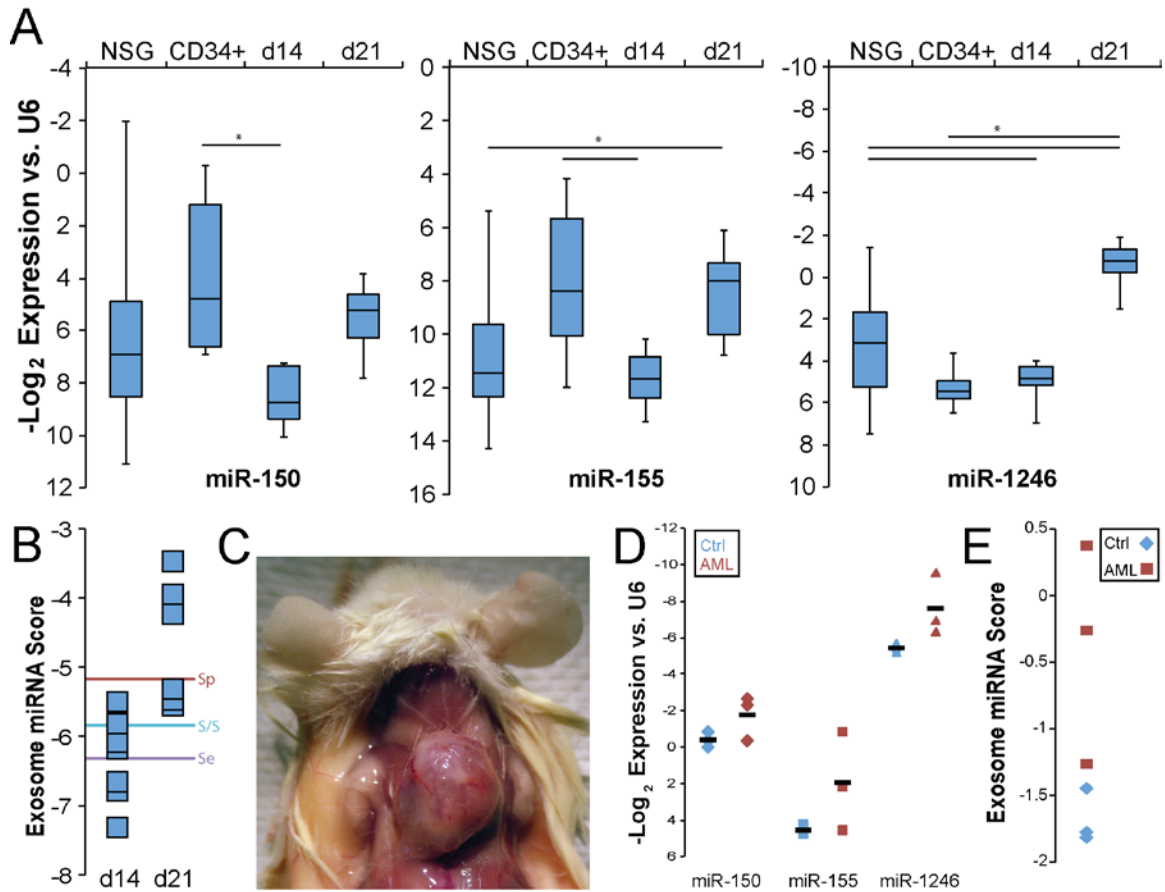


Figure 4.6: Expansion of the Scope of the Serum Exosome miRNA Biomarker

(A) Comparing serum exosome miRNA levels in HL-60. Exosomes were isolated from peripheral blood of control NSG mice as well as NSG mice engrafted with HL-60 (after 14 or 21 days; d14 and d21, respectively) or human CD34+ cells. MicroRNA levels were measured by qRT-PCR. *, $p < 0.05$ by Student's *t*. (B) Evaluation of score performance. miRNA panel scores were calculated for HL-60-engrafted mice at 14 and 21 day time. The lines correspond to alphas chosen as described in Figure 4B. (C) Chloromas in HL-60-engrafted NSG mice. (D) Patient serum / plasma exosome miRNA. Exosomes were isolated from serum or plasma from AML patients (red) or normal subjects (black), and miRNA levels of miR-150, -155, and -1246 were measured. Means are represented as horizontal bars. (E) Evaluation of score in human samples. miRNA panel scores were calculated for the serum miRNA levels depicted in D.

We had the opportunity to investigate the feasibility of our biomarker panel in a small set of patient plasma and serum samples, both previously validated as equivalent sources of circulating miRNA¹⁵³. Evaluating three AML patients and three normal subjects, we found that all three individual exosome miRNA in our panel were detectable in circulating human exosomes, and were markedly

Animal	% <i>hsa</i> -CD45+			
	PB, 3wk	PB, 4wk	BM, 4wk	Tumor, 4wk
3N	0.3	3.53	0	98.04
4N	0	0	0	97.97
5N	0	0	11.04	98.18
6N	0	0	0	98.02
1-2N	0	0.01	0.05	97.79
1-5N	0.01	0	0	52.76
1-6N	0	22.2	0	98.58

Table 4.2: Peripheral Blood and Bone Marrow Chimerism of HL-60-engrafted Mice

NSG mice were given 5×10^6 HL-60 cells via tail vein injection. At 3wk and 4wk post-injection, peripheral blood (PB) chimerism was measured by flow cytometry for human CD45. At 4wk post-injection, animals were sacrificed, and bone marrow (BM) chimerism was measured by flow cytometry for human CD45. In all animals, a chloroma was present (representative photograph in **Fig. 4.6C**) at 4wk, from which homogenized cells were >97% positive for human CD45 by flow cytometry.

different in the AML patients compared to the normal subjects (**Fig. 4.6D**). We calculated panel scores from these miRNA levels, which resulted in a clear cutoff between patients and controls (**Fig. 4.6E**). This difference tended toward, but did not reach significance ($p = 0.057$ for the overall miRNA panel score), reflecting the small sample size. We consider this result encouraging for further development of exosome miRNA panels to be tested prospectively in AML patient serum.

Discussion

The substantial morbidity and mortality experienced by AML patients in relapse creates an urgent need for efficient and cost-effective MRD surveillance. Whereas chemotherapy effectively eliminates peripheral AML blasts, most treatment regimens fail to eradicate residual leukemic cells within the bone marrow microenvironment^{146,147}. In an effort to overcome the limitations of compartmental relapse and reliance on measuring malignant cells directly, we

set out to develop exosomal miRNA, as biomarkers of disease, a prospect not limited to AML^{138,140,154}.

Detection of serum exosome miRNA circumvents both the need for an invasive marrow aspiration procedure and the reliance on the presence of leukemic blasts in the periphery. While the endothelium presents a barrier to leukemia cell egress from the marrow¹⁵⁵, exosomes are able to equilibrate with the bloodstream⁷⁰, and thus are detectable in systemic circulation. Detection of these exosomes peripherally, therefore, could potentially provide evidence of early (including extramedullary) leukemia relapse. Several recent publications indicate a correlation of select circulating miRNA, singly or as a panel of markers, with disease burden in CLL and GVHD^{126,156}. These tools rely either on direct measures of cellular miRNA, or on total cell-free miRNA in plasma, and have unfortunately not yet produced clinically useful biomarkers¹⁵⁷. Analysis of circulating exosomes allows evaluation of a population to which AML is known to directly contribute, excluding such populations as HDL-associated and protein-bound miRNA¹⁵⁸.

Xenotransplantation of human cells into immunodeficient mice, in particular NOD/SCID/IL-2 γ ^{null} (NSG) mice, is well established as a model for the systematic *in vivo* study of human AML biology^{142,143}. Molm-14, a cell line derived from a patient with monocytic leukemia, is positive for the FLT3-ITD mutation¹⁴⁴, a negative prognostic indicator¹⁵⁹ and characteristic of an aggressive, rapidly progressive disease. In earlier studies, we had established that Molm-14 and HL60 cells, like those of primary patient-derived AML samples,

produced exosomes rich in miRNA¹³³. We therefore selected these cell lines to provide consistency for development of this biomarker platform not present using primary AML xenografts with more variable kinetics¹⁶⁰.

Our recent finding that exosomes transport a preponderance of miRNA, and that the miRNA cargo is not simply a random sampling of cellular content¹³³ supports the view of AML-derived exosomes as containing specifically selected miRNA populations. Accordingly, our experiments demonstrate reproducible miRNA perturbations in peripheral blood exosomes, while less abundant AML-specific mRNA transcripts could not be detected in AML exosomes¹³³, even with substantial peripheral blood chimerism. In a series of microarray and qRT-PCR experiments we were able to combine multiple measures to derive a panel of miRNA that were not only exported in exosomes by AML, but correlated with the presence of leukemia (**Fig 2, 4**). While miR-1246 and miR-155 individually correlated well with AML in our model (**Fig 4**), the analysis of multiple miRNA in combinations allowed us to arrive at the subset most representative of AML disease status. We show that careful analysis of this panel of miRNA, rather than reliance on a single target miRNA level to indicate disease improves both sensitivity and specificity (**Fig 4**). When directly compared to the immunophenotypic MRD thresholds of 0.1%, commonly used with AML bone marrow samples, or 0.015% with AML peripheral blood samples, our panel of markers was equally sensitive in Molm-14-engrafted mice and more sensitive in HL-60-engrafted mice, often detecting leukemia in mice with zero chimerism by flow (**Fig 4B, 5B**). These observations are echoed in patient serum exosome

miRNA samples that similarly varies between leukemia patients and controls. These results support the position that serum exosomal miRNA can add sensitivity and specificity to the minimally invasive detection of residual or recurrent AML, conferring additional advantage as a cell-free marker unaffected by chemotherapy. Intriguingly, our data indicate that this serum exosome population may reflect contributions from both leukemic blasts and marrow stromal cells modified by the presence of the malignancy. While other multi-component biomarkers have been identified¹⁶¹ (including, potentially, circulating cell-free nucleic acid^{127,141}), to our knowledge this is the first such leukemia biomarker to represent multiple components of the malignant microenvironment.

In aggregate, we demonstrate the feasibility of isolating exosomal miRNA from small volumes of murine serum, allowing for discrimination between AML-bearing and control NSG mice. Through comparison with existing metrics over the course of disease and treatment, we establish exosomal miRNA as a sensitive and robust indicator in our xenograft model. A small set of primary patient samples suggests feasibility and discriminatory potential of this marker as a clinical tool. These experiments provide a platform for the development of clinical AML biomarkers with the potential to provide improved detection of occult disease in a minimally invasive methodology.

Materials & Methods

Cell culture

The AML cell lines U937, HL-60, and Molm-14 were cultured in RPMI media (Life Technologies) with 10% FBS in a Thermo Scientific cell culture incubator at 5% CO₂. Cell lines were obtained as previously reported¹³³; Molm-14 were authenticated by PCR for characteristic FLT3-ITD prior to engraftment. Primary human CD34⁺ hematopoietic progenitor cells and primary patient and control serum / plasma were collected according to an OHSU IRB-approved protocol. CD34⁺ cells were purified from cord blood using MACS cell separation (Miltenyi Biotec) and cultured in serum-free expansion media (StemCell Technologies) supplemented with 100 U/ml penicillin/streptomycin, 40 ng/ml Flt-3, 25 ng/ml SCF, and 50 ng/ml TPO (Miltenyi Biotec). Primary murine stromal cells were BM stromal cells were obtained by culturing whole BM cells isolated from the experimental animals in IMDM (Life Technologies) with 20% Vesicle-free FBS¹³³ for 4 days, then washing 2x with versene.

Mice and xenografts

NOD/SCID/IL-2 γ ^{null} mice (NSG) were purchased from The Jackson Laboratory. Animals were maintained in a pathogen-free barrier facility following an OHSU IACUC-approved protocol. Animals 6-8 weeks old were used in the experiments. 1x10⁵ Molm-14 cells/human cord blood-derived CD34⁺ cells or 5X10⁶ HL-60 cells per animal were engrafted into non-irradiated animals by *i.v.* tail-vein injection. Retroorbital blood draws were conducted as necessary to obtain serum exosomes or peripheral blood for human CD45 chimerism analysis by flow cytometry. Animals were sacrificed at indicated time points, when peripheral blood, spleen, and bone marrow were collected from each animal. For

cytarabine-treated animals, ara-C was administered by intraperitoneal injection at 300mg/kg every third day for three total injections¹⁶² starting 14d post-engraftment.

Exosome preparation and RNA extraction

Exosomes from *in vitro* cultures were isolated by differential centrifugation as described previously¹³³. Briefly, AML cells were cultured for 48 hrs, the culture media was spun at 300xg for 10 min to remove cells, then the supernatant was spun at 2,000xg for 20 min and 10,000xg for 20 min to remove cell debris. The supernatant was centrifuged at 100,000xg for 2 hrs to pellet exosomes. Exosomes from NSG serum were extracted using ExoQuick (System Biosciences). RNA was extracted from exosomes or cells using the miRNeasy kit (Qiagen) according to manufacturer's instructions.

RNA analysis and qRT-PCR

RNA was extracted from exosomes and cells using miRNeasy or RNeasy kits and quantified using a Nanodrop 2000c (Thermo). RNA integrity was measured using the Agilent Bioanalyzer 'Pico Chip' (Agilent). For RT-PCR, RNAs were converted into cDNA using the SuperScript III First Strand Synthesis Kit (Invitrogen) with oligo-dT priming, followed by PCR. A SYBR Green PCR kit (Applied Biosystems) was used for quantitative PCR. In the case of miRNA, reverse transcription and qRT-PCR were performed using mature human miRNA Taqman assays (Applied Biosystems), normalized to U6 snRNA.

Immunohistochemistry (IHC) staining

Femur IHC staining for human CD45 was performed by the Histology Core Facility at the Oregon Health and Science University. In brief, a femur was removed from each experimental mouse and fixed in 10% formalin for 24 hrs at 4 °C, then transferred to cold 70% ethanol for the storage until sectioning. The fixed femur was embedded in paraffin and sectioned at 5- μ m thickness. The femur slides were rehydrated and high-pressure treated. The treated slides were blocked and then stained with mouse anti-human CD45 antibody (Clone HI30, BioLegend) at 1:150 dilution and then biotinylated anti-mouse IgG. Mouse IgG1 isotype was used as the control. The images of antibody-stained slide were taken with a Leica ICC50 microscope equipped with HD camera using 20X lens. The image processing was performed using Adobe Photoshop (Adobe).

Flow cytometry analysis

Murine peripheral blood or bone marrow cells were labeled with antibodies to murine CD45 (Clone 30-F11) and human CD45 (Clone HI30, BioLegend) and analyzed by FACSCalibur (BD Biosciences). All data was analyzed using FlowJo software (Tree Star).

Transmission Electron Microscopy

10 μ l of Exosome preparations were deposited onto glow discharged carbon formvar 400 Mesh copper grids (Ted Pella 01822-F) for 3 min, rinsed 15 secs in water, wicked on Whatman filter paper 1, stained for 45 secs in filtered 1.33 %

(w/v) uranyl acetate, wicked and air dried. Samples were imaged at 120 kV on a FEI Tecnai™ Spirit TEM system. Images were acquired as 2048 × 2048 pixel, 16-bit gray scale files using the FEI's TEM Imaging & Analysis (TIA) interface on an Eagle™ 2K CCD multiscan camera.

Microarrays

Microarray assays were performed in the OHSU Gene Profiling Shared Resource. For each sample, a 130 ng of total RNA was labeled using the Flash-Tag Biotin HSR miRNA Labeling Kit (Affymetrix) by polyadenylation and ligation with biotinylated 3'DNA dendrimers. Labeled RNA was mixed with hybridization controls and incubated overnight with the GeneChip miRNA 3.0 array (Affymetrix) as per manufacturer recommendations. Arrays were scanned using the GeneChip Scanner 3000 7G with autoloader (Affymetrix). Image processing was performed using Affymetrix GeneChip Command Console software followed by analysis with Expression Console software (Affymetrix). Array performance and general data quality were assessed using Signal All, mean background intensity, number of detected probe sets, % P, all probe set mean, all probe set standard deviation, all probe set RLE mean, and % species specific small RNA probe sets detected. All arrays passed standard performance quality thresholds.

Microarray statistical analysis and data visualization

Individual array data (.cel files) were uploaded to R software package and analyzed using Bioconductor's Oligo package. Normalization was conducted on all samples in a single set using RMA Background and Quantile Normalization

sub-routine. Signal intensities were log₂ transformed and probe set values summarized using Median Polish Summarization Method. Final data set included paired samples from exosome cell. Further analysis included 3391 mature and pre-mature human miRNA probe sets. Data visualization tools (e.g., box plot, hierarchical clustering, matrix plots and multi-dimensional scaling) were used to assess the general data quality and outliers. To determine differentially expressed miRNA genes, the mixed model was used to assess differences in miRNA probe expression between exosome samples and cell samples. Unadjusted statistical significance was set at $p \leq 0.05$ with FDR correction at $p \leq 0.10$ for multiple testing where relevant. Fold Change values of 2.0 were used as a cut-off to identify up- and down-regulated probes.

Normalized log₂ transformed signal data for all human mature miRNAs were imported into Partek Genomics Suite 6.6 software and then filtered to include only miRNA signal data of interest prior to generating individual heat maps. The Tools Discover Hierarchical Clustering subroutine was invoked to create each clustered heat map. Samples and miRNA were clustered using Pearson's Dissimilarity as the measure of distance with complete linkage.

Statistical analysis

The results are presented as mean \pm standard deviation or SEM (where indicated). The 2-tailed Student *t*-test was used for comparison between groups. A value of $p < 0.05$ was considered statistically significant. To elucidate combinations of serum miRNA that could discriminate between engrafted mice

(evaluated through 14 and 21 days) versus control mice, we estimated linear combinations of markers via logistic regression and evaluated the resulting receiver operating characteristic (ROC) curves (plots of sensitivity versus 1 minus specificity) using R.

Complete blood count

Blood was drawn from mice retroorbitally into EDTA-treated Microvettes (Sarstedt). Counts were generated using a Hemavet HV950 (Drew Scientific).

CHAPTER 5: AML Exosome MicroRNA Target Analysis

Abstract

AML-derived exosomes deliver an actively selected and concentrated subset of cellular microRNA to multiple cell types within the bone marrow microenvironment. In aggregate, the content of these exosomes is sufficient to suppress hematopoietic function when delivered to the marrow via intrafemoral injection. This functional suppression may be related to molecular changes observed *in vitro* upon treatment of HSPC or stroma with AML exosomes. The experiments described in this chapter address this relationship, by evaluating several of the most concentrated microRNA in AML exosomes. Through broad characterization of microRNA targeting, combined with specific validation experiments and the utilization of public bioinformatics resources, these experiments begin to clarify the complex effects of the delivery of exosomal microRNA to the different recipient cell types within the bone marrow.

Introduction

Having gained an appreciation for the substantial enrichment of miRNA in exosomes secreted by AML blasts, and the marked selection of particular miRNA species that occurs, we became interested in the regulatory role this population of small RNA has within the marrow. As each miRNA has the capacity to regulate many targets, and as exosome delivery is not a targeted process, exosome-transferred miRNA have the potential to regulate many processes in many cell types simultaneously, with differing transcripts being suppressed in different recipient cells. The total effect of exosomal miRNA is therefore a combination of the effects of the many individual miRNA contained within the

exosomes, overlaid on the expression profile of the various recipient cells. In order to gain an understanding of what this communication signifies in the context of AML, it is necessary to take both a broad and a narrow view; to capture all the potential activity of a particular miRNA, and then focus that set of targets within the transcriptome of each cell type of interest. Despite this, it is possible to restrict the set of miRNA of interest before taking any experimental approach; the fact that miRNA regulation of a given target is dose-dependent (albeit in relationship to the *a priori* expression level of target mRNAs) implies that the most enriched miRNA in exosomes are those most potently regulating the recipient cells. Further, the scope of our investigation can be limited by the set of observations we are attempting to explain - the suppression of clonogenicity in HSPC, and the failure of hematopoietic support in marrow stroma. As other groups have provided baseline assessment of the transcriptomes of our cell populations of interest¹⁶³, and as there is substantial existing research into miRNA in AML, our experimental design gained the benefit of some insight into which particular miRNA are likely to be of significance, or to target hematopoietically relevant transcripts.

Results

Our initial investigations into AML exosome miRNA content revealed more than one thousand unique species of miRNA to be present; it was necessary to pare down this list for more in-depth targeting studies. Fortunately, our data repeatedly presented the same group of candidate miRNA as promising throughout our experimentation.

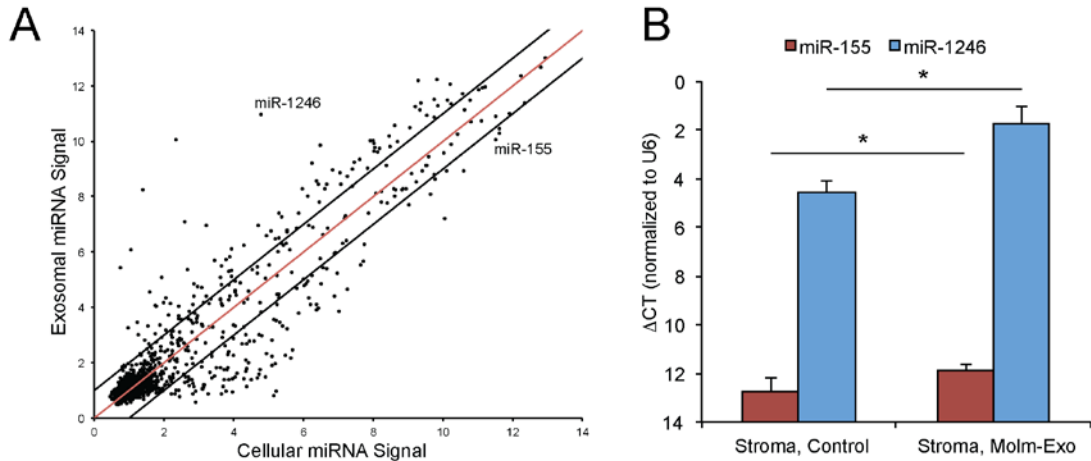


Figure 5.1: Packaging and Import of miRs -155 and -1246

(A) Microarray comparison of Molm-14 cell and exosome miRNA. miR-155 and -1246 are indicated. The heavy black lines indicate 2-fold change between cell and exosome. (B) Marrow stromal cells from orthopedic patients without malignancy were exposed overnight to exosomes from Molm-14, then miR-155 and -1246 were assayed by qRT-PCR normalized to U6 snRNA. *, $p < 0.01$.

MicroRNA-155 is well known in both malignancy and hematopoietic contexts. It is responsible for regulation of hematopoietic differentiation through inhibition of PU.1¹⁶⁴, and provides a mechanistic link between Notch signaling and NF- κ B in the control of marrow stromal cytokine secretion¹⁶⁵. Its activation through STAT5 signaling has been shown to support the leukemogenic potential of HSPC¹⁶⁶, it is inversely associated with response to chemoimmunotherapy in CLL¹⁶⁷, and its overexpression causes a B-cell malignancy in transgenic mice¹⁶⁸.

MicroRNA-1246, on the other hand, is almost entirely novel. Very little work has been done on this microRNA to date, and although a small number of reports suggest potential links to cancer, it has no known hematopoietic relevance¹⁶⁹⁻¹⁷¹. However, it was consistently among the most prevalent miRNA in our microarray studies of AML cell lines, and only present at very low levels in the cells and exosomes of nonmalignant CD34+ cells. In our biomarker studies,

it was the single best individual predictor of disease status among all miRNA evaluated.

Examining the levels of these microRNA in Molm-14 exosomes in the microarray data we generated reveals that while miR-1246 is highly selected for inclusion into exosomes, miR-155 is present in exosomes at a slightly lower level than its cellular representation indicates. However, its absolute signal level is still similar to that of miR-1246, due to its overrepresentation in the producing cells (**Fig. 5.1A**). In order to verify that these particular miRNA are efficiently transferred to nearby cells by AML exosomes, we treated human marrow stromal samples with exosomes derived from Molm-14 overnight, and then washed the cells and assayed for miR-155 and -1246, finding both miRNA to be significantly increased in recipient cells versus controls (**Fig. 5.1B**), as we had already found for miR-155 in exosome-exposed c-Kit⁺ HSPC (**Fig. 2.5F**).

Having selected miRNA for initial investigation, we began with a survey of all targets of miR-155 using RISCTrap. This technology utilizes a dominant negative GW182 protein in order to capture mRNA targets inside RISC complexes without degrading them. In a cell expressing this protein and transfected with a miRNA of interest, the mRNA targeted by this miRNA will be enriched in these complexes, which can be immunoprecipitated using a FLAG tag on the modified GW182. After subsequent enrichment for polyadenylated transcripts (and so selection for mRNA), the precipitated RNA are sequenced and compared to other transfected miRNA or scramble in order to identify the target set of mRNA of the miRNA of interest¹⁷² (**Fig. 5.2A**). After comparison to

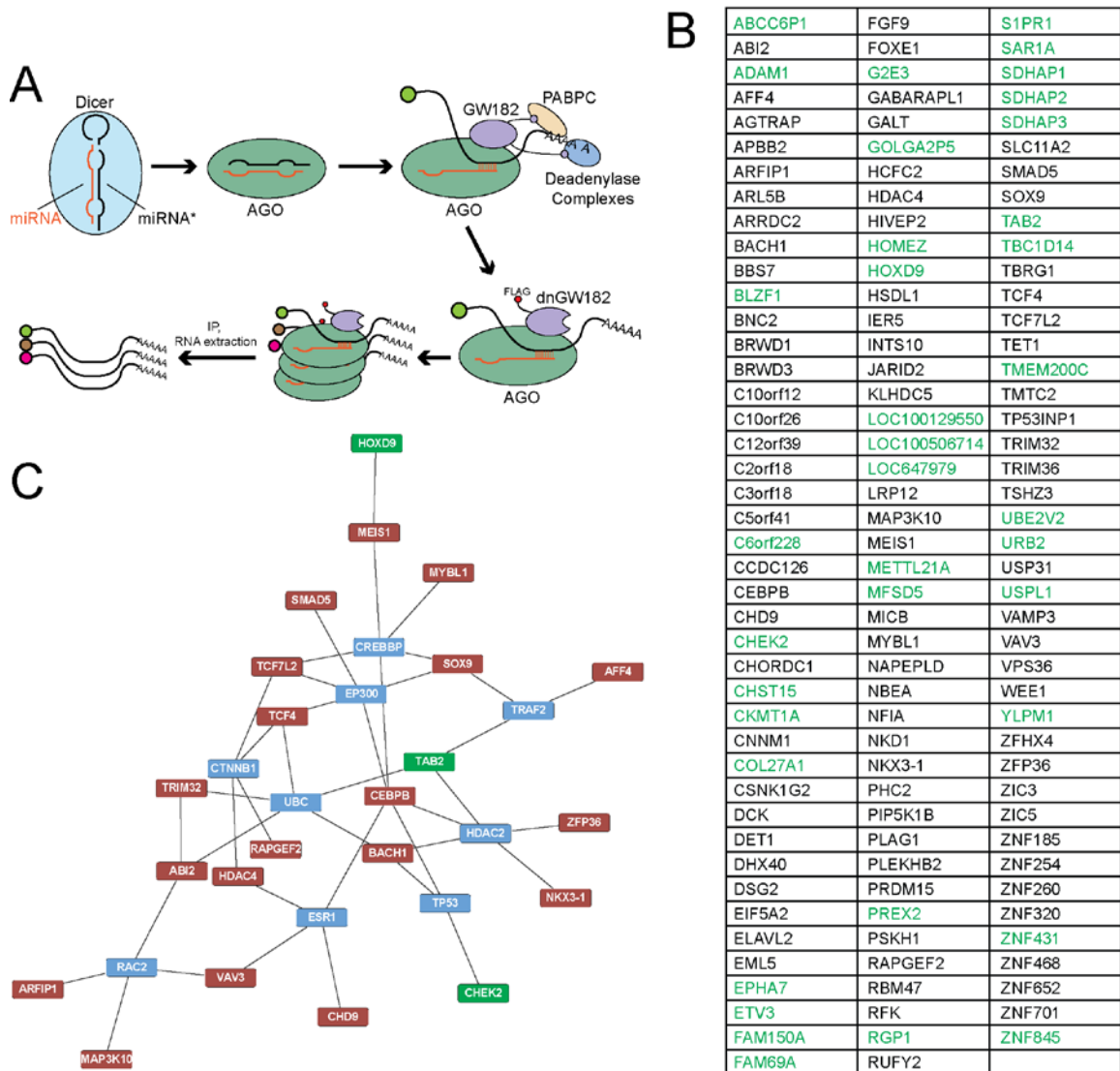


Figure 5.2: RISCTrap mRNA Targeting of miR-155

(A) Schematic diagram of RISCTrap target analysis. (B) mRNA targets of miR-155, by significant enrichment ($FDR > 0.15$) in cells transfected with miR-155 versus -132 and -137. Targets in green are those not predicted by the miRWalk database. (C) Central interaction network of miR-155 targets, based on STRING protein interaction database query. Central cluster of 4th and higher degree nodes is shown. Proteins in green were those not predicted by miRWalk but identified by RISCTrap, proteins in red were identified as miR-155 targets by RISCTrap, proteins in blue are neither.

the control miRNAs miR-132 and -137, a set of targets were selected based on significant enrichment in the miR-155 transfected samples ($FDR < 0.15$; details of statistical analysis in ¹⁷²) (Fig. 5.2B). Comparing this list to predicted targets using the miRWalk database¹⁷³, 94/128 were predicted by at least one of six

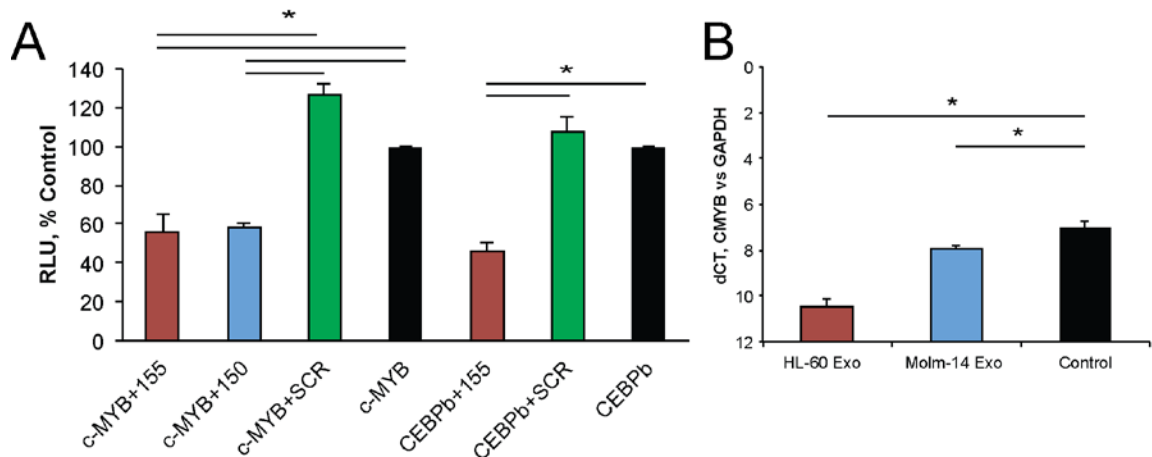


Figure 5.3: Validation of miRNA Targeting

(A) 3'UTR luciferase reporter assay demonstrating direct suppression of CEBPb by miR-155 and of c-MYB by miR-150 and -155. *, $p < 0.01$. (B) Transcript levels of c-MYB in c-Kit⁺ HSPC exposed to HL-60- or Molm-14-derived exosomes overnight, normalized to GAPDH. *, $p < 0.01$.

prediction algorithms (targets not predicted in green in **Fig. 5.2B**), while 24/128 had been experimentally validated. The results of this comparison supported the validity of our experimentally determined target set.

We next took advantage of the STRING protein interaction database¹⁷⁴ to identify connected networks of proteins regulated by this miRNA. After identifying all proteins interacting with the targets identified by RISCTrap, the list was reduced to experimentally-supported interactions between human proteins, and then to quaternary or higher-degree nodes within the resulting interaction network. This process yielded a clear cluster of interacting protein nodes, most of which were identified as direct targets of miR-155, but several of which were included by virtue of being interacting partners of many direct targets (**Fig. 5.2C**).

Beginning with this broad network of targets, we began investigations on specific targeting. Using a dual-luciferase 3'UTR reporter system, we validated the targets c-MYB and CEBP β (**Fig. 5.3A**), demonstrating clear suppression of

these targets by miR-155 (and -150, in the case of c-Myb, implying multiple targeting by AML exosomes). These results were then mechanistically linked with the observed transfer of miR-155 to c-Kit⁺ cells by evaluating transcript levels of c-MYB in c-Kit⁺ cells exposed to AML exosomes (**Fig. 5.3B**). In aggregate, these results provide the first direct demonstration of suppression of a hematopoietic target by AML exosome miRNA.

Discussion

In the hematopoietic niche, HSC are maintained primarily in quiescence, protected from the immune system and from apoptosis. In the leukemic niche, HSC are no longer retained, and leukemic cells are instead the recipients of pro-growth and anti-apoptotic signaling. Conversion of the marrow microenvironment from one to the other requires the subversion of several cell types. As exosomal microRNA are capable of targeting multiple transcripts in disparate cells, are efficiently and selectively packaged, and trafficked to nearby cells without entry restriction, they represent a uniquely parsimonious means by which this may be accomplished. Many studies have demonstrated correlations between miRNA expression in AML blasts and leukemic potential, progression, or prognosis^{166,175-177}, but to date mechanistic links between these phenomena have been largely speculative.

In order to address this problem, we chose to focus on miRNA candidates selected for high levels of incorporation into AML-derived exosomes, as well as either a marked selection in exosome incorporation or a firmly established role in

hematopoiesis and leukemia. The RISCTrap technology provided us with the means to globally assess the targets of our selected miRNA, providing a set of enriched target mRNA to consider in the context of leukemia and hematopoiesis. We first used it to assess the target set of miR-155, reasoning that starting with a well-studied miRNA would enable us to both assess the effectiveness of the assay (through comparison with other targeting studies), and provide a foundation on which to base our subsequent experiments. Our results confirmed previous predicted or validated targets, including MEIS1¹⁷⁸, HDAC4¹⁷⁹, CEBP β ¹⁸⁰, and TAB2¹⁸¹, while also suggesting previously unanticipated targets, such as CHEK2 and HOXD9.

The first demonstration of TAB2 targeting by miR-155 involved MSC, wherein the authors demonstrated that such targeting produced a suppression of iNOS, interfering with the immune modulating effects of MSC in culture¹⁸¹. HDAC4 suppression has been shown to derange endothelial cell proliferation and localization as one of many downstream mediators of VEGF¹⁸². CEBP β , when upregulated in HSC, produces myeloid differentiation and proliferation¹⁸³. MEIS1 suppression by exosomal miR-155 is a promising prospect for further study, as it presents an unexpected target population for AML-derived exosomes: megakaryocytes. MEIS1 expression is essentially unique to megakaryocytes among differentiated blood lineages¹⁸⁴, where it is an important transcriptional activator of CXCL4¹⁸⁵, among other genes. As recent evidence suggests that megakaryocyte-derived CXCL4 is necessary for HSC quiescence¹⁸⁶, its suppression could be a significant factor in hematopoietic failure secondary to

AML. In aggregate, these targets and their relevant cell populations illustrate the potency of nonselective exosomal transfer of miRNA within the marrow niche.

Beyond the individual direct mRNA targets of miRNA, interrogating the networks these proteins participate in with the STRING interaction database allows us to recognize potential other, indirect mediators of miRNA effects in these cells. In the case of miR-155, proteins of meaningful impact that interact heavily with direct miR-155 targets include CTNNB1 (which regulates HSC self-renewal)¹⁸⁷, HDAC2 (which regulates HSC homeostasis and differentiation)¹⁸⁸, and ESR1 (which is implicated in B-cell differentiation)¹⁸⁹. Indirect manipulations of any of these proteins have the potential for significant phenotypic impact on hematopoiesis.

Focusing on the specific targets CEBP β and c-MYB, we validated both targeting by miR-155 and knockdown in exosome-receiving cKit⁺ cells (**Fig. 5.3**), demonstrating that exosome transfer of miR-155 from AML blasts to HSPC is sufficient to suppress c-MYB expression. This protein has previously been shown to directly regulate HSC self-renewal, and the loss of c-MYB in LSK cells causes a deficit in colony forming capacity by CFU-C¹¹⁸, phenocopying our previous observations with *in vitro* and *in vivo* exosome delivery. In sum, the experiments detailed in this chapter demonstrate the direct targeting of recipient cell transcript by exosomal miRNA, and support a role for cMYB suppression in HSPC in the hematopoietic suppression seen in AML.

Materials & Methods

Microarrays

Microarray assays were performed in the OHSU Gene Profiling Shared Resource. For each sample, a 130 ng of total RNA was labeled using the Flash-Tag Biotin HSR miRNA Labeling Kit (Affymetrix) by polyadenylation and ligation with biotinylated 3'DNA dendrimers. Labeled RNA was mixed with hybridization controls and incubated overnight with the GeneChip miRNA 3.0 array (Affymetrix) as per manufacturer recommendations. Arrays were scanned using the GeneChip Scanner 3000 7G with autoloader (Affymetrix). Image processing was performed using Affymetrix GeneChip Command Console software followed by analysis with Expression Console software (Affymetrix). Array performance and general data quality were assessed using Signal All, mean background intensity, number of detected probe sets, % P, all probe set mean, all probe set standard deviation, all probe set RLE mean, and % species specific small RNA probe sets detected. All arrays passed standard performance quality thresholds.

Microarray statistical analysis and data visualization

Individual array data (.cel files) were uploaded to R software package and analyzed using Bioconductor's Oligo package. Normalization was conducted on all samples in a single set using RMA Background and Quantile Normalization sub-routine. Signal intensities were log₂ transformed and probe set values summarized using Median Polish Summarization Method. Final data set included paired samples from exosome cell. Further analysis included 3391 mature and

pre-mature human miRNA probe sets . Data visualization tools (e.g., box plot, hierarchical clustering, matrix plots and multi-dimensional scaling) were used to assess the general data quality and outliers. To determine differentially expressed miRNA genes, the mixed model was used to assess differences in miRNA probe expression between exosome samples and cell samples. Unadjusted statistical significance was set at $p \leq 0.05$ with FDR correction at $p \leq 0.10$ for multiple testing where relevant. Fold Change values of 2.0 were used as a cut-off to identify up- and down-regulated probes.

RNA analysis and qRT-PCR

RNA was extracted from exosomes and cells using miRNeasy or RNeasy kits and quantified using a Nanodrop 2000c (Thermo). For RT-PCR, RNAs were converted into cDNA using the SuperScript III First Strand Synthesis Kit (Invitrogen) with oligo-dT priming, followed by PCR. A SYBR Green PCR kit (Applied Biosystems) was used for quantitative PCR. In the case of miRNA, reverse transcription and qRT-PCR were performed using mature human miRNA Taqman assays (Applied Biosystems), normalized to U6 snRNA.

RISCTrap

RISCTrap was performed in collaboration with the Richard H. Goodman laboratory (OHSU), as described in ¹⁷². Briefly, 6×10^6 HEK293T were cotransfected with 20 μ g of expression plasmid for Flag-dnGW182 and 50 nM miRNA mimics, using Lipofectamine 2000 (Invitrogen). Twenty-four hours later, cells were rinsed with cold PBS and harvested in cold lysis buffer. Cleared

lysates were incubated for 2h at 4°C with 10 µL of preblocked Flag–M2 agarose. After washing, bound RNA was eluted by Trizol extraction (Invitrogen) and mRNA was enriched by generation of double-stranded cDNA followed by a 16-h T7 IVT reaction. The TruSeq v2 library protocol was used on 200 ng of mRNA-enriched material from each sample. Samples were pooled into three lanes, with each biological replicate sequenced in a separate lane on a HiSeq v3 platform using a single-read 100-bp protocol. Reads were mapped using TopHat v1.4.0 to a human reference genome. We determined a baseline for the dataset (minimum of 200 counts per target), removed nonpolyadenylated transcripts, and normalized to the median of geometric ratios. Transcript-specific variance estimates were obtained by fitting the negative binomial model, and significantly enriched targets were determined with ANOVA among the biological replicates. STRING database¹⁷⁴ analysis was performed using Cytoscape software¹⁹⁰. Interaction edges were limited by selecting for human transcripts only, including only edges with experimental support, then filtering for quaternary and higher-degree nodes and pruning those nodes remaining unconnected.

Luciferase Assays

The 3' untranslated regions of proteins of interest were cloned into the psiCHECK2 dual reporter vector (Promega). 100ng of this vector, along with 25µM miRNA mimic, was introduced into 4.0×10^5 HEK293 cells using Lipofectamine 2000 (Life Technologies). 48 hours later, luciferase activity was measured using the Dual Luciferase Assay (Promega).

CHAPTER 6: Conclusions and Future Directions

Future directions

AML Vesicle Biogenesis and Trafficking

It is generally agreed that the biogenesis of exosomes occurs upon fusion of the late endosome (or multivesicular body) with the plasma membrane, thereby releasing the intraluminal vesicles (ILVs) into the extracellular space¹⁹¹. Despite this, the mechanisms leading to the packaging of particular molecules and the targeting of late endosomes to the plasma membrane rather than the lysosome are far from clear. While the ESCRT protein complexes have been shown to play a role both in the formation of these ILVs and to cargo selection¹⁹², ILVs can also be generated independently of the ESCRT proteins¹⁹³. Mechanisms have been proposed whereby both mRNA¹⁹⁴ and miRNA¹⁹⁵ can be sorted into exosomes, however, neither of these mechanisms is purported to be exclusive or consistent across cell types. In the case of miRNA, generation of new mature miRNA (through continued processing of precursors) has been shown to occur within exosomes, further complicating their biogenesis¹⁹⁶. As the work presented in this thesis demonstrates, however, cargo selection is substantially different in malignant cells compared to nonmalignant HSPC controls. A more complete understanding of exosome biogenesis and packaging will be necessary in order to explain the reasons behind the shift in exosome content that occurs in leukemogenesis, as analysis of the microRNA content in cells and exosomes suggests that these changes are not simply reflective of changes in transcription in the producing cells (**Fig. 2.4A**).

Although it has been assumed that exosome uptake by a recipient cell requires specific receptor-ligand interactions¹⁹¹, numerous such interacting pairs have been proposed¹⁹⁷⁻¹⁹⁹, none of which have been shown to universally enable or restrict exosome uptake. It therefore remains to be elucidated which, if any, of these mechanisms are at play within the tumor microenvironment. Considering the permissive apparent nature of exosome uptake, however, it is perhaps more likely that a more general mechanism – such as the endocytosis of membranes containing external-leaflet phosphatidylserine^{200,201} – is responsible for exosome uptake in this context. Additional research into exosome biogenesis, cargo selection, and uptake will reveal the specific molecular mechanisms by which molecules are transferred in exosomes between AML blasts and other cells, which could allow for modification of cargo content or the inhibition of exosome secretion or uptake. These developments would enable additional angles of experimental approach, in addition to having potential therapeutic applications.

Impact on the Marrow Niche / AML Exosome MicroRNA Target Analysis

The fundamental importance of the microenvironment to a developing cancer has been recognized for more than a century²⁰². Similarly, the necessity of stromal support for hematopoietic stem cells is well established, and has generated a substantial literature delineating the roles of many cell types in this capacity. Recent reports indicate that myeloid leukemias are capable of co-opting these cell populations, converting the marrow from a hematopoietic microenvironment to a leukemic niche^{42,203,204}. Upon development of a chronic-phase myeloid malignancy, murine marrow cells were shown to shift in

composition and function, becoming less capable of supporting HSC, and promoting the expansion of leukemic cells⁴². Additionally, numerous experimental perturbations of the marrow stroma have been shown to independently produce oncogenesis²⁰⁵, including the specific disruption of miRNA maturation in osteolineage cells²⁰⁶ and the derepression of miR-155 expression via ablated Notch signaling¹⁶⁵. The work presented in this thesis demonstrates that stromal cells are altered by leukemic engraftment, and themselves secrete exosomes containing abnormal microRNA content, perhaps contributing to the self-reinforcing nature of the leukemic niche noted by others⁴². Collectively, these studies support a model of homeostatic *versus* malignant hematopoiesis that hinges upon the coordinated action of stromal cell populations, and specifically upon the activity of microRNA within those cells. This model suggests major flaws in the strategy of traditional therapeutic approaches to AML, which rely upon targeting either the rapid cell divisions or specific mutated proteins in leukemic blasts themselves. If AML is truly a disease of the marrow compartment, a view supported by this thesis as well as the referenced studies, new types of therapy will be necessary to manage this disease. It is, however, encouraging to note that displacement of leukemic cells from the hematopoietic niche allows them to be replaced, and indeed outcompeted, by nonmalignant HSC in a transplant setting²⁰³, suggesting that the microenvironmental changes introduced by AML may be reversible²⁰⁷. In order to address this possibility, and to determine whether such a reversal can be supported with medical intervention, future studies will be required to examine

the extent of microenvironmental dysfunction, the concomitant alterations in residual HSC, and the mediators of these changes.

As regulation of a messenger RNA by a miRNA is greatly dependent upon the respective concentrations (doses) of the two transcripts, the most prominent miRNAs transferred in exosomes are a logical starting point for such investigations, given that intrafemoral exosome injection is sufficient to induce marrow dysfunction (**Fig. 3.3**). Due to the promiscuous nature of miRNA target regulation⁹¹, my initial investigations into the role of miR-155 in recipient cells centered around the use of RISCTrap, combined with a protein interaction database, to identify likely candidate pathways regulated by this miRNA. This combined interrogation of the experimental data described here and publicly available data has already yielded promising results in cMYB and CEBP β (**Fig. 5.3**), but as our investigations into miR-1246 and other overrepresented miRNA components of AML exosomes proceed – using similar methods, but each time expanding the data used to inform the STRING database query – we will create an increasingly representative, higher resolution picture of the regulatory influence of AML exosomal miRNA. This data can then be used to inform directed molecular, *in vitro*, and *in vivo* studies to test the validity and relevance of these changes in particular target cell populations, and in whole organism models of disease. The ultimate goal of this research is to clarify how specifically the marrow microenvironment is altered by leukemia, enabling interventions that would render leukemic blasts more vulnerable to chemotherapy, reduce the

occurrence of relapse, and relieve the hematopoietic suppression that accompanies AML.

AML Exosomes as Serum Biomarkers

Recently, both circulating cell-free RNA and circulating exosomes have become popular targets of study for the development of biomarkers in numerous malignancies^{59,70,72}, work that builds on the increased output of exosomes by cancer cells⁷⁰ and the equilibration of exosomes from multiple tissues with the bloodstream⁶⁵. Our observation that leukemic exosome miRNA content differs substantially from that of the producing cell as well as from that of exosomes from nonmalignant hematopoietic cells (**Fig. 2.4A**) suggested that serum exosome miRNA could potentially harbor site-independent indicators of disease in AML, and the studies in Chapter 4 of this thesis support that potential. It is clear, however, that the limited number of AML patient samples presented (**Fig. 4.6**) is an incomplete representation of the diversity of AML patients, and that the ultimate utility of any potential biomarker will require evaluation in numerous individual patients over time. We have already begun the expansion of these studies into additional patient samples, collected at time of diagnosis. With this additional data, we will begin to be able to correlate serum exosome miRNA biomarker performance with leukemia subtype and mutation status, which will ideally enable us to refine the applicability and sensitivity of the marker. It is also likely that marker performance could be improved by expansion to additional targets. Ideally, this would be done using an unbiased, inclusive assay, such as deep sequencing, on multiple clinical samples of distinct AML subtypes in order

to identify the most broadly applicable marker set, as well as to identify subsets of disease for which other, more specific miRNA could be measured. Ideally, the eventual product of these investigations would be a set of related serum exosome miRNA markers, some broadly applicable across the spectrum of leukemic disease (useful in the detection of secondary disease in patients who have received chemotherapeutics for non-hematologic malignancies, for example), and some specific to a more narrowly defined disease, with enhanced sensitivity (for use in relapse detection). These markers, once defined, could greatly inform patient care, allowing for more timely identification of disease status, and improving risk stratification and treatment selection. The work performed in this thesis provides a promising first step in this direction.

Conclusions

At the outset of our studies, it had not previously been demonstrated that AML blasts secreted exosomes, and the first study to be published describing extracellular vesicles in AML did not examine their RNA content²⁰⁸. Although it was appreciated that advancing AML disrupted and converted the hematopoietic microenvironment⁴², a role for exosomes in this process had not been described. In this thesis, I establish that AML blasts constitutively secrete extracellular vesicles in the sub-100nm size range that are of endocytic origin and typical exosome morphology and density, and that these exosomes represent the majority of extracellular vesicles secreted by these cells. Using low-oxygen tissue culture conditions, I demonstrate that the hypoxic nature of the marrow microenvironment encourages the production of exosomes by AML, without

significantly altering their overall RNA concentration or microRNA content. This likely contributes to the levels of AML-derived serum exosomes in a nascent marrow-resident leukemia, driving the potential for earlier detection. Bioanalyzer examination of total exosome RNA demonstrates that there is a substantial increase in the representation of small RNA, including miRNA, in exosomal RNA as compared to the RNA of the producing cells, a finding that holds across all leukemic and stromal exosomes tested. Employing microarray analysis and qRT-PCR, I show for the first time that AML exosomal miRNA is both primarily mature, and distinct both from that of AML blasts and that of exosomes from nonmalignant hematopoietic cells. Further, these exosomes are taken up both by marrow stromal cells and by HSPC, causing substantial increases in the levels of select miRNA in the recipients. Together, these findings suggest a model of AML niche communications wherein oncogenesis coincides with a transformation of exosomal content, delivering selected miRNA cargo to nearby stroma and HSPC, and thereby manipulating the function of recipient cells.

In order to demonstrate the plausibility of this model, I show that exposure to AML exosomes causes marked phenotypic change in recipient cells. Stromal cells exhibit decreased expression of key niche factors *Scf* and *Cxcl12*, while MEFs showed increased proliferation and expression of proangiogenic *Vegf* following transfer (and functional translation) of *Igf-IR*. Further, stroma altered by AML engraftment produce exosomes *ex vivo* that are themselves distinct in miRNA cargo, despite the absence of AML blasts for multiple passages in culture. In HSPC, exosome-exposed cells lose their ability to home to a higher

concentration of CXCL12, through decreased surface expression of CXCR4. In Molm-14 xenograft, this produces mobilization of progenitors from the marrow into the peripheral blood, shown as a decrease in clonogenicity in the marrow combined with an increase in clonogenicity among PBMCs. In all models, exposure to AML-derived exosomes yields a dysregulation of transcription factors including *cMyb* and *Hoxa9*, along with a significant suppression in the ability of these cells to form colonies in culture. This occurs both *in vitro* and *in vivo*, with either the direct presence of AML cells or the introduction of purified exosomes, and holds in human progenitors as well as murine. In aggregate, these results support a direct role for AML-derived exosomes in the depletion of functional HSPC from the marrow, both by durable alteration of the hematopoietic niche and by direct effects on the HSPC themselves.

The secretion of exosomes with malignancy-specific miRNA content suggests the potential for an exosome biomarker. I pursued this possibility by examining serum exosome miRNA in several xenograft models of AML. Exosomal miRNA can be reliably assayed by qRT-PCR in less than 50 μ L of serum, easily obtainable from engrafted mice. After establishing consistent kinetics in our models, I evaluated several miRNA in the serum of engrafted mice over the course of disease, finding one panel of markers to be substantially more sensitive and specific than peripheral blood flow cytometry, while being less vulnerable to the confounding influence of chemotherapy than other measures. In a separate, extramedullary disease model, as well as in a limited set of primary patient samples, I show that this panel of serum exosome miRNA is

applicable more broadly. The biomarker development described in this thesis provides a foundation for the development and testing of a promising minimally invasive biomarker for AML.

Finally, I pursued a more mechanistic line of inquiry in my investigation of exosomal miRNA trafficking within the marrow microenvironment, focusing first on miR-155, a microRNA of established relevance to both hematopoiesis and leukemia, and one that is highly enriched in AML exosomes. By collaborating with Drs. Lulu Cambronne and Rongkun Shen, the inventors of the RISCTrap technology, we provide a survey of the mRNA targets of this miRNA, which both confirmed previously reported targets and identified potential novel ones. In addition to these directly regulated targets of miR-155, I was able to determine additional targets that are likely to be regulated indirectly through the suppression of interacting partners through the use of the STRING database, which provided a regulatory network that will be further refined as additional miRNAs are studied. Among these targets was the RNA encoding the protein cMYB, noted to govern self-renewal in HSC. Using a 3'UTR luciferase assay, I demonstrate that this transcript is indeed a direct target of miR-155. Combined with the evidence in this thesis that exosome exposure both substantially increases miR-155 levels and decreases *cMyb*, this strongly suggests a contributing mechanism to hematopoietic suppression in AML.

In total, the experiments described in this thesis characterize the secretion of exosomes by AML, describe their miRNA content, and demonstrate its trafficking to neighboring cells of multiple types within the bone marrow. These

exosomes are sufficient to disrupt HSPC function, and create lasting dysregulation of stromal cells. The exosomal distribution of signaling molecules to diverse cell types within the marrow therefore represents a single mechanism whereby AML coordinately regulates the marrow microenvironment. This regulation is entirely separate and distinct from traditional signaling modalities, and therefore represents a new compartmental signaling paradigm. Further, AML-derived exosomes equilibrate with the bloodstream, where they can be detected, and their miRNA can provide early evidence of leukemia. These experiments represent a necessary groundwork for an understanding of the role that exosomes play in the establishment of leukemia and the suppression of hematopoiesis that accompanies it.

REFERENCES

1. Piller G. Leukaemia - a brief historical review from ancient times to 1950. *British journal of haematology* 2001;112:282-92.
2. Tallman MS. Acute myeloid leukemia; decided victories, disappointments, and detente: an historical perspective. *Hematology / the Education Program of the American Society of Hematology American Society of Hematology Education Program* 2008:390.
3. Bennett JM, Catovsky D, Daniel MT, et al. Proposals for the classification of the acute leukaemias. French-American-British (FAB) co-operative group. *British journal of haematology* 1976;33:451-8.
4. Bennett JM, Catovsky D, Daniel MT, et al. Proposed revised criteria for the classification of acute myeloid leukemia. A report of the French-American-British Cooperative Group. *Annals of internal medicine* 1985;103:620-5.
5. Vardiman JW, Thiele J, Arber DA, et al. The 2008 revision of the World Health Organization (WHO) classification of myeloid neoplasms and acute leukemia: rationale and important changes. *Blood* 2009;114:937-51.
6. Khalidi HS, Medeiros LJ, Chang KL, Brynes RK, Slovak ML, Arber DA. The immunophenotype of adult acute myeloid leukemia: high frequency of lymphoid antigen expression and comparison of immunophenotype, French-American-British classification, and karyotypic abnormalities. *American journal of clinical pathology* 1998;109:211-20.
7. Head DR. Revised classification of acute myeloid leukemia. *Leukemia* 1996;10:1826-31.
8. Leith CP, Kopecky KJ, Godwin J, et al. Acute myeloid leukemia in the elderly: assessment of multidrug resistance (MDR1) and cytogenetics distinguishes biologic subgroups with remarkably distinct responses to standard chemotherapy. A Southwest Oncology Group study. *Blood* 1997;89:3323-9.
9. Kohlmann A, Bullinger L, Thiede C, et al. Gene expression profiling in AML with normal karyotype can predict mutations for molecular markers and allows novel insights into perturbed biological pathways. *Leukemia* 2010;24:1216-20.
10. Howlader N NA, Krapcho M, Neyman N, Aminou R, Waldron W, Altekruse SF, Kosary CL, Ruhl J, Tatalovich Z, Cho H, Mariotto A, Eisner MP, Lewis DR, Chen HS, Feuer EJ, Cronin KA, Edwards BK (eds). SEER Cancer Statistics Review, 1975-2008. In. 2011 ed. Bethesda, MD: National Cancer Institute; 2010.
11. Rowe JM, Tallman MS. How I treat acute myeloid leukemia. *Blood* 2010;116:3147-56.
12. Barrett A, Barrett AJ, Powles RL. Total body irradiation and marrow transplantation for acute leukaemia. The Royal Marsden Hospital experience. *Pathologie-biologie* 1979;27:357-9.
13. Dicke KA, Zander AR, Spitzer G, et al. Autologous bone marrow transplantation in relapsed adult acute leukemia. *Experimental hematology* 1979;7 Suppl 5:170-87.

14. Faulk K, Gore L, Cooper T. Overview of therapy and strategies for optimizing outcomes in de novo pediatric acute myeloid leukemia. *Paediatric drugs* 2014;16:213-27.
15. Lowenberg B, Downing JR, Burnett A. Acute myeloid leukemia. *The New England journal of medicine* 1999;341:1051-62.
16. Forman SJ, Rowe JM. The myth of the second remission of acute leukemia in the adult. *Blood* 2013;121:1077-82.
17. Paietta E. Minimal residual disease in acute myeloid leukemia: coming of age. *Hematology / the Education Program of the American Society of Hematology American Society of Hematology Education Program* 2012;2012:35-42.
18. Al-Mawali A, Gillis D, Lewis I. The role of multiparameter flow cytometry for detection of minimal residual disease in acute myeloid leukemia. *American journal of clinical pathology* 2009;131:16-26.
19. Thol F, Kolking B, Damm F, et al. Next-generation sequencing for minimal residual disease monitoring in acute myeloid leukemia patients with FLT3-ITD or NPM1 mutations. *Genes, chromosomes & cancer* 2012;51:689-95.
20. McKee LC, Jr., Collins RD. Intravascular leukocyte thrombi and aggregates as a cause of morbidity and mortality in leukemia. *Medicine* 1974;53:463-78.
21. Lehrnbecher T, Sung L. Anti-infective prophylaxis in pediatric patients with acute myeloid leukemia. *Expert review of hematology* 2014;7:819-30.
22. Tuzuner N, Cox C, Rowe JM, Bennett JM. Bone marrow cellularity in myeloid stem cell disorders: impact of age correction. *Leukemia research* 1994;18:559-64.
23. Li XP, Liu WF, Ji SR, Wu SH, Sun JJ, Fan YZ. Isolated pancreatic granulocytic sarcoma: a case report and review of the literature. *World journal of gastroenterology : WJG* 2011;17:540-2.
24. Geyh SR-P, M.; Khandanpour, C.; Cadeddu, R.P.; Jäger, P.; Zilkens, C.; Dührsen, U.; Wilk, C.M.; Fenk, R.; Gattermann, N.; Germing, U.; Kobbe, G.; Lyko, F.; Haas, R.; Schroeder, T. Functional Inhibition of Mesenchymal Stem and Progenitor Cells (MSPC) Significantly Contributes to Hematopoietic Insufficiency with Acute Myeloid Leukemia (AML). In: 56th ASH Annual Meeting and Exposition. San Francisco, CA; 2014.
25. Schofield R. The relationship between the spleen colony-forming cell and the haemopoietic stem cell. *Blood cells* 1978;4:7-25.
26. Smith JN, Calvi LM. Concise review: Current concepts in bone marrow microenvironmental regulation of hematopoietic stem and progenitor cells. *Stem Cells* 2013;31:1044-50.
27. Tabe Y, Konopleva M. Advances in understanding the leukaemia microenvironment. *British journal of haematology* 2014;164:767-78.
28. Wang L, Benedito R, Bixel MG, et al. Identification of a clonally expanding haematopoietic compartment in bone marrow. *The EMBO journal* 2013;32:219-30.
29. Mendelson A, Frenette PS. Hematopoietic stem cell niche maintenance during homeostasis and regeneration. *Nature medicine* 2014;20:833-46.

30. Harrison JS, Rameshwar P, Chang V, Bandari P. Oxygen saturation in the bone marrow of healthy volunteers. *Blood* 2002;99:394.
31. Spencer JA, Ferraro F, Roussakis E, et al. Direct measurement of local oxygen concentration in the bone marrow of live animals. *Nature* 2014;508:269-73.
32. Morrison SJ, Scadden DT. The bone marrow niche for haematopoietic stem cells. *Nature* 2014;505:327-34.
33. Mercier FE, Ragu C, Scadden DT. The bone marrow at the crossroads of blood and immunity. *Nature reviews Immunology* 2012;12:49-60.
34. Sugiyama T, Kohara H, Noda M, Nagasawa T. Maintenance of the hematopoietic stem cell pool by CXCL12-CXCR4 chemokine signaling in bone marrow stromal cell niches. *Immunity* 2006;25:977-88.
35. Fujisaki J, Wu J, Carlson AL, et al. In vivo imaging of Treg cells providing immune privilege to the haematopoietic stem-cell niche. *Nature* 2011;474:216-9.
36. Winkler IG, Sims NA, Pettit AR, et al. Bone marrow macrophages maintain hematopoietic stem cell (HSC) niches and their depletion mobilizes HSCs. *Blood* 2010;116:4815-28.
37. Katayama Y, Battista M, Kao WM, et al. Signals from the sympathetic nervous system regulate hematopoietic stem cell egress from bone marrow. *Cell* 2006;124:407-21.
38. Yamazaki S, Ema H, Karlsson G, et al. Nonmyelinating Schwann cells maintain hematopoietic stem cell hibernation in the bone marrow niche. *Cell* 2011;147:1146-58.
39. Wiseman DH, Greystoke BF, Somerville TC. The variety of leukemic stem cells in myeloid malignancy. *Oncogene* 2014;33:3091-8.
40. Messinger Y, Chelstrom L, Gunther R, Uckun FM. Selective homing of human leukemic B-cell precursors to specific lymphohematopoietic microenvironments in SCID mice: a role for the beta 1 integrin family surface adhesion molecules VLA-4 and VLA-5. *Leukemia & lymphoma* 1996;23:61-9.
41. Duhrsen U, Hossfeld DK. Stromal abnormalities in neoplastic bone marrow diseases. *Annals of hematology* 1996;73:53-70.
42. Schepers K, Pietras EM, Reynaud D, et al. Myeloproliferative neoplasia remodels the endosteal bone marrow niche into a self-reinforcing leukemic niche. *Cell stem cell* 2013;13:285-99.
43. Evans AG, Calvi LM. Notch signaling in the malignant bone marrow microenvironment: implications for a niche-based model of oncogenesis. *Annals of the New York Academy of Sciences* 2015;1335:63-77.
44. Poulos MG, Gars EJ, Gutkin MC, et al. Activation of the vascular niche supports leukemic progression and resistance to chemotherapy. *Experimental hematology* 2014;42:976-86 e3.
45. Konopleva MY, Jordan CT. Leukemia stem cells and microenvironment: biology and therapeutic targeting. *Journal of clinical oncology : official journal of the American Society of Clinical Oncology* 2011;29:591-9.
46. Trams EG, Lauter CJ, Salem N, Jr., Heine U. Exfoliation of membrane ecto-enzymes in the form of micro-vesicles. *Biochimica et biophysica acta* 1981;645:63-70.

47. Thery C, Zitvogel L, Amigorena S. Exosomes: composition, biogenesis and function. *Nature reviews Immunology* 2002;2:569-79.
48. Harding C, Heuser J, Stahl P. Receptor-mediated endocytosis of transferrin and recycling of the transferrin receptor in rat reticulocytes. *The Journal of cell biology* 1983;97:329-39.
49. van Niel G, Porto-Carreiro I, Simoes S, Raposo G. Exosomes: a common pathway for a specialized function. *Journal of biochemistry* 2006;140:13-21.
50. Bobrie A, Colombo M, Krumeich S, Raposo G, Thery C. Diverse subpopulations of vesicles secreted by different intracellular mechanisms are present in exosome preparations obtained by differential ultracentrifugation. *Journal of extracellular vesicles* 2012;1.
51. Gould SJ, Raposo G. As we wait: coping with an imperfect nomenclature for extracellular vesicles. *Journal of extracellular vesicles* 2013;2.
52. Johnstone RM, Bianchini A, Teng K. Reticulocyte maturation and exosome release: transferrin receptor containing exosomes shows multiple plasma membrane functions. *Blood* 1989;74:1844-51.
53. Raposo G, Nijman HW, Stoorvogel W, et al. B lymphocytes secrete antigen-presenting vesicles. *The Journal of experimental medicine* 1996;183:1161-72.
54. Gould SJ, Booth AM, Hildreth JE. The Trojan exosome hypothesis. *Proceedings of the National Academy of Sciences of the United States of America* 2003;100:10592-7.
55. Sidhu SS, Mengistab AT, Tauscher AN, LaVail J, Basbaum C. The microvesicle as a vehicle for EMMPRIN in tumor-stromal interactions. *Oncogene* 2004;23:956-63.
56. Hawari FI, Rouhani FN, Cui X, et al. Release of full-length 55-kDa TNF receptor 1 in exosome-like vesicles: a mechanism for generation of soluble cytokine receptors. *Proceedings of the National Academy of Sciences of the United States of America* 2004;101:1297-302.
57. Valadi H, Ekstrom K, Bossios A, Sjostrand M, Lee JJ, Lotvall JO. Exosome-mediated transfer of mRNAs and microRNAs is a novel mechanism of genetic exchange between cells. *Nature cell biology* 2007;9:654-9.
58. Huber V, Filipazzi P, Iero M, Fais S, Rivoltini L. More insights into the immunosuppressive potential of tumor exosomes. *Journal of translational medicine* 2008;6:63.
59. Skog J, Wurdinger T, van Rijn S, et al. Glioblastoma microvesicles transport RNA and proteins that promote tumour growth and provide diagnostic biomarkers. *Nature cell biology* 2008;10:1470-6.
60. Smalheiser NR. Do Neural Cells Communicate with Endothelial Cells via Secretory Exosomes and Microvesicles? *Cardiovascular psychiatry and neurology* 2009;2009:383086.
61. Skinner AM, O'Neill SL, Kurre P. Cellular microvesicle pathways can be targeted to transfer genetic information between non-immune cells. *PloS one* 2009;4:e6219.

62. Bruno S, Grange C, Deregibus MC, et al. Mesenchymal stem cell-derived microvesicles protect against acute tubular injury. *Journal of the American Society of Nephrology* : JASN 2009;20:1053-67.
63. Deng ZB, Poliakov A, Hardy RW, et al. Adipose tissue exosome-like vesicles mediate activation of macrophage-induced insulin resistance. *Diabetes* 2009;58:2498-505.
64. Admyre C, Grunewald J, Thyberg J, et al. Exosomes with major histocompatibility complex class II and co-stimulatory molecules are present in human BAL fluid. *The European respiratory journal* 2003;22:578-83.
65. Caby MP, Lankar D, Vincendeau-Scherrer C, Raposo G, Bonnerot C. Exosomal-like vesicles are present in human blood plasma. *International immunology* 2005;17:879-87.
66. Bard MP, Hegmans JP, Hemmes A, et al. Proteomic analysis of exosomes isolated from human malignant pleural effusions. *American journal of respiratory cell and molecular biology* 2004;31:114-21.
67. Hoorn EJ, Pisitkun T, Zietse R, et al. Prospects for urinary proteomics: exosomes as a source of urinary biomarkers. *Nephrology (Carlton)* 2005;10:283-90.
68. Ogawa Y, Kanai-Azuma M, Akimoto Y, Kawakami H, Yanoshita R. Exosome-like vesicles with dipeptidyl peptidase IV in human saliva. *Biological & pharmaceutical bulletin* 2008;31:1059-62.
69. Harrington MG, Fonteh AN, Oborina E, et al. The morphology and biochemistry of nanostructures provide evidence for synthesis and signaling functions in human cerebrospinal fluid. *Cerebrospinal fluid research* 2009;6:10.
70. Taylor DD, Gercel-Taylor C. MicroRNA signatures of tumor-derived exosomes as diagnostic biomarkers of ovarian cancer. *Gynecologic oncology* 2008;110:13-21.
71. Mitchell PJ, Welton J, Staffurth J, et al. Can urinary exosomes act as treatment response markers in prostate cancer? *Journal of translational medicine* 2009;7:4.
72. Rosell R, Wei J, Taron M. Circulating MicroRNA Signatures of Tumor-Derived Exosomes for Early Diagnosis of Non-Small-Cell Lung Cancer. *Clinical lung cancer* 2009;10:8-9.
73. Saenz-Cuesta M, Osorio-Querejeta I, Otaegui D. Extracellular Vesicles in Multiple Sclerosis: What are They Telling Us? *Frontiers in cellular neuroscience* 2014;8:100.
74. Kruh-Garcia NA, Wolfe LM, Chaisson LH, et al. Detection of *Mycobacterium tuberculosis* peptides in the exosomes of patients with active and latent *M. tuberculosis* infection using MRM-MS. *PloS one* 2014;9:e103811.
75. Wu SC, Yang JC, Rau CS, et al. Profiling circulating microRNA expression in experimental sepsis using cecal ligation and puncture. *PloS one* 2013;8:e77936.
76. Alvarez S, Suazo C, Boltansky A, et al. Urinary exosomes as a source of kidney dysfunction biomarker in renal transplantation. *Transplantation proceedings* 2013;45:3719-23.

77. Katakowski M, Buller B, Zheng X, et al. Exosomes from marrow stromal cells expressing miR-146b inhibit glioma growth. *Cancer letters* 2013;335:201-4.
78. Roccaro AM, Sacco A, Maiso P, et al. BM mesenchymal stromal cell-derived exosomes facilitate multiple myeloma progression. *The Journal of clinical investigation* 2013;123:1542-55.
79. Tan CY, Lai RC, Wong W, Dan YY, Lim SK, Ho HK. Mesenchymal stem cell-derived exosomes promote hepatic regeneration in drug-induced liver injury models. *Stem cell research & therapy* 2014;5:76.
80. Zhang Y, Chopp M, Meng Y, et al. Effect of exosomes derived from multipotential mesenchymal stromal cells on functional recovery and neurovascular plasticity in rats after traumatic brain injury. *Journal of neurosurgery* 2015:1-12.
81. Zhu YG, Feng XM, Abbott J, et al. Human mesenchymal stem cell microvesicles for treatment of Escherichia coli endotoxin-induced acute lung injury in mice. *Stem Cells* 2014;32:116-25.
82. Kordelas L, Rebmann V, Ludwig AK, et al. MSC-derived exosomes: a novel tool to treat therapy-refractory graft-versus-host disease. *Leukemia* 2014;28:970-3.
83. Peinado H, Aleckovic M, Lavotshkin S, et al. Melanoma exosomes educate bone marrow progenitor cells toward a pro-metastatic phenotype through MET. *Nature medicine* 2012;18:883-91.
84. Zhang HG, Grizzle WE. Exosomes and cancer: a newly described pathway of immune suppression. *Clinical cancer research : an official journal of the American Association for Cancer Research* 2011;17:959-64.
85. Haga H, Yan IK, Takahashi K, Wood J, Zubair A, Patel T. Tumour cell-derived extracellular vesicles interact with mesenchymal stem cells to modulate the microenvironment and enhance cholangiocarcinoma growth. *Journal of extracellular vesicles* 2015;4:24900.
86. Wang J, Hendrix A, Hernot S, et al. Bone marrow stromal cell-derived exosomes as communicators in drug resistance in multiple myeloma cells. *Blood* 2014;124:555-66.
87. Lee RC, Ambros V. An extensive class of small RNAs in *Caenorhabditis elegans*. *Science* 2001;294:862-4.
88. Lau NC, Lim LP, Weinstein EG, Bartel DP. An abundant class of tiny RNAs with probable regulatory roles in *Caenorhabditis elegans*. *Science* 2001;294:858-62.
89. Lagos-Quintana M, Rauhut R, Lendeckel W, Tuschl T. Identification of novel genes coding for small expressed RNAs. *Science* 2001;294:853-8.
90. Ambros V. The functions of animal microRNAs. *Nature* 2004;431:350-5.
91. Friedman RC, Farh KK, Burge CB, Bartel DP. Most mammalian mRNAs are conserved targets of microRNAs. *Genome research* 2009;19:92-105.
92. Ha M, Kim VN. Regulation of microRNA biogenesis. *Nature reviews Molecular cell biology* 2014;15:509-24.
93. Yates LA, Norbury CJ, Gilbert RJ. The long and short of microRNA. *Cell* 2013;153:516-9.
94. Griffiths-Jones S. What's in a name? In: miRBase blog; 2011.

95. Braun JE, Huntzinger E, Fauser M, Izaurralde E. GW182 proteins directly recruit cytoplasmic deadenylase complexes to miRNA targets. *Molecular cell* 2011;44:120-33.
96. Huntzinger E, Izaurralde E. Gene silencing by microRNAs: contributions of translational repression and mRNA decay. *Nature reviews Genetics* 2011;12:99-110.
97. Chen CZ, Li L, Lodish HF, Bartel DP. MicroRNAs modulate hematopoietic lineage differentiation. *Science* 2004;303:83-6.
98. Bissels U, Bosio A, Wagner W. MicroRNAs are shaping the hematopoietic landscape. *Haematologica* 2012;97:160-7.
99. Schoolmeesters A, Eklund T, Leake D, et al. Functional profiling reveals critical role for miRNA in differentiation of human mesenchymal stem cells. *PLoS one* 2009;4:e5605.
100. Costa A, Afonso J, Osorio C, et al. miR-363-5p regulates endothelial cell properties and their communication with hematopoietic precursor cells. *Journal of hematology & oncology* 2013;6:87.
101. Vasilatou D, Papageorgiou S, Pappa V, Papageorgiou E, Dervenoulas J. The role of microRNAs in normal and malignant hematopoiesis. *European journal of haematology* 2010;84:1-16.
102. Vidal M, Mangeat P, Hoekstra D. Aggregation reroutes molecules from a recycling to a vesicle-mediated secretion pathway during reticulocyte maturation. *Journal of cell science* 1997;110 (Pt 16):1867-77.
103. King HW, Michael MZ, Gleadle JM. Hypoxic enhancement of exosome release by breast cancer cells. *BMC cancer* 2012;12:421.
104. Chen XX, Lin J, Qian J, et al. Dysregulation of miR-124-1 predicts favorable prognosis in acute myeloid leukemia. *Clinical biochemistry* 2014;47:63-6.
105. Spinello I, Quaranta MT, Riccioni R, et al. MicroRNA-146a and AMD3100, two ways to control CXCR4 expression in acute myeloid leukemias. *Blood cancer journal* 2011;1:e26.
106. Palma CA, Al Sheikha D, Lim TK, et al. MicroRNA-155 as an inducer of apoptosis and cell differentiation in Acute Myeloid Leukaemia. *Molecular cancer* 2014;13:79.
107. Su R, Lin HS, Zhang XH, et al. MiR-181 family: regulators of myeloid differentiation and acute myeloid leukemia as well as potential therapeutic targets. *Oncogene* 2014;0.
108. Lee DW, Futami M, Carroll M, et al. Loss of SHIP-1 protein expression in high-risk myelodysplastic syndromes is associated with miR-210 and miR-155. *Oncogene* 2012;31:4085-94.
109. Ufkin ML, Peterson S, Yang X, Driscoll H, Duarte C, Sathyanarayana P. miR-125a regulates cell cycle, proliferation, and apoptosis by targeting the ErbB pathway in acute myeloid leukemia. *Leukemia research* 2014;38:402-10.
110. Nakano T, Kodama H, Honjo T. Generation of lymphohematopoietic cells from embryonic stem cells in culture. *Science* 1994;265:1098-101.
111. O'Connell RM, Chaudhuri AA, Rao DS, Gibson WS, Balazs AB, Baltimore D. MicroRNAs enriched in hematopoietic stem cells differentially regulate long-

term hematopoietic output. Proceedings of the National Academy of Sciences of the United States of America 2010;107:14235-40.

112. O'Connell RM, Rao DS, Chaudhuri AA, et al. Sustained expression of microRNA-155 in hematopoietic stem cells causes a myeloproliferative disorder. The Journal of experimental medicine 2008;205:585-94.

113. Roberts CT, Jr., Kurre P. Vesicle trafficking and RNA transfer add complexity and connectivity to cell-cell communication. Cancer research 2013;73:3200-5.

114. Mizuno S, Chijiwa T, Okamura T, et al. Expression of DNA methyltransferases DNMT1, 3A, and 3B in normal hematopoiesis and in acute and chronic myelogenous leukemia. Blood 2001;97:1172-9.

115. Nakajima K, Crisma AR, Silva GB, Rogero MM, Fock RA, Borelli P. Malnutrition suppresses cell cycle progression of hematopoietic progenitor cells in mice via cyclin D1 down-regulation. Nutrition 2014;30:82-9.

116. Ramos-Mejia V, Navarro-Montero O, Ayllon V, et al. HOXA9 promotes hematopoietic commitment of human embryonic stem cells. Blood 2014;124:3065-75.

117. Pulikkan JA, Peramangalam PS, Dengler V, et al. C/EBPalpha regulated microRNA-34a targets E2F3 during granulopoiesis and is down-regulated in AML with CEBPA mutations. Blood 2010;116:5638-49.

118. Lieu YK, Reddy EP. Conditional c-myc knockout in adult hematopoietic stem cells leads to loss of self-renewal due to impaired proliferation and accelerated differentiation. Proceedings of the National Academy of Sciences of the United States of America 2009;106:21689-94.

119. Zhao JL, Ma C, O'Connell RM, et al. Conversion of danger signals into cytokine signals by hematopoietic stem and progenitor cells for regulation of stress-induced hematopoiesis. Cell stem cell 2014;14:445-59.

120. Yin JA, O'Brien MA, Hills RK, Daly SB, Wheatley K, Burnett AK. Minimal residual disease monitoring by quantitative RT-PCR in core binding factor AML allows risk stratification and predicts relapse: results of the United Kingdom MRC AML-15 trial. Blood 2012;120:2826-35.

121. Loken MR, Alonzo TA, Pardo L, et al. Residual disease detected by multidimensional flow cytometry signifies high relapse risk in patients with de novo acute myeloid leukemia: a report from Children's Oncology Group. Blood 2012;120:1581-8.

122. Buonamici S, Ottaviani E, Testoni N, et al. Real-time quantitation of minimal residual disease in inv(16)-positive acute myeloid leukemia may indicate risk for clinical relapse and may identify patients in a curable state. Blood 2002;99:443-9.

123. Dohner H, Estey EH, Amadori S, et al. Diagnosis and management of acute myeloid leukemia in adults: recommendations from an international expert panel, on behalf of the European LeukemiaNet. Blood 2010;115:453-74.

124. Hageman IM, Peek AM, de Haas V, Damen-Korbijn CM, Kaspers GJ. Value of routine bone marrow examination in pediatric acute myeloid leukemia (AML): a study of the Dutch Childhood Oncology Group (DCOG). Pediatric blood & cancer 2012;59:1239-44.

125. Rickmann M, Macke L, Sundarasetty BS, et al. Monitoring dendritic cell and cytokine biomarkers during remission prior to relapse in patients with FLT3-ITD acute myeloid leukemia. *Annals of hematology* 2013;92:1079-90.
126. Xiao B, Wang Y, Li W, et al. Plasma microRNA signature as a noninvasive biomarker for acute graft-versus-host disease. *Blood* 2013;122:3365-75.
127. Lim SH, Becker TM, Chua W, et al. Circulating tumour cells and circulating free nucleic acid as prognostic and predictive biomarkers in colorectal cancer. *Cancer letters* 2014;346:24-33.
128. Raghavachari N, Liu P, Barb JJ, et al. Integrated analysis of miRNA and mRNA during differentiation of human CD34+ cells delineates the regulatory roles of microRNA in hematopoiesis. *Experimental hematology* 2014;42:14-27 e1-2.
129. Morris VA, Zhang A, Yang T, et al. MicroRNA-150 expression induces myeloid differentiation of human acute leukemia cells and normal hematopoietic progenitors. *PloS one* 2013;8:e75815.
130. Marcucci G, Radmacher MD, Maharry K, et al. MicroRNA expression in cytogenetically normal acute myeloid leukemia. *The New England journal of medicine* 2008;358:1919-28.
131. Garzon R, Garofalo M, Martelli MP, et al. Distinctive microRNA signature of acute myeloid leukemia bearing cytoplasmic mutated nucleophosmin. *Proceedings of the National Academy of Sciences of the United States of America* 2008;105:3945-50.
132. Wang Y, Li Z, He C, et al. MicroRNAs expression signatures are associated with lineage and survival in acute leukemias. *Blood cells, molecules & diseases* 2010;44:191-7.
133. Huan J, Hornick NI, Shurtleff MJ, et al. RNA trafficking by acute myelogenous leukemia exosomes. *Cancer research* 2013;73:918-29.
134. Simons M, Raposo G. Exosomes--vesicular carriers for intercellular communication. *Current opinion in cell biology* 2009;21:575-81.
135. Cheng L, Sun X, Scicluna BJ, Coleman BM, Hill AF. Characterization and deep sequencing analysis of exosomal and non-exosomal miRNA in human urine. *Kidney international* 2013.
136. Street JM, Barran PE, Mackay CL, et al. Identification and proteomic profiling of exosomes in human cerebrospinal fluid. *Journal of translational medicine* 2012;10:5.
137. Aoki J, Ohashi K, Mitsuhashi M, et al. Posttransplantation Bone Marrow Assessment by Quantifying Hematopoietic Cell-Derived mRNAs in Plasma Exosomes/Microvesicles. *Clinical chemistry* 2014.
138. Manterola L, Guruceaga E, Gallego Perez-Larraya J, et al. A small noncoding RNA signature found in exosomes of GBM patient serum as a diagnostic tool. *Neuro-oncology* 2014.
139. Hong CS, Muller L, Whiteside TL, Boyiadzis M. Plasma exosomes as markers of therapeutic response in patients with acute myeloid leukemia. *Frontiers in immunology* 2014;5:160.

140. Liu J, Sun H, Wang X, et al. Increased Exosomal MicroRNA-21 and MicroRNA-146a Levels in the Cervicovaginal Lavage Specimens of Patients with Cervical Cancer. *International journal of molecular sciences* 2014;15:758-73.
141. Fayyad-Kazan H, Bitar N, Najjar M, et al. Circulating miR-150 and miR-342 in plasma are novel potential biomarkers for acute myeloid leukemia. *Journal of translational medicine* 2013;11:31.
142. Sanchez PV, Perry RL, Sarry JE, et al. A robust xenotransplantation model for acute myeloid leukemia. *Leukemia* 2009;23:2109-17.
143. Agliano A, Martin-Padura I, Mancuso P, et al. Human acute leukemia cells injected in NOD/LtSz-scid/IL-2Rgamma null mice generate a faster and more efficient disease compared to other NOD/scid-related strains. *International journal of cancer Journal international du cancer* 2008;123:2222-7.
144. Matsuo Y, MacLeod RA, Uphoff CC, et al. Two acute monocytic leukemia (AML-M5a) cell lines (MOLM-13 and MOLM-14) with interclonal phenotypic heterogeneity showing MLL-AF9 fusion resulting from an occult chromosome insertion, ins(11;9)(q23;p22p23). *Leukemia* 1997;11:1469-77.
145. Mony U, Jawad M, Seedhouse C, Russell N, Pallis M. Resistance to FLT3 inhibition in an in vitro model of primary AML cells with a stem cell phenotype in a defined microenvironment. *Leukemia* 2008;22:1395-401.
146. Jacamo R, Chen Y, Wang Z, et al. Reciprocal leukemia-stroma VCAM-1/VLA-4-dependent activation of NF-kappaB mediates chemoresistance. *Blood* 2014;123:2691-702.
147. Garrido SM, Appelbaum FR, Willman CL, Banker DE. Acute myeloid leukemia cells are protected from spontaneous and drug-induced apoptosis by direct contact with a human bone marrow stromal cell line (HS-5). *Experimental hematology* 2001;29:448-57.
148. Barbash S, Shifman S, Soreq H. Global coevolution of human MicroRNAs and their target genes. *Molecular biology and evolution* 2014;31:1237-47.
149. Rommer A, Steinleitner K, Hackl H, et al. Overexpression of primary microRNA 221/222 in acute myeloid leukemia. *BMC cancer* 2013;13:364.
150. Woiterski J, Ebinger M, Witte KE, et al. Engraftment of low numbers of pediatric acute lymphoid and myeloid leukemias into NOD/SCID/IL2Rcgammanull mice reflects individual leukemogenicity and highly correlates with clinical outcome. *International journal of cancer Journal international du cancer* 2013;133:1547-56.
151. Reese ND, Schiller GJ. High-dose cytarabine (HD araC) in the treatment of leukemias: a review. *Current hematologic malignancy reports* 2013;8:141-8.
152. Kampa-Schittenhelm KM, Heinrich MC, Akmut F, Dohner H, Dohner K, Schittenhelm MM. Quizartinib (AC220) is a potent second generation class III tyrosine kinase inhibitor that displays a distinct inhibition profile against mutant-FLT3, -PDGFRA and -KIT isoforms. *Molecular cancer* 2013;12:19.
153. Mitchell PS, Parkin RK, Kroh EM, et al. Circulating microRNAs as stable blood-based markers for cancer detection. *Proceedings of the National Academy of Sciences of the United States of America* 2008;105:10513-8.

154. Katsuda T, Kosaka N, Ochiya T. The roles of extracellular vesicles in cancer biology: towards the development of novel cancer biomarkers. *Proteomics* 2013.
155. Bazarbachi A, Abou Merhi R, Gessain A, et al. Human T-cell lymphotropic virus type I-infected cells extravasate through the endothelial barrier by a local angiogenesis-like mechanism. *Cancer research* 2004;64:2039-46.
156. Ferrajoli A, Shanafelt TD, Ivan C, et al. Prognostic value of miR-155 in individuals with monoclonal B-cell lymphocytosis and patients with B chronic lymphocytic leukemia. *Blood* 2013;122:1891-9.
157. Kern SE. Why your new cancer biomarker may never work: recurrent patterns and remarkable diversity in biomarker failures. *Cancer research* 2012;72:6097-101.
158. Turchinovich A, Samatov TR, Tonevitsky AG, Burwinkel B. Circulating miRNAs: cell-cell communication function? *Frontiers in genetics* 2013;4:119.
159. Estey EH. Acute myeloid leukemia: 2013 update on risk-stratification and management. *American journal of hematology* 2013;88:318-27.
160. Miraki-Moud F, Anjos-Afonso F, Hodby KA, et al. Acute myeloid leukemia does not deplete normal hematopoietic stem cells but induces cytopenias by impeding their differentiation. *Proceedings of the National Academy of Sciences of the United States of America* 2013;110:13576-81.
161. Joosten SA, Goeman JJ, Sutherland JS, et al. Identification of biomarkers for tuberculosis disease using a novel dual-color RT-MLPA assay. *Genes and immunity* 2012;13:71-82.
162. Lim WS, Tardi PG, Dos Santos N, et al. Leukemia-selective uptake and cytotoxicity of CPX-351, a synergistic fixed-ratio cytarabine:daunorubicin formulation, in bone marrow xenografts. *Leukemia research* 2010;34:1214-23.
163. Ren J, Jin P, Sabatino M, et al. Global transcriptome analysis of human bone marrow stromal cells (BMSC) reveals proliferative, mobile and interactive cells that produce abundant extracellular matrix proteins, some of which may affect BMSC potency. *Cytotherapy* 2011;13:661-74.
164. Lu D, Nakagawa R, Lazzaro S, et al. The miR-155-PU.1 axis acts on Pax5 to enable efficient terminal B cell differentiation. *The Journal of experimental medicine* 2014;211:2183-98.
165. Wang L, Zhang H, Rodriguez S, et al. Notch-dependent repression of miR-155 in the bone marrow niche regulates hematopoiesis in an NF-kappaB-dependent manner. *Cell stem cell* 2014;15:51-65.
166. Zhang H, Goudeva L, Immenschuh S, et al. MiR-155 is associated with the leukemogenic potential of the class IV granulocyte colony stimulating factor receptor in CD34+ progenitor cells. *Mol Med* 2014.
167. Guinn D, Ruppert AS, Maddocks K, et al. miR-155 expression is associated with chemoimmunotherapy outcome and is modulated by Bruton's tyrosine kinase inhibition with Ibrutinib. *Leukemia* 2014.
168. Costinean S, Zanesi N, Pekarsky Y, et al. Pre-B cell proliferation and lymphoblastic leukemia/high-grade lymphoma in E(mu)-miR155 transgenic mice. *Proceedings of the National Academy of Sciences of the United States of America* 2006;103:7024-9.

169. Chen J, Yao D, Zhao S, et al. MiR-1246 promotes SiHa cervical cancer cell proliferation, invasion, and migration through suppression of its target gene thrombospondin 2. *Archives of gynecology and obstetrics* 2014;290:725-32.
170. Takeshita N, Hoshino I, Mori M, et al. Serum microRNA expression profile: miR-1246 as a novel diagnostic and prognostic biomarker for oesophageal squamous cell carcinoma. *British journal of cancer* 2013;108:644-52.
171. Liao JM, Zhou X, Zhang Y, Lu H. MiR-1246: a new link of the p53 family with cancer and Down syndrome. *Cell Cycle* 2012;11:2624-30.
172. Cambronne XA, Shen R, Auer PL, Goodman RH. Capturing microRNA targets using an RNA-induced silencing complex (RISC)-trap approach. *Proceedings of the National Academy of Sciences of the United States of America* 2012;109:20473-8.
173. Dweep H, Gretz N, Sticht C. miRWalk database for miRNA-target interactions. *Methods Mol Biol* 2014;1182:289-305.
174. Szklarczyk D, Franceschini A, Wyder S, et al. STRING v10: protein-protein interaction networks, integrated over the tree of life. *Nucleic acids research* 2015;43:D447-52.
175. Wang X, Li J, Dong K, et al. Tumor suppressor miR-34a targets PD-L1 and functions as a potential immunotherapeutic target in acute myeloid leukemia. *Cellular signalling* 2015;27:443-52.
176. Organista-Nava J, Gomez-Gomez Y, Illades-Aguir B, et al. High miR-24 expression is associated with risk of relapse and poor survival in acute leukemia. *Oncology reports* 2015;33:1639-49.
177. Weng H, Lal K, Yang FF, Chen J. The pathological role and prognostic impact of miR-181 in acute myeloid leukemia. *Cancer genetics* 2015.
178. Romania P, Lulli V, Pelosi E, Biffoni M, Peschle C, Marziali G. MicroRNA 155 modulates megakaryopoiesis at progenitor and precursor level by targeting Ets-1 and Meis1 transcription factors. *British journal of haematology* 2008;143:570-80.
179. Sandhu SK, Volinia S, Costinean S, et al. miR-155 targets histone deacetylase 4 (HDAC4) and impairs transcriptional activity of B-cell lymphoma 6 (BCL6) in the Emu-miR-155 transgenic mouse model. *Proceedings of the National Academy of Sciences of the United States of America* 2012;109:20047-52.
180. Worm J, Stenvang J, Petri A, et al. Silencing of microRNA-155 in mice during acute inflammatory response leads to derepression of c/ebp Beta and down-regulation of G-CSF. *Nucleic acids research* 2009;37:5784-92.
181. Xu C, Ren G, Cao G, et al. miR-155 regulates immune modulatory properties of mesenchymal stem cells by targeting TAK1-binding protein 2. *The Journal of biological chemistry* 2013;288:11074-9.
182. Wang S, Li X, Parra M, Verdin E, Bassel-Duby R, Olson EN. Control of endothelial cell proliferation and migration by VEGF signaling to histone deacetylase 7. *Proceedings of the National Academy of Sciences of the United States of America* 2008;105:7738-43.

183. Hayashi Y, Hirai H, Kamio N, et al. C/EBPbeta promotes BCR-ABL-mediated myeloid expansion and leukemic stem cell exhaustion. *Leukemia* 2013;27:619-28.
184. Watkins NA, Gusnanto A, de Bono B, et al. A HaemAtlas: characterizing gene expression in differentiated human blood cells. *Blood* 2009;113:e1-9.
185. Okada Y, Nagai R, Sato T, et al. Homeodomain proteins MEIS1 and PBXs regulate the lineage-specific transcription of the platelet factor 4 gene. *Blood* 2003;101:4748-56.
186. Bruns I, Lucas D, Pinho S, et al. Megakaryocytes regulate hematopoietic stem cell quiescence through CXCL4 secretion. *Nature medicine* 2014;20:1315-20.
187. Huang J, Nguyen-McCarty M, Hexner EO, Danet-Desnoyers G, Klein PS. Maintenance of hematopoietic stem cells through regulation of Wnt and mTOR pathways. *Nature medicine* 2012;18:1778-85.
188. Heideman MR, Lancini C, Proost N, Yanover E, Jacobs H, Dannenberg JH. Sin3a-associated Hdac1 and Hdac2 are essential for hematopoietic stem cell homeostasis and contribute differentially to hematopoiesis. *Haematologica* 2014;99:1292-303.
189. Thurmond TS, Murante FG, Staples JE, Silverstone AE, Korach KS, Gasiewicz TA. Role of estrogen receptor alpha in hematopoietic stem cell development and B lymphocyte maturation in the male mouse. *Endocrinology* 2000;141:2309-18.
190. Smoot ME, Ono K, Ruscheinski J, Wang PL, Ideker T. Cytoscape 2.8: new features for data integration and network visualization. *Bioinformatics* 2011;27:431-2.
191. Colombo M, Raposo G, Thery C. Biogenesis, secretion, and intercellular interactions of exosomes and other extracellular vesicles. *Annual review of cell and developmental biology* 2014;30:255-89.
192. Hanson PI, Cashikar A. Multivesicular body morphogenesis. *Annual review of cell and developmental biology* 2012;28:337-62.
193. Stuffers S, Sem Wegner C, Stenmark H, Brech A. Multivesicular endosome biogenesis in the absence of ESCRTs. *Traffic* 2009;10:925-37.
194. Bolukbasi MF, Mizrak A, Ozdener GB, et al. miR-1289 and "Zipcode"-like Sequence Enrich mRNAs in Microvesicles. *Molecular therapy Nucleic acids* 2012;1:e10.
195. Villarroya-Beltri C, Gutierrez-Vazquez C, Sanchez-Cabo F, et al. Sumoylated hnRNPA2B1 controls the sorting of miRNAs into exosomes through binding to specific motifs. *Nature communications* 2013;4:2980.
196. Melo SA, Sugimoto H, O'Connell JT, et al. Cancer exosomes perform cell-independent microRNA biogenesis and promote tumorigenesis. *Cancer cell* 2014;26:707-21.
197. Morelli AE, Larregina AT, Shufesky WJ, et al. Endocytosis, intracellular sorting, and processing of exosomes by dendritic cells. *Blood* 2004;104:3257-66.
198. Rana S, Yue S, Stadel D, Zoller M. Toward tailored exosomes: the exosomal tetraspanin web contributes to target cell selection. *The international journal of biochemistry & cell biology* 2012;44:1574-84.

199. Christianson HC, Svensson KJ, van Kuppevelt TH, Li JP, Belting M. Cancer cell exosomes depend on cell-surface heparan sulfate proteoglycans for their internalization and functional activity. *Proceedings of the National Academy of Sciences of the United States of America* 2013;110:17380-5.
200. Miyanishi M, Tada K, Koike M, Uchiyama Y, Kitamura T, Nagata S. Identification of Tim4 as a phosphatidylserine receptor. *Nature* 2007;450:435-9.
201. Hanayama R, Tanaka M, Miwa K, Shinohara A, Iwamatsu A, Nagata S. Identification of a factor that links apoptotic cells to phagocytes. *Nature* 2002;417:182-7.
202. Paget S. The distribution of secondary growths in cancer of the breast. 1889. *Cancer metastasis reviews* 1989;8:98-101.
203. Boyd AL, Campbell CJ, Hopkins CI, et al. Niche displacement of human leukemic stem cells uniquely allows their competitive replacement with healthy HSPCs. *The Journal of experimental medicine* 2014;211:1925-35.
204. Nwajei F, Konopleva M. The bone marrow microenvironment as niche retreats for hematopoietic and leukemic stem cells. *Advances in hematology* 2013;2013:953982.
205. Evans AG, Calvi LM. Notch signaling in the malignant bone marrow microenvironment: implications for a niche-based model of oncogenesis. *Annals of the New York Academy of Sciences* 2015;1335:63-77.
206. Raaijmakers MH, Mukherjee S, Guo S, et al. Bone progenitor dysfunction induces myelodysplasia and secondary leukaemia. *Nature* 2010;464:852-7.
207. Georgiou KR, Foster BK, Xian CJ. Damage and recovery of the bone marrow microenvironment induced by cancer chemotherapy - potential regulatory role of chemokine CXCL12/receptor CXCR4 signalling. *Current molecular medicine* 2010;10:440-53.
208. Szczepanski MJ, Szajnik M, Welsh A, Whiteside TL, Boyiadzis M. Blast-derived microvesicles in sera from patients with acute myeloid leukemia suppress natural killer cell function via membrane-associated transforming growth factor-beta1. *Haematologica* 2011;96:1302-9.